REPUBLIC OF TURKEY
GAZIANTEP UNIVERSITY
GRADUATE SCHOOL OF
NATURAL & APPLIED SCIENCES

SELF-COMPACTING GEOPOLYMER & CONCRETE FILLED POLYMER TUBES

Ph.D. THESIS

IN

CIVIL ENGINEERING

BY
ALI KHALID HUSSEIN
MARCH 2019

Self-Compacting Geopolymer & Concrete Filled Polymer Tubes

Ph.D. Thesis

In

Civil Engineering

University of Gaziantep

Supervisor

Prof. Dr. Abdulkadir Çevik

Co-Supervisor

Assist. Prof. Dr. Ahmet Emin Kurtoğlu

By

Ali Khalid Hussein

March 2019

REPUBLIC OF TURKEY
UNIVERSITY OF GAZİANTEP
GRADUATE SCHOOL OF NATURAL & APPLIED SCIENCES
CIVIL ENGINEERING DEPARTMENT

Name of the thesis: Self-Compacting Geopolymer & Concrete Filled Polymer Tubes

Name of the student: Ali Khalid HUSSEIN

Exam date: March 20, 2019

Approval of the Graduate School of Natural and Applied Sciences.

Prof. Dr. A. Necmeddin YAZICI
Director

I certify that this thesis satisfies all the requirements as a thesis for the degree of Doctor of Philosophy.

Prof. Dr. Hanifi ÇANAKCI
Head of Department

This is to certify that we have read this thesis and that in our opinion it is fully adequate, in scope and quality, as a thesis for the degree of Doctor of Philosophy.

Assist. Prof. Dr. Ahmet Emin Kurtoğlu	Prof. Dr. Abdulkadir ÇEVİK
Co. Supervisor	Supervisor

Examining Committee Members: Signature

Prof. Dr. Abdulkadir ÇEVİK   ………………………….

Prof. Dr. İbrahim H. GÜZELBEY   …………………………

Assoc. Prof. Dr. Amjad KHABAZ   …………………………

Assist. Prof. Dr. Mehmet Eren GÜLŞAN   …………………………

Assist. Prof. Dr. Hüseyin Çağan KILINÇ   …………………………

State that all those data on that file have been provided and shown according to academics protocols and honest carry out. Furthermore, i state that, as needed by these guidelines and as well, carry out, I possess completely mentioned and referenced all of the materials and outcomes which are not unique for this study.

Ali Khalid HUSSEIN

ABSTRACT
SELF-COMPACTING GEOPOLYMER & CONCRETE FILLED POLYMER TUBES

HUSSEIN, Ali Khalid

Ph.D. in Civil Engineering

Supervisor: Prof. Dr. Abdulkadir ÇEVİK

Co-Supervisor: Assist. Prof. Dr. Ahmet EminKurtoğlu

March 2019

162 page

This thesis examines the flexural and axial behaviour of self-compacting concrete and geopolymer filled polymer tubes. The study consists of 3 parts. The first part of the study investigates the short-term durability and mechanical characteristics of self-compacting concrete (SCC)-filled glass reinforced polymer (GRP) tubular columns under axial compression. A total of fourty specimens were prepared and submerged in water or acid solution prior to axial compression tests. Test variables included the exposure type, specimen/tube geometry (i.e., diameter, height and thickness) and steel fiber presence. The second part investigates the mechanical properties and short term durability performance of self-compacting concrete (SCC)–filled high density polyethylene (HDPE) tubes with and without steel fibers. A total of 45 cylinder specimens were prepared and subjected to aggressive substances such as sulfate or acid contents. Test variables included the environmental exposure conditions, tube thickness, inside diameter, tube height and steel fiber presence. The third part of the thesis demonstrates an experimental investigation on the flexural behavior of high-density polyethylene (HDPE)-steel double skin tubular (DST) tube beams-filled with self compacting geopolymer concrete (SCGP). The fundamental parameters of the experimental investigation include the diameter of (HDPE) tubes, cross-sectional shapes of interior steel reinforcement, and the presence (or absence) of (SCGC) concrete filling inside of steel tube. This experimental program involves twenty-two beams and they are partitioned into two groups based on diameter (i.e. 11 and 12 mm).

Keywords: Polymer tubes, fiber reinforced polymer (FRP), confinement, self-compacting concrete, self-compacting geopolymer, composite beams, and short columns.

ÖZET
KENDİLİĞİNDEN YERLEŞEN JEOPOLİMER VE BETON DOLGULU POLİMER TÜPLER

HUSSEIN, Ali Khalid

İnşaat Mühendisliği Doktora
Danışman: Prof. Dr. Abdulkadir ÇEVİK
**Yardımcı Danışman: Dr. Öğr. Üyesi Ahmet EminKurtoğlu**
Mart 2019

162 sayfa

Bu tezde, kendiliğinden yerleşen beton ve jeopolimer beton doldurulmuş polimer tüplerin eğilme davranışı ve basınç altında davranışları incelenmiştir. Çalışma 3 bölümden oluşmaktadır. İlk bölümde, kendiliğinden yerleşen beton (KYB) doldurulmuş cam takviyeli polimer (CTP) tüp kolonların kısa vadeli durabilitesi ve eksenel basınç altındaki davranışı incelenmiştir. Toplam 40 adet numune hazırlanmış olup eksenel basınç deneylerinden önce, numuneler su veya asit çözeltisinde bekletilmiştir. Deneylerde değişken parametreler; deney öncesi çevresel maruziyet koşulu, numune geometrisi (çap, yükseklik ve kalınlık) ve çelik lif mevcudiyeti olarak belirlenmiştir. İkinci bölümde, kendiliğinden yerleşen beton (KYB) ile doldurulmuş yüksek yoğunluklu polietilen (HDPE) tüplerin çelik lifli veya lifsiz halde mekanik özellikleri ve kısa süreli durabilite performansı irdelenmiştir. Toplam 45 numune hazırlanmış olup numuneler sülfat veya asit solüsyonu gibi agresif ortamlara maruz bırakılmıştır. Test değişkenleri; çevresel maruziyet koşulları, tüp kalınlığı, iç çap, tüp yüksekliği ve çelik lif mevcudiyeti olarak belirlenmiştir. Tezin üçüncü bölümünde, kendiliğinden yerleşen jeopolimer beton (KYJB) ile doldurulmuş yüksek yoğunluklu polietilen (HDPE) ve çelik çift cidarlı boru (ÇCB) tüplerin eğilme davranışı üzerinde deneysel bir araştırma yapılmıştır. Deneysel çalışmanın temel parametreleri; dış boru çapı, iç çelik boru kesit geometrisi ve KYJB mevcudiyeti olarak belirlenmiştir. Bu deneyler için, iki grup halinde (11 mm ve 12 mm çaplı) 22 adet numune üretilmiştir.

Anahtar Kelimeler: Polimer tüpler, fiber takviyeli polimer (FRP), sargılama, kendiliğinden yerleşen beton, kendiliğinden yerleşen jeopolimer, kompozit kirişler ve kısa kolonlar.

To My Parents, I am grateful to God for having parents like you. Your unconditional love and support made my every achievement possible.
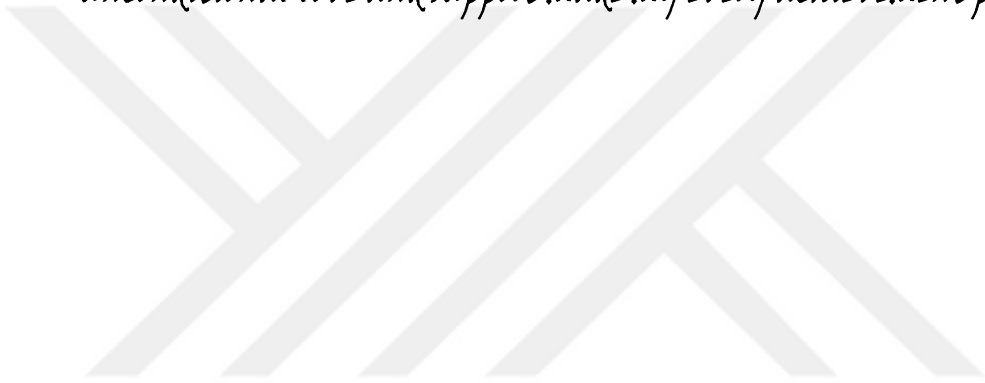
ACKNOWLEDGEMENT

First of all, I want to consider the chance to be grateful for Allah for His success as well as for providing me the achievement, power, and bravery to do this thesis. Without him, I would not have been capable to make this happen thesis.

I want expressing my honest appreciation to my supervisor Prof. Abdulkadir ÇEVİK for the constant assist of my Ph.D. research for his tolerance, inspiration, and great education. I am grateful to God for advantage me with a teacher as you. Likewise I want expressing my exceptional appreciation to my cost supervisor Assist. Prof. Dr. Ahmet EminKurtoğlu for his central assistance helping to produce me. As well I want expressing my special appreciation to my teacher Assist. Prof. Dr. Mehmet Eren GÜLŞAN for his critical assistance helping to produce me.

My phrases aren't enough expressing my deep appreciation to my family (**My Parents, My Brothers, and Sisters**) because they were definitely assisting and motivate me during my research and maintained in contact and provided self-confidence in every stage of my research. I am very thankful to them for understandings, helps, tolerance, and encouragements.

TABLE OF CONTENTS

LIST OF TABLES

LIST OF FIGUERS

xiii

xv

LIST OF SYMBOLS/ABERVIATIONS

FRP: Fibre-reinforced polymer

RC: Reinforced concrete

VARTM: Vacuum assisted resin transfer molding

CFFTs: Concrete-filled FRP tubes

DSTMs: Double-skin tubular members

SCC: Self-compacting concrete

SCG: Self-compacting Geopolymers

SFRC: Steel Fiber Reinforced Concrete

GPC: Geopolymers concrete

HG: Hollow GRP

Al: Aluminum

Si: Silica

GRP: Glass reinforced polymer

LVDTs: Linear variable displacement transducers

HDPE: High density polyethylene

DST: Double skin tubular

Gravel: G

Sand: S

Portland cement: PC

Water: W

ASTM C39 / C39M – 12: Standard Test Method for Compressive Strength of Cylindrical Concrete Specimens

EFNARC: European federation dedicated to specialist construction chemicals and concrete systems

CHAPTER 1

INTRODUCTION

1.1 Fiber reinforced polymer (FRP)

In the last three decades, advanced fibre-reinforced polymer (FRP) composites have attracted worldwide interests as an emerging construction material for the repair, strengthening and as well, retrofit of existing constructions. FRP composite have many advantages, including the great strength to weight percentage, remarkable corrosion resistor, tailor ability of mechanized benefits and ease for installation (Hollaway & Teng, 2008). General research interests include flexural and shear strengthening of reinforced concrete (RC) beams (Chun & Park, 2002; Ernst, Bridge, & Wheeler, 2010; Qian & Liu, 2006), seismic retrofit and strengthening of RC columns (Lam & Teng, 2003; Teng & Lam, 2002), flexural strengthening and buckling prevention of steel structures (Teng, Yu, & Fernando, 2012), and retrofit of masonry structures (Rovero, Focacci, & Stipo, 2012). Various attempts are also designed to include FRP in new construction, seeking at remarkable durable constructions which only require very low protection (Zaman, Gutub, & Wafa, 2013). It should, however, be noted that FRP composites also have their disadvantages, including their low shear strength, relatively low elastic modulus, relatively high cost and poor fire resistance (Teng, Yu, Wong, & Dong, 2007). As a result, when used in new construction, FRP composites are preferred to be combined with traditional construction materials (e.g. steel and concrete). Various forms of hybrid members incorporating FRP composites have been proposed and investigated worldwide. FRP products generally available in the market include fibre sheets for forming FRP via a wet lay-up process, FRP bars/cables, FRP profiles/panels and FRP tubes (Sciolti, Frigione, & Aiello, 2010). Fibre sheets are generally preferred in the strengthening and retrofit of existing structures due to their flexibility in shape. Pultruded FRP bars have been extensively investigated as an alternate to traditional steel bars for concrete structures located in an aggressive environment (Barris, Torres, Comas, & Mias, 2013; Manalo, Benmokrane, Park, & Lutze, 2014). Type of concrete structures reinforced with FRP bars has been covered

by several design guidelines (Benmokrane, El-Salakawy, El-Ragaby, & Lackey, 2006; R. Wang, Han, & Tao, 2015). FRP cables are advantageous to traditional steel cables in terms of their light weight as well as corrosion and fatigue resistance. The first bridge with FRP cables was constructed as early as 1992 in the USA (Khalifa, Hodhod, & Zaki, 1996). For long span cable stayed bridges, the sag of an FRP cable is generally smaller than a corresponding steel cable, leading to a higher global stiffness and higher natural frequencies. FRP cables are thus an excellent alternative to steel cables (X. Wang & Wu, 2011). In addition, it is easy to embed fibre optical sensors into FRP cables during the manufacturing process, making it easy to monitor the condition of the cables during its service life. FRP profiles are generally manufactured via a pultrusion process, where the fibres are mainly oriented in the longitudinal direction. Many different cross section shapes can be achieved, such as those shown in Figure 1.1, (Zhao, 2017). The profiles can serve as the main girders of a bridge or connected by bolts to form a truss bridge. However, because of the low elastic modulus of the FRP, the design of structures with FRP profile girders is generally controlled by deformation instead of load carrying capacity. Complex FRP panels made via a vacuum served botanical switch molding (VARTM) procedure have also been proposed to serve as light weight bridge decks (e.g. Figures 1.2 and 1.3), (Zhao, 2017). FRP panels also suffer from the weakness of low elastic modulus. Alternatively, the voids of FRP panels can be partially or completely filled with concrete or foam to enhance its stiffness and ultimate strength (e.g. Figures 1.4 and 1.5) (Zhao, 2017). Concrete-filled FRP tubes (CFFTs) are usually the most used types of hybrid members manufactured from concrete and FRP. For the strengthening/retrofit of existing columns, the FRP tube/jacket could be formed via a wet lay-up procedure using fibre sheets. For new construction, prefabricated FRP tubes are preferred, which also function as the formwork for casting concrete (Mirmiran & Shahawy, 1995). When a CFFT is under central compression, the concrete primary is exposed to lateral confinement from the FRP tube, resulting in tri-axial compressive stresses in the concrete, the FRP pipe is subsequently exposed to hoop tension (Ozbakkaloglu, 2013). Seeing that FRP behaves nearly linear elastically, the lateral confinement in the concrete primary can increase continually with the improvement of lateral deformation (Matthys, Toutanji, & Taerwe, 2006). Consequently, both strength and ductility of the concrete primary could be significantly improved. The optimal combination of two brittle materials (i.e. FRP and concrete) thus leads to a highly ductile compression

member. Although the FRP tube can also be used as longitudinal reinforcement by adopting fibres at or close to the longitudinal direction,

as suggested by some researchers, the incorporation of longitudinal fibres in an FRP tube, however, suffers from several disadvantages (Mirmiran, 2003): (1) the shear force to be transferred between the concrete and the FRP tube increases, and the bond at the bi-material interface may become critical; (2) the FRP tube ruptures suddenly when loaded beyond its tensile capacity, leading to reduced ductility of the member (B. Wang et al., 2009) (3) FRP tubes with a large axial stiffness is prone to buckling under axial compression (Zhu, Ahmad, & Mirmiran, 2005), which compromises the confinement effectiveness. As a result, researchers (Dai, Bai, & Teng, 2011) have suggested that the fibres of the FRP tube should be mainly oriented in or close to the hoop direction, with the bending moment being resisted by additional internal reinforcement (Figure 1.6).

Figure 1.1 FRP profiles of various cross-section shapes (Zhao, 2017)
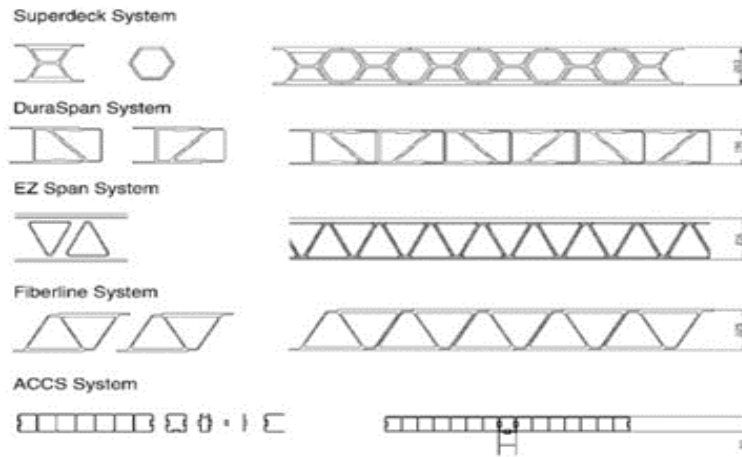
Figure 1.2 Complex FRP panels as light-weight bridge decks (Zhao, 2017)
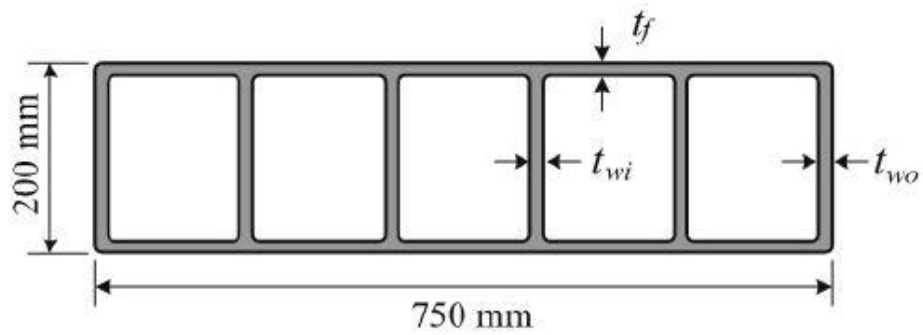
Figure 1.3 FRP deck panel (Zhao, 2017)

Figure 1.4 FRP panels filled with foam material (Zhao, 2017)
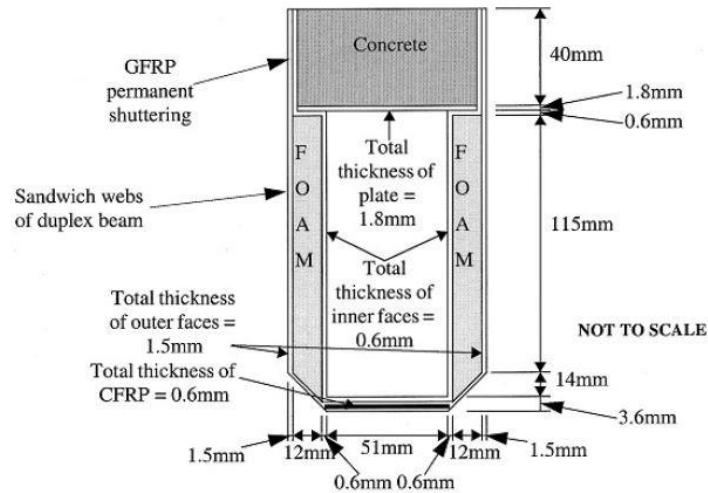
Figure 1.5 Partially filled FRP profile as bridge girder (Zhao, 2017)
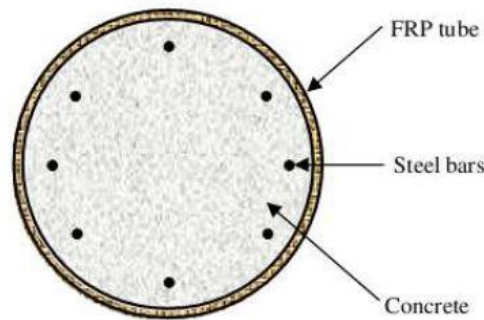
Figure 1.6 Concrete-filled FRP tube (CFFT) with internal steel reinforcement (Zhao, 2017)

1.2 Hybrid FRP concrete steel double skin

Tube members Double-skin tubular members (DSTMs) refer to members consisting of an external pipe, an interior pipe and a concrete infill between two pipes. Examples include DSTMs with two steel tubes (Figure 1.7). (De Lorenzis & Teng, 2007; Pan, Guo, Li, Tang, & Huang, 2017; Tao Yu & Remennikov, 2013; T Yu, Wong, Teng, Dong, & Lam, 2006) proposed hybrid FRP-concrete-steel double-skin tubular members, that include an interior steel pipe, an exterior FRP pipe and as well , concrete filled in between. The unique combination of the three components in a structural element leads to several positive aspects over existing structural forms. Compared with DSTMs with two steel tubes, hybrid DSTMs have many advantages including

21

(Anuradha et al., 2013): (1) more ductile response of concrete due to better confinement from the FRP pipe that doesn't buckle; (2) does not require fire defense of the outer pipe as it only serves as a form for casting concrete and a confining system 4 for the ultimate limit state; (3) better corrosion resistance like the steel pipe is perfectly saved by the FRP tube and the concrete. Compared to DSTMs with two FRP pipes (Tao Yu & Teng, 2012), the key benefits of hybrid DSTMs consist of: (1) capability to assist structure load because of the existence of a stiff/strong interior steel pipe; (2) ease for connection with other members taking advantage of the inner steel tube; (3) does not require fire cover of the outer pipe; (4) better confinement to the concrete due to the stiff/strong inner steel pipe. Hybrid DSTMs are also expected to possess the following advantages (Idris & Ozbakkaloglu, 2015): (1) remarkable ductility as a concrete is good confined as well as the steel pipe acts as ductile longitudinal reinforcement; (2) light weight due to the enhanced concrete strength and a large inner void; (3) ease for construction as the prefabricated FRP tube and steel pipe work as the formwork for casting concrete with no steel cages needed. A large number of research has been carried out on hybrid DSTMs seeing that their technology. The current research, however, has been primarily centered on the use of hybrid DSTMs as compression members (i.e. hybrid double-skin tubular columns or hybrid DSTCs). Only a few studies (Celik et al., 2015; Ouchi, Nakamura, Osterberg, Hallberg, & Lwin, 2003; Persson, 2001; Teng, Yu, & Wong, 2011) were dedicated to the behavior of hybrid DSTMs as flexural members (i.e. hybrid double-skin tubular beams or hybrid DSTBs). These minor existing research completely involved only small-scale beam tests, which confirmed the excellent ductility of hybrid DSTBs (Vejmelková, Keppert, Grzeszczyk, Skaliński, & Černý, 2011).
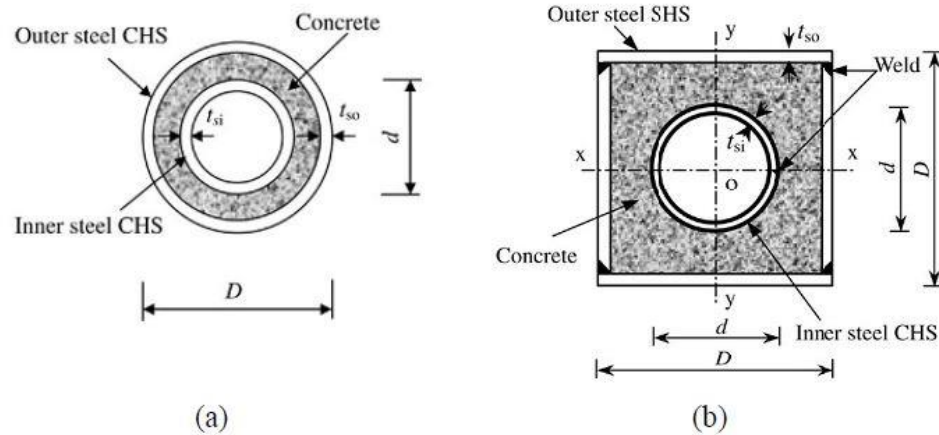
Figure 1.7 Double-skin tubular members (DSTMs) with two steel tubes (Zhao, 2017)

1.3 Self compacting concrete (SCC)

Recent studies have exhibited that reinforced concrete is composed of construction material with strong effective effect since its establishment due to its low-cost characteristics, environment friendly, strong strength and hardness characteristics, in addition to the ease of manufacturing in the site, is the most requested and the use of a wide range of building materials, which are more than any other material. Recent studies have shown that global demand for concrete is about 10 billion tons per year (Okamura & Ouchi, 1999). In recent decades, a number of research has been presented in the development of the construction industry. "'Self-compacting concrete (SCC)' " is, in turn, one of the most significant advances in concrete technology (Behr, Rosentritt, Regnet, Lang, & Handel, 2004).

It has been designed (SCC) in order to flow under its own mass, resistance to separation, in order to provide durability requirements, compression molds and pump capacity. Due to its high quality, most durable, dense and uniform surface texture and better strength characteristics, (SCC) has contributed significantly to improving the quality of concrete structures and opening new horizons for the application of concrete to build a fast track (Topcu, Bilir, & Uygunoğlu, 2009).

Material used in concrete is the same as used in (SCC), but the ingredients used in the form contain less quantity than the aggregates and the quantity of powder (cement and filler particles smaller than 0.125 mm). Glass filler, Fly ash, silica fume AS a

supplement, fillers and super-plastic materials are used ViscoCrete (SikaNorge AS) or SSP 2000 (Scancem Chemicals AS) etc. are added. High segregation resistance and High flow ability of SCC are obtained by using, (Grdic, Toplicic-Curcic, Despotovic, & Ristic, 2010):

1-A larger amount of precision, i.e., The total particle content posted (Coarse aggregate: 50% of concrete and sand-size: 40% of the size of the mortar).

2-Low values for water / powder ratio (0.3-0.4).

3-A higher dosage stabilizer and plasticizer.

SCC, self-concrete specifications can be given as a material of superior performance that flows under the influence of its own weight without the need to use the vibrator to achieve uniformity by filling the entire structure even when access to the very narrow distances between reinforcing rods is obstructed. The basic understanding was first introduced to self-compacting concrete in Japan in the 1980s. For a number of decades and years starting in 1983, there was a fundamental problem about the issue of the durability of concrete constructions and as well, was a significant challenge in Japan. This was necessitated by sufficient and appropriate pressure by skilled labor to obtain permanent concrete structures. Studies by researchers and academics to find a suitable solution to this problem led to the creation of self-adjusting concrete, first reported in 1989 (Song & Hwang, 2004). Since the development and actual innovation of SCC in 1989, the use of SCC in structures has increased dramatically and widely. The primary causes of the usage of self-adhesive concrete could be described the examples below, (Yoo, Yoon, & Banthia, 2015):

1-It has a strong effect in reducing or preventing noise, especially in concrete production plants.

2-Effectively powerful in facilitating the construction of the fast track with a minimal use of labor.

3-It is effective in ensuring the compactness is excellent in the structure: especially in areas with high concentration reinforcement where there is pressure by mechanical vibration is very difficult to achieve when using ordinary concrete.

Separation of doubt represents an actual problem, it is possible to impede prevention around reinforcement, and this causes drying shrinkage of high-grade and non-uniform

compressive strength when concrete hardening occurs. In addition, it is possible to observe the separation of SCC either in a fixed form or in the form of dynamic motion during the flow of concrete. This separation is highly undesirable because it will in turn lead to the appearance of the properties and characteristics of the material classes (shrinkage, Poisson's ratio, modulus of elasticity and creep) which in turn cause a lack of uniformity in the stresses and strength resulting from internal restraint through volumetric changes (Yoo, Shin, Yang, & Yoon, 2014).

Thus, differences in characteristics (and durability) are closely correlated with the specific effects of elements on the rheological properties of the mixture, the effects of the physical properties (i.e. size and specific density) of the aggregate, and the date of the mixing (Deluce & Vecchio, 2013). As such, it can be seen that the concrete SCC was a remarkable development and addition to that it was more revolutionary in the concrete industry in recent years. Although the main reason was originally to overcome the shortage of skilled labor, it has also been used now for both concrete and precast concrete sites (Altun, Haktanir, & Ari, 2007).

1- Safe working environment

2- Reduced noise levels, due to absence of vibration and

3- Greater bond strength

4- Increased durability

5- Better surface finish

6-. Faster construction

7- Reduction in manpower

8- Uniform and complete consolidation

9- Ease in placement

1.4 Steel fiber reinforced concrete (SFRC)

Steel fiber reinforced concrete (SFRC) is a compound materials containing the traditional components of Portland cement concrete. (Additives, concrete, fine concrete, hydraulic cement), and dispersing short cut steel fibers randomly. Just as with all FRC materials, compared to plain concrete the most noticeable differences are

improved ductility and post-cracking performance. In North America, the use of SFRC has grown over the years, albeit very slowly. In addition extensive experimental research has been conducted on SFRC. However, despite this fact the use of SFRC in structural applications remains very limited in the construction industry (Alwan, Naaman, & Guerrero, 1999). One of the main reasons returns to deficiency of dependable prediction designs and the insufficient detailed design and style recommendations for engineers. Other reasons include the price SFRC and the conventional nature of the construction industry. Current widespread use of fibers is mostly in non-structural applications, where fibers are generally used as an alternative for the steel bars and wire mesh used to control cracking Other examples include nonstructural applications, panels, large concrete containers, concrete pavements and industrial flooring. Generally, these types of structures and solutions are characterized by having open surface spaces and movements limitations, which in turn leads to a high possibility of cracking (Altun et al., 2007). For these applications, fiber has a number of advantages over traditional rebar including uniform distribution of the fibers in the concrete matrix and savings in labor cost and construction time due to the ability of fibers to partially or completely replace traditional reinforcement. In addition to the present utilize of fibers in nonstructural functions there may be benefit in using this material in some structural functions. The usage of fibers significantly enhances the diagonal-tension capacity of concrete, leading to improved shear resistance. Hence the use of fibers in beams and columns can potentially be used to replace traditional shear and transverse reinforcement. The addition of fibers also improves the energy-absorption capacity of concrete; hence the use of fibers may be beneficial in seismic and blast applications (beams, columns, walls) (Alwan et al., 1999).

1.4.1 Steel fiber typologies

Various steel fiber configurations can be used. For example, some steel fibers have hooked ends while others have deformed or twisted shapes to improve pullout behavior.

1.4.2 Hooked and steel fibers

Hooked-end steel fibers represent the most common fiber type used by researchers and in the construction industry. These fibers provide superior performance when

compared to straight fibers because of the effect of the hooks on pullout resistance. After the initial deboning of the fiber from the concrete matrix, the hooked-ends must deform, resulting in an improvement in pullout strength. Currently hooked-end fibers are manufactured by Bekaert under the Dramix brand. Extensive experimental data on the use of this type of fiber is available in the literature. The fibers are added to the concrete during mixing as glued bundles and disperse homogeneously during the mixing process (Deluce & Vecchio, 2013).

1.5 Geopolymers concrete

The process of Geopolymerization was fueled by the need to develop nonflammable and noncombustible plastic materials after some horrific fires broke out in France in the early 1970s. Joseph Davidovits, a French chemist, is widely considered as the father or this process. While trying to develop an inorganic polymer material is organic, found that the thermal conditions of water have an effect on the effective installation of organic plastic and metal heat-resistant, such as zeolite. This discovery helped him develop three dimensional semi-crystalline materials that consist of silicaalumina bonds. The first applications of these materials were in constriction manufacture, such as fire-resistant chip-board panels, which were composed of a wooden primary facing two Silifas Q nanocomposite coatings, that the complete panel was developed in a one-step process (Xu & Van Deventer, 2000) After the fire resistant chip-board panels, Davidovits experimented with ceramics by replacing quartz with synthesized cordiorite, (Si5AlO18) Al3Mg2, in a naturally occurring mixture of kaoline and quartz. He obtained a unique material; SILIFACE COR70 that had excellent mechanical and thermal properties but poor absorption properties. It was through this observation that Davidovits was able to coin the term "Geopolymer". A Geopolymer is formed when a chemical reaction occurs where the aluminum (Al) and Silica (Si) in a trace material of geological origin or it by product (such as fly ash) react with an alkaline liquid to produce a binder. The chemical reaction is a polymerization reaction. Geopolymers are family members of inorganic polymers. The chemical structure of the Geopolymer materials is comparable to organic zeolitic materials. However, the microstructures of Geopolymer materials are amorphous instead of crystalline (Villa, Pecina, Torres, & Gómez, 2010). Essentially the two main constituents of Geopolymers are the trace material and the activator solution. The trace material is an element containing a large number of Aluminum (Al) and Silica (SI)

since they are the basis of geopolymer reactions. The activator solution is an alkaline solution composed of diluted alkali metals. Potassium and Sodium are known to be the preferred metals for these solutions (Andini et al., 2008).

The chemical reaction during Geopolymerizaton usually contains the steps below.

1- Dissolution of Al atoms and Si from the cradle material through the action of hydroxide ions.

2- Setting or polycondensation/polymerisation of monomers into polymeric structures.

3- Condensation or orientation or Transportation of precursor ions into monomers.

1.6 Organization of thesis

Chapter 1. This chapter provides as an intro, describes the benefits and as well, application of concrete filled FRP pipes in civil engineering infrastructures, accompanied by the main goal and scope of this research.

Chapter 2: This chapter shows the first part in this thesis, that's named "Experimental investigation on the short-term durability of self-compacting concrete-filled GRP tubular columns." It shows the outcomes of an experimental analysis on the axial behavior of 40 short columns.

Chapter 3: This chapter shows the second part in this thesis, that's titled "Mechanical Characterization and Durability of HDPE-confined Self-Compacting Concrete Tubular Columns Exposed to Severe Environment." It shows the outcomes of an experimental analysis on the axial behavior of 45 short columns.

Chapter 4: This chapter shows the third part in this thesis, that's titled "Flexural behavior of ultra-high ductile geopolymer HDPE tubes." It shows the outcomes of an experimental analysis on the flexural behavior of 45 composite beams.

Chapter 5: A conclusion of this analysis is provided in this chapter. The chapter also reveals the typical findings sucked from the work shown in this thesis.

CHAPTER 2

SHORT-TERM DURABILITY OF SELF-COMPACTING CONCRETE-FILLED GRP TUBULAR COLUMNS

2.1 Introduction

One of the major concerns in construction industry is the durability of reinforced concrete members exposed to aggressive substances. Marine structures are mainly subjected to deterioration such as salt crystallization-induced concrete corrosion, steel corrosion and surface degradation caused by chemicals inside sea water. RC bridge piers, for instance, are deteriorated mainly by the degradation of splash-tidal zones and corrosion of steel rebar. Reasons for deterioration include freeze-thaw cycles, wetting and drying, high salt and/or acid contents. Corrosion of steel reinforcement and/or salt crystallization damage at the splash/tidal zones are the main reasons for failure of structures in coastal areas where the groundwater with high salt and sulfate content is present. Numerous corrosion control systems (e.g. control permeability formwork, polymer wraps) have been applied to prevent these zones from deterioration. These methods, however, have disadvantages such as high cost and time-consuming (Karimi, Tait, & El-Dakhakhni, 2011a, 2011b; Saafi, Toutanji, & Li, 1999).

According to current estimations, billions of dollars are spent annually for the maintenance and/or the repairing of deteriorated marine structures worldwide. Due to this high cost, alternative ideas such as manufacturing beams or columns by encasing concrete in plastic tubes have attracted great attention recently. Concrete filled plastic tubes appear to be a promising alternative to conventional reinforcement columns/beams in terms of durability (Mirmiran, Shahawy, & Beitleman, 2001), mechanical enhancement, environmental and economic advantages such as the elimination of reusable formworks and reduced material and labour costs. Past studies have demonstrated that the confinement of concrete can enhance both the mechanical and long term performance of concrete (normal strength concrete) (Abdulla, 2017; Thériault & Neale, 2000), high strength concrete, self-compacting concrete, recycled aggregate concrete. Various forms of confinement

types and materials (i.e. steel tubes, PVC tubes, FRP tubes or hybrid composite tubes) have been studied to investigate the effect of confining jackets on mechanical behavior and/or (Alsubari, Shafigh, & Jumaat, 2015; El Chabib, Nehdi, & El Naggar, 2005; Fakharifar & Chen, 2016; Tiberti, Minelli, & Plizzari, 2015). Most studies covering the durability (A. Z. Fam & Rizkalla, 2001) and mechanical behavior of such systems have used fiber reinforced polymer (FRP) composites as confining material. One major disadvantage of this composite, however, is the cost of material and labour. Thus, the introduction of new concrete protection materials for confinement and strengthening methods is significant for engineers in practice.

Apparently, glass reinforced polymer (GRP) pipes provide a more economical alternative in terms of manufacture and application. However, further research on durability concerns are to be resolved before putting this concept into application. Although a number of studies have investigated the mechanical behavior and durability of FRP-confined and/or PVC-confined normal concrete, an extensive investigation on the self-compacting concrete (SCC) filled GRP tubular systems is not present. Current study reports the results of an experimental work in which the mechanical characterization and short term durability of SCC-filled square GRP pipes were investigated for the first time in literature. Investigated parameters were the influences of GRP confinement, geometry, steel fiber addition in SCC, and acid attack.

2.2 Experimental program

A total of fourty specimens were prepared, cured and tested within the experimental program. The specimens were divided into four groups in accordance with tube dimensions as shown in Table 2.1and all specimens had square cross section. Out of fourty specimens, sixteen GRP tubes were filled with SCC, sixteen specimens were prepared as unconfined SCC and eight specimens were kept as hollow GRP tube (HG). Unconfined specimens were manufactured by filling the molds of equal size and removing them after the hardening of SCC. For the manufacturing GRP-confined SCC, a GRP tube was cut to required length and affixed at one end with silicon glue to a wood board to prevent water and concrete seepage, as shown in Fig. 2.1 a,b,c, respectively. This combination was used as a stay-in-place formwork before casting the confined specimens. All cast specimens including quality control reference cylinders according to ASTM C39-12 were kept in the water tank at 20°C for 28 days

to assure required curing conditions. Additionally, all tubes were checked to be free of initial cracks or defects that could be caused by cutting process.

The specimens were designated according to confinement material (HG for hollow GRP pipe, GCSCC for GRP tube + SCC and USCC for unconfined SCC samples), group number (G1, G2 and G3), steel fiber percentage (0% or 1%) and exposure type (W or A for water or acid, respectively). For instance, GCSCC-G3-0%-A addresses the SCC filled GRP tube specimen of the group G3, containing no steel fiber (0%) and exposed to acidic solution. Table 2.2 lists the test metrics of all specimens tested within the experimental program, (HAKIMI, 2017). It has been placed epoxy layer (5 mm) on the top of surface composite columns in order to ensure the distribution of stresses on the entire surface of the composite columns.

Figure 2.1 (a) Cutting of GRP tube
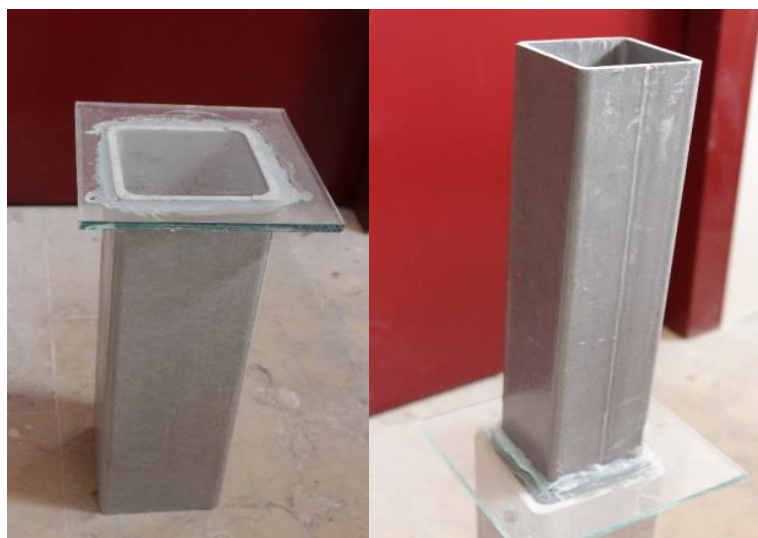
Figure 2.1 (b) GRP tubes before casting
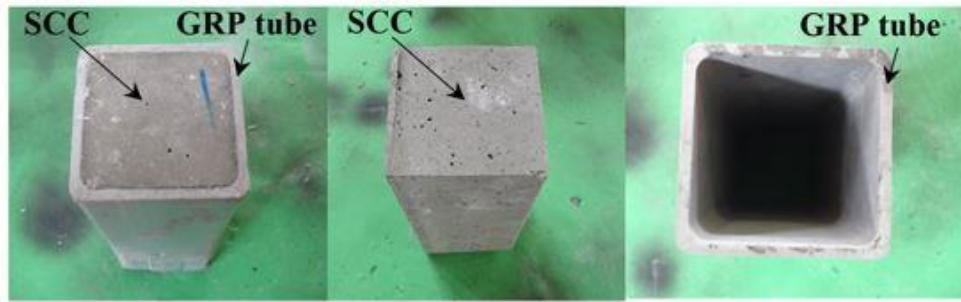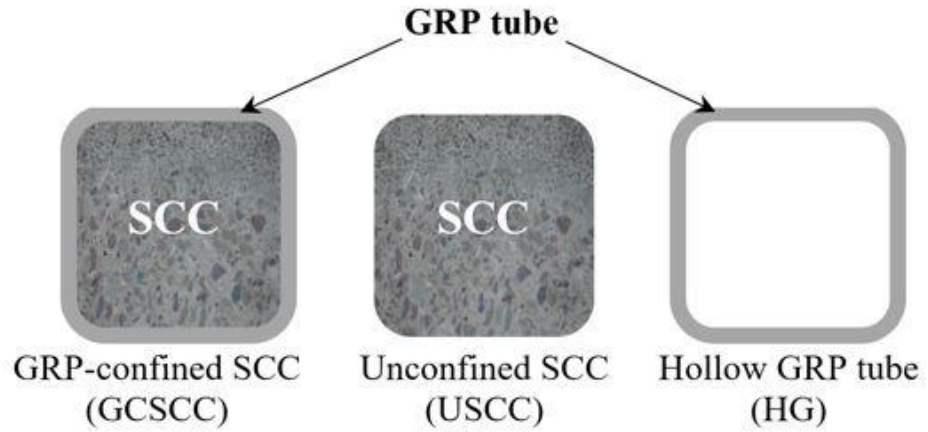
Figure 2.1 (c) Preparation of test specimens

Table 2.1 Geometry details of GRP tubes

Group details				
Group number	**Interior Dimension cm**	**Height cm**	**Thickness cm**	**Sample Designation**
1	(10 X 10)	60	0.8	Group 1
2	(10 X 10)	30	0.8	Group 2
3	(7.5 X 7.5)	60	0.43	Group 3
4	(7.5 X 7.5)	30	0.43	Group 4

Table 2.2 Test metrics and designation of specimens

Group 1 (G1)			
GRP-confined SCC (GCSCC)			
No	Steel fiber ratio	Environment	Sample Designation
#1	0 %	Water	GC-SCC-G1-0%-W
#2	1 %	Water	GC-SCC-G1-1%-W
#3	0 %	Acid	GC-SCC-G1-0%-A

#4	1 %	Acid	GC-SCC-G1-1%-A
Unconfined SCC (USCC)			
#5	0 %	Water	USCC-G1-0%-W
#6	1 %	Water	USCC-G1-1%-W
#7	0 %	Acid	USCC-G1-0%-A
#8	1 %	Acid	USCC-G1-1%-A
Hollow GRP tube (HG)			
#9	-	Water	HG-G1-W
#10	-	Acid	HG-G1-A
Group 2 (G2)			
GRP-confined SCC (GCSCC)			
No	**Steel fiber ratio**	**Environment**	**Sample Designation**
#11	0 %	Water	GC-SCC-G2-0%-W
#12	1 %	Water	GC-SCC-G2-1%-W
#13	0 %	Acid	GC-SCC-G2-0%-A
#14	1 %	Acid	GC-SCC-G2-1%-A
Unconfined SCC (USCC)			
#15	0 %	Water	USCC-G2-0%-W
#16	1 %	Water	USCC-G2-1%-W
#17	0 %	Acid	USCC-G2-0%-A
#18	1 %	Acid	USCC-G2-1%-A
Hollow GRP tube (HG)			
#19	-	Water	HG-G2-W
#20	-	Acid	HG-G2-A
Group 3 (G3)			
GRP-confined SCC (GCSCC)			
No	Steel fiber ratio	Environment	Sample Designation
#21	0 %	Water	GC-SCC-G3-0%-W
#22	1 %	Water	GC-SCC-G3-1%-W
#23	0 %	Acid	GC-SCC-G3-0%-A
#24	1 %	Acid	GC-SCC-G3-1%-A
Unconfined SCC (USCC)			
#25	0 %	Water	USCC-G3-0%-W
#26	1 %	Water	USCC-G3-1%-W
#27	0 %	Acid	USCC-G3-0%-A
#28	1 %	Acid	USCC-G3-1%-A
Hollow GRP tube (HG)			
#29	-	Water	HG-G3-W
#30	-	Acid	HG-G3-A
Group 4 (G4)			
GRP-confined SCC (GCSCC)			
No	**Steel fiber ratio**	**Environment**	**Sample Designation**
#31	0 %	Water	GC-SCC-G4-0%-W
#32	1 %	Water	GC-SCC-G4-1%-W
#33	0 %	Acid	GC-SCC-G4-0%-A
#34	1 %	Acid	GC-SCC-G4-1%-A

Unconfined SCC (USCC)			
#35	0 %	Water	USCC-G4-0%-W
#36	1 %	Water	USCC-G4-1%-W
#37	0 %	Acid	USCC-G4-0%-A
#38	1 %	Acid	USCC-G4-1%-A
Hollow GRP tube (HG)			
#39	-	Water	HG-G4-W
#40	-	Acid	HG-G4-A

2.3 Material properties

2.3.1 Self compacting concrete

Self-compacting concrete (SCC) mix with an unconfined compressive strength of 32 MPa at 28 days was considered for the fabrication of all unconfined and confined cylinder specimens. Portland cement (ASTM type I) was used as binder. Local sand with a fineness modulus of 2.6 mm and dry crushed limestone with a maximum size of 12 mm was used as coarse aggregate. Three cubic and three cylinder samples were cast and cured under the same curing conditions. These samples were then tested as per ASTM standards to ensure the required compressive strength. Table 2.3 presents the concrete proportions used in the fabrication of fresh SCC with and without steel fibers.

As stated in Table 2.4, all SCC requirements as per EFNARC standard were found satisfactory. The compressive and tensile strength results were obtained by averaging the outcomes of three tests for cylinder and cube samples. Quality control specimens were also cast from the same SCC mix.

Table 2.3 SCC mix proportions

Material	Value (kg/m3)	
	without SF (0%)	with SF (1%)
Gravel	730	1005
Sand	900	1425
Portland cement	300	450
FlyAsh Admixture	250	412.5
Water	200	255
Super plasticizer	4	8.625
Steel Fiber	-	58.85

Table 2.4 Fresh and hardened SCC properties

Parameter	Value	Limits (EFNARC)
Air content (%)		
Slump (mm)	650	520-700
Unit weight (kg/m^3)		
V-funnel flow (s)	8	≤ 12
T-50 (s)	4	2-5
Blocking ratio (H_2/H_1)	0.9	0.8-1
Splitting tensile strength* (MPa)	3.21	-
Compressive strength* (MPa)	32	-
* tested after standard water curing		

2.3.2 GRP pipes

Glass reinforced plastic (GRP) pipes were used as confinement material. GRP pipes exhibit various advantages such as high corrosion resistance, long service life of more than 50 years. Using GRP pipes for confinement can also provide suitable curing conditions for concrete due to low conductivity. Table 2.5 summarizes the physical properties of GRP pipes provided by the manufacturer.

Table 2.5 Physical properties of GRP pipes

Parameter	Value
Class	PE 40
Density	0.945-0.965 g/cm3
Breaking elongation	min 350%
Elastic modulus	>600 MPa
Ultimate tensile strength	26 MPa
Working temperature	min. -80 °C, max. 100 °C
Thermal conductivity	0.29 kcal/m hr °C
Service life	>50 years

2.3.3 Steel fiber

The addition of steel fiber in concrete leads to a number of enhancements in the behaviour of structural member. In compression, steel fibers do not significantly affect the ascending curve of the compressive stress-strain response. However, they cause the descending post-peak response curve to decline in a shallower fashion than the curve of plain concrete, resulting in an increased ductility and toughness. The

researchers observed an enhancement of only 15% in compression. However, the peak strain increases significantly with the provision of steel fibers.

On the other hand, the addition of steel fibers induces a much more noticeable effect on the tensile behavior. The strain softening behavior is observed in the concrete with typical fiber volume content. This results in the composite having greater ductility and energy absorption capabilities than the plain concrete. In addition, because the fibers bridge the cracks in the composite and aid in the transfer of forces across the cracks, crack widths are less than those in plain concrete. If the reinforcing bars are present, multiple cracks can form even for a strain-softening material. As compared to the plain concrete, there will be more cracks at shorter spacing and with smaller width.

Steel hooked fibers (SF), shown in Fig. 2.2, were added in the self-compacting concrete mix to see the effect of SF on the load strain behavior of unconfined and SCC filled GRP square columns under axial compression. Table 2.6 lists the properties of SF used in this study.

Figure 2.2 Steel fibers

Table 2.6 Steel fiber properties

Fiber type	Length (mm)	Diameter (mm)	Density (g/cm³)	Aspect ratio	Tensile strength MPa
Steel hooked fiber	50.3	0.75	7.8	67	1100

2.4 Instrumentation and testing

Experimental part of this study has two stages. First stage involves the durability tests where, after curing period, specimens were immersed in water or 1% acid solution for a period of 30 days. It was ensured that each solution was in room temperature during the durability tests. Second stage consists of axial compression tests on specimens exposed to severe environment. Prior to testing, surfaces of both confined and unconfined specimens were carefully leveled to remove irregularities, unevenness and to provide uniform load distribution.

Four linear variable displacement transducers (LVDTs) were mounted to measure the platen-to-platen as well as the lateral displacement of the specimen, as illustrated in Fig. 2.3. Specimens were tested under axial compression using a 3000 kN-capacity universal testing machine at an approximate rate of 0.2 mm/min in displacement controlled mode. The load was applied to entire section, i.e. pipe wall section for GC specimens, concrete section for USCC specimens and, concrete and pipe wall for GCSCC specimens.

Load and deflection values were monitored using a data acquisition system with a frequency capacity of 5 Hz. Corresponding axial strain values were then calculated in accordance with the deflection values received from LVDTs. After the termination of experiments, a portion of GRP tubes were cut in order to inspect the effect of chemicals on the inner face of GCSCC specimens, as shown in Fig. 2.4.
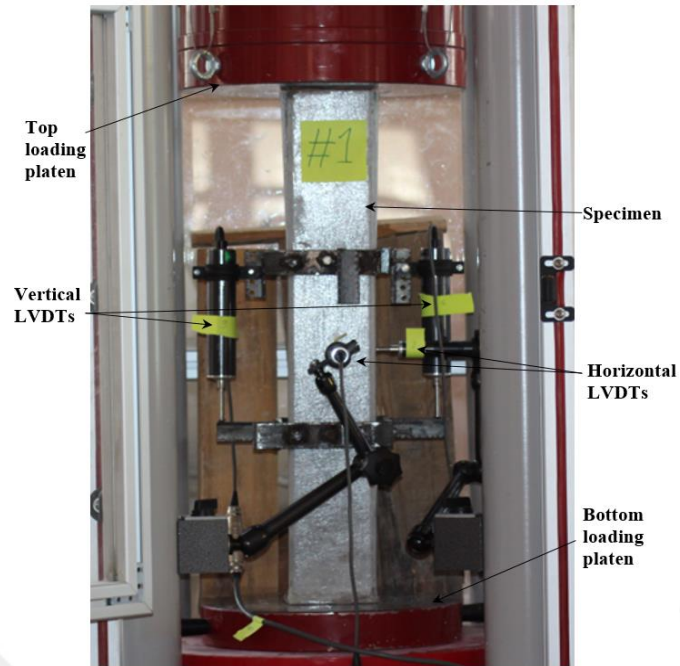
Figure 2.3 Test setup

2.5 Results and discussion

2.5.1 Surface degradation

Visual inspection ensured that a serious degradation was occurred on the surface layer of unconfined specimens due to the direct acidic exposure. On the other hand, for confined specimens, GRP pipe layer reduced the rate of attack significantly. Subsequently, no significant degradation was evident on the concrete surface and GRP pipe surface for confined specimens exposed to acid solution. Besides, confined specimens exhibited fairly ductile behavior as the concrete core continued to push towards the GRP wall, resulting in significant plastic deformation without disintegration.

Figure 2.4 Surface degradation after acid exposure

2.5.2 Failure modes

Fig. 2.5 a,b,c, shows the examples of specimens subjected to axial compression up to failure. As far as the confined specimens are concern, almost all specimens failed in shear through the corner regions of GRP pipes as well as the crushing of concrete. This type of failure is attributed to the fact that the fibers in GRP pipes are oriented towards the vertical direction and are not able to withstand the lateral dilation of concrete.

Figure 2.5 (a) Some of confined samples after testing

Figure 2.5 (b) Specimens after testing

Figure 2.5 (c) Specimens after testing

2.5.3 Load – strain behavior

Typically, axial compression of confined concrete results in lateral expansion of concrete core due to Poisson's effect, followed by a gradual development of passive pressure on confining material. Hence, two main factors play significant roles in the behavior of confined concrete: (1) radial stiffness of confining material (i.e. FRP, PVC or GRP), (2) lateral expansion of concrete core.

Fig. 2.6 a,b,c,d, shows the load strain curves for specimens without steel fiber. For confined specimens (GCSCC), load strain behavior is composed of three regions. The first region consists of linear ascending line and is similar to that of USCC specimens since the concrete core cracking is not reached to a level that allows the expansion of concrete. Hence, the confinement effect is not fully involved in the behavior in this region. In the second region, where nonlinear transition occurs around the peak load, an unstable expansion of concrete core is initiated due to significant cracking, resulted in an excessive drop in load. The behavior is similar for both confined and unconfined specimens in the first two regions. Finally, the contribution of confinement is fully engaged in the third region where a post-peak strain-softening was exhibited. In this region, slowly descending or ascending curve was observed depending on tube thickness. A smooth and consistent type of load-strain behavior was observed for all hollow section tubes, with a gradual post-peak reduction.
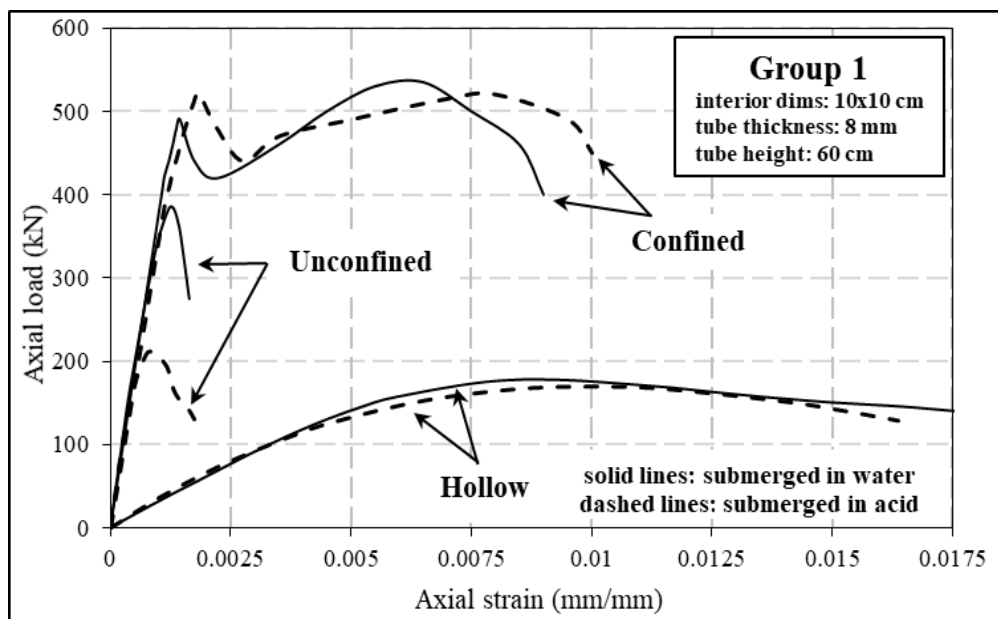

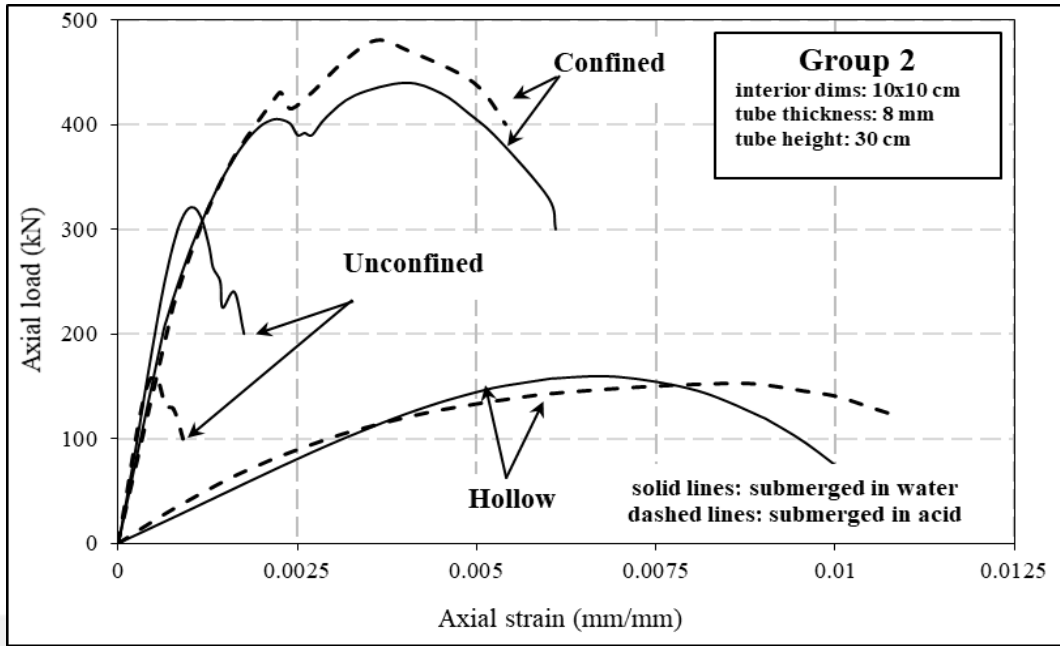**Figure 2.6 (a)** Load – strain curves for Group 1

41

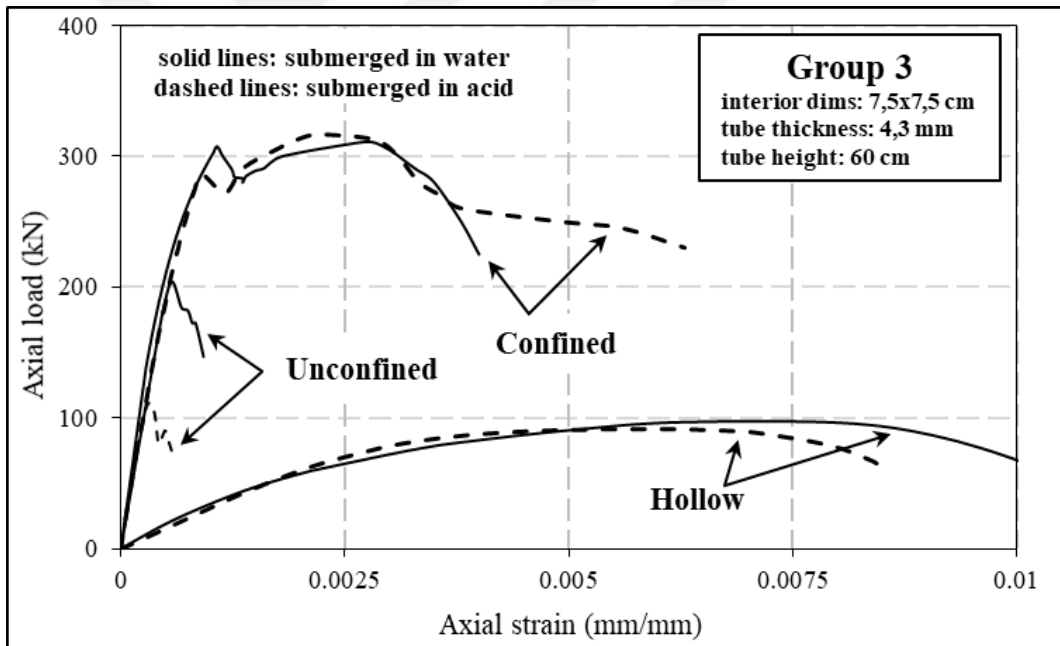**Figure 2.6 (b)** Load – strain curves for Group 2

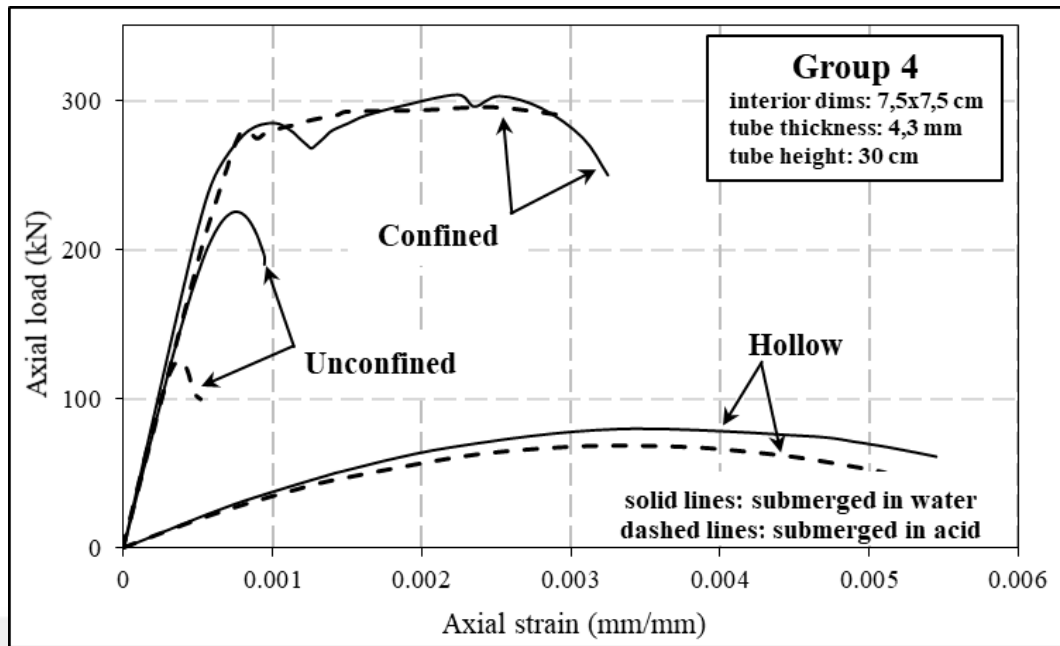**Figure 2.6 (c)** Load – strain curves for Group 3

Figure 2.6 (d) Load – strain curves for Group 4

2.5.4 Influence of confinement

Fig. 2.6 a,b,c,d, also compares the varying behavior of specimens exposed to acid or water. All confined specimens exhibited nearly the same behavior regardless of exposure type, due to the favorable role of GRP pipes in protecting the concrete core against acidic solution. Load carrying capacity of unconfined specimens in acid environment, however, was almost two times lower than their confined counterparts. Unconfined specimens end up facing a brittle failure whereas the confinement effect starts to engage in confined specimens followed by a straight plateau region. Significant post-peak strain-softening behavior and ductility enhancement is observed in all confined specimens.

2.5.5 Influence of steel fiber

Fig. 2.7 a,b,c,d, depicts the load-strain curves for confined and unconfined specimens. Only the specimens exposed to water were considered for plotting the curves since the effect of steel fibers on durability is anticipated to be negligible. Fig. 2.7 a,b,c,d, shows that, as far as the ascending portions of the curves are concerned, a slight increase in the peak load is evident for specimens with steel fibers, irrespective of the geometry and confinement. The effect of steel fibers on post-peak behavior is sound and the ductility is largely enhanced by SF contribution especially for the confined specimens.

43

This can be the result of higher energy absorption caused by the combined effect of confinement and steel fiber presence.
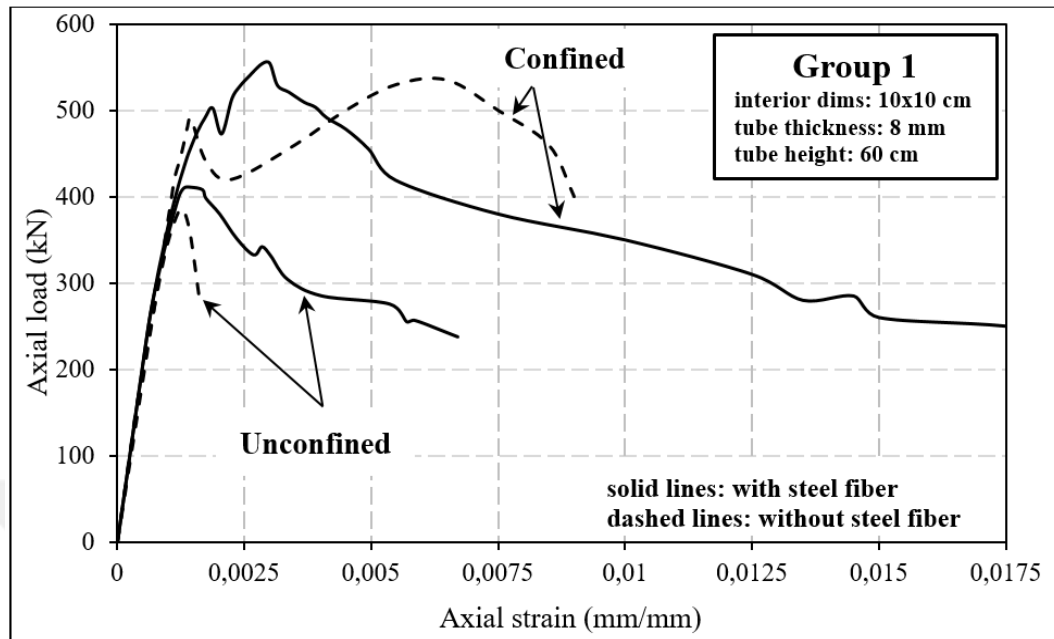
Figure 2.7 (a) Load – strain curves for Group 1
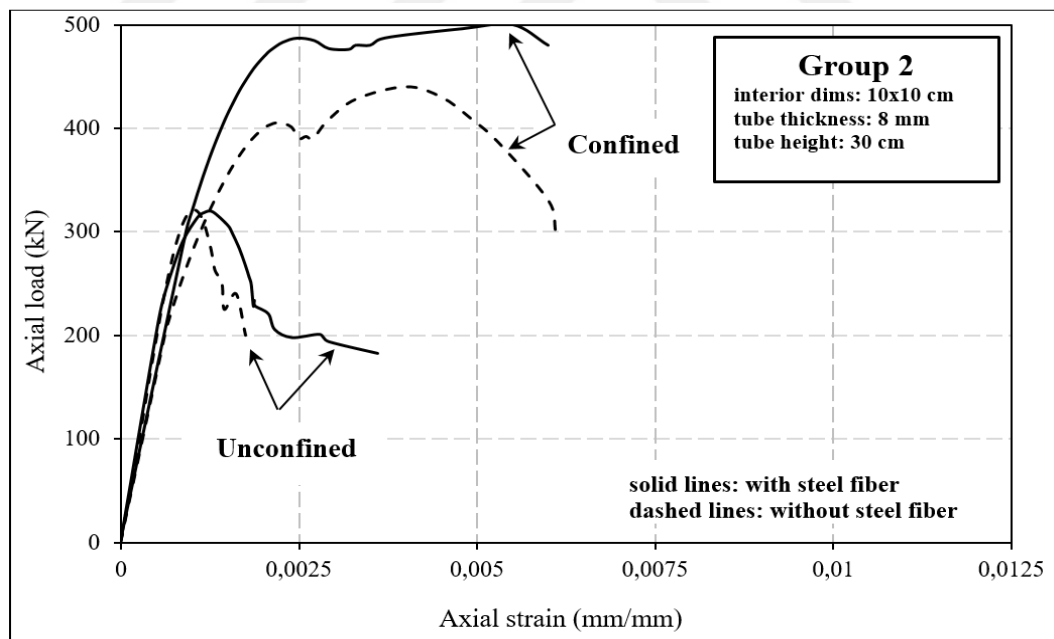
Figure 2.7 (b) Load – strain curves for Group 2
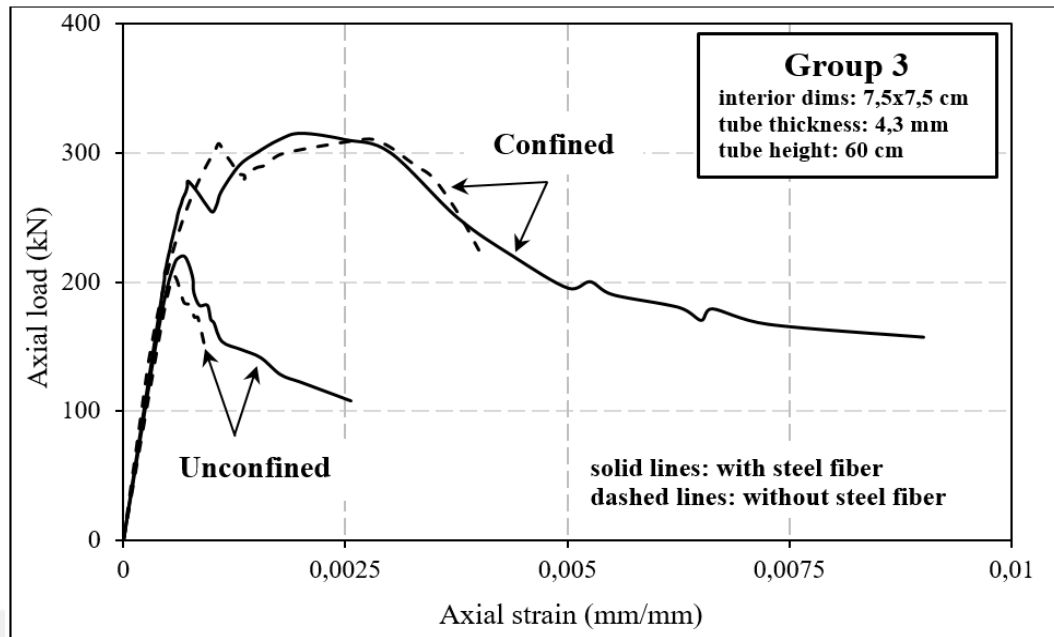
Figure 2.7 (c) Load – strain curves for Group 3
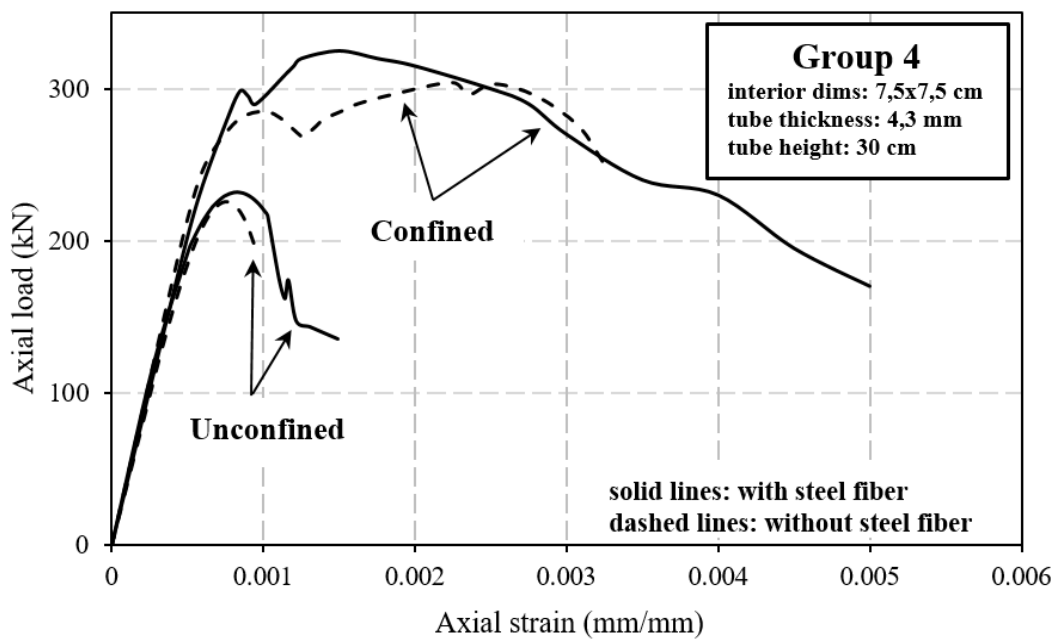
Figure 2.7 (d) Load – strain curves for Group 4

2.5.7 Influence of chemical exposure

Figure. 2.7 a,b,c,d, shows the load-strain behavior of confined, unconfined and hollow specimens exposed to water or acidic environment. It is evident from the figures that the exposure type had almost no effect both on the peak load and the post-peak behavior of confined and hollow samples, which clearly demonstrates the high

protection capacity of GRP pipes against severe attacks. On the other hand, the peak load of unconfined specimens exposed to acidic environment was almost half of the samples exposed to water. The stress-strain curves of the specimens and the detailed photos of the experimental work are presented in Appendix A.

CHAPTER 3

MECHANICAL CHARACTERIZATON AND DURABLTY OF HDPE-CONFINED SELF-COMPACTING CONCRETE TUBULAR COLUMNS EXPOSED TO SEVERE ENVIRONMENT

3.1 Introduction

Durability of reinforced concrete structures under severe environmental conditions is one of the major concerns in construction industry. Marine structures are mainly subjected to deterioration such as the corrosion of steel and salt crystallization-induced concrete corrosion. According to current estimations, billions of dollars are spent annually for the maintenance and/or the repairing of deteriorated marine structures worldwide. Due to this high cost, a great interest has been shown in alternative composite materials such as tubular columns/piles obtained by filling the FRP, PVC or HDPE pipes with concrete (Fanella & Naaman, 1985).

Reinforced concrete bridge piers, for instance, are deteriorated specifically by the degradation of splash/tidal zones and corrosion of steel rebar. Reasons for deterioration include wetting and drying, freeze-thaw cycles, high salt and/or acid contents and chloride penetration. Corrosion of steel reinforcement and/or salt crystallization damage at the splash/tidal zones are the main reasons for failure of structures in coastal areas where the groundwater with high salt and sulfate content is present. Numerous corrosion control systems (e.g. control permeability formwork, polymer wraps) have been applied to prevent these zones from deterioration. These methods, however, have disadvantages such as high cost and time-consuming (Gupta & Verma, 2016). Past studies have demonstrated that the confinement of concrete can enhance both the mechanical and long term performance of concrete, i.e., normal strength (440, 1996; Choi, Kim, Rhee, & Kang, 2014; Jiang, Ma, & Wu, 2014; Mander, Priestley, & Park, 1988; A Nanni, Norris, & Bradford, 1993; Antonio Nanni & Bradford, 1995) recycled aggregate concrete,

(440, 1996; ASTM C39/C39M-01, 2003; Feng, Cheng, Bai, & Ye, 2015; Gupta & Verma, 2016; Huang, Yu, Zhang, & Wang, 2017; Jamaluddin et al., 2017; Jiang et al., 2014; Mander et al., 1988; Ozbakkaloglu & Lim, 2013). Various forms of confinement types and materials (i.e. steel tubes, PVC tubes, FRP tubes or hybrid composite tubes) have been studied to investigate the effect of confining jackets on mechanical behavior and/or durability (Song & Hwang, 2004; Vincent &Ozbakkaloglu, 2013). HDPE-confined concrete tubes provide alternative composite system to solve durability problems of structures exposed to aggressive substances. HDPE confinement provides isolation for concrete from aggressive substances such as sulfate and/or acid contents, prevent the penetration of chloride ions into concrete and, thus, protect steel reinforcement and concrete from corrosion-induced damage. Moreover, HDPE pipes can function as natural formwork that allows the concrete curing even in bad conditions. Therefore, the core concrete can perform better even under severe conditions such as in bridge piers, columns and other type of structures in marine and saline environments. The main objective is to provide extended service life and reduce the maintenance cost of such structures.

Although a number of studies have investigated the mechanical behavior and durability of FRP-confined and/or PVC-confined normal concrete (Zaghi, Saiidi, & Mirmiran, 2012), an extensive investigation on the HDPE-confined concrete tubular systems is not present. Current study reports the results of an experimental work in which the mechanical characterization and short term durability of self-compacting concrete (SCC) filled HDPE pipes were investigated for the first time in literature. Investigated parameters were the influences of HDPE confinement, tube thickness, steel fiber addition in SCC, and chemical attacks (i.e., sulfate or acid exposure).

3.2 Experimental program

A total of fourty-five specimens were manufactured, as stated in Table 3.1, cured and tested within the experimental program. Out of fourty-five samples, thirty-six of them were filled with SCC while remaining eight specimens were kept as hollow tubes. SCC-filled specimens were divided into three subgroups in accordance with their diameters and thicknesses.

A HDPE tube for each specimen was cut to required length and affixed at one end with silicon glue to a wood board to avoid the water and concrete seepage, as shown in Fig.

3.1 (a) and Fig. 3.1 (b), respectively. This combination was used as a stay-in-place formwork before casting the confined and unconfined specimens. For unconfined specimens, HDPE tube was removed after 24 hours of hardening period (Fig. 3.1 (c,d)). All cast specimens including quality control reference cylinders according to ASTM C39-12 were kept in the water tank at 20°C for 28 days to assure required curing conditions.

The cylinder specimens were designated according to confinement material (H for hollow section, HSCC for HDPE tube + SCC and USCC for unconfined SCC cylinders), group number (G1, G2 and G3), steel fiber percentage (0% or 1%) and exposure type (W, A or S for water, acid or sulfate, respectively). For instance, HSCC-F3-0%-A addresses the SCC filled HDPE tube specimen of the group G3 (with inside diameter of 14 mm), containing no steel fiber and exposed to acidic solution.
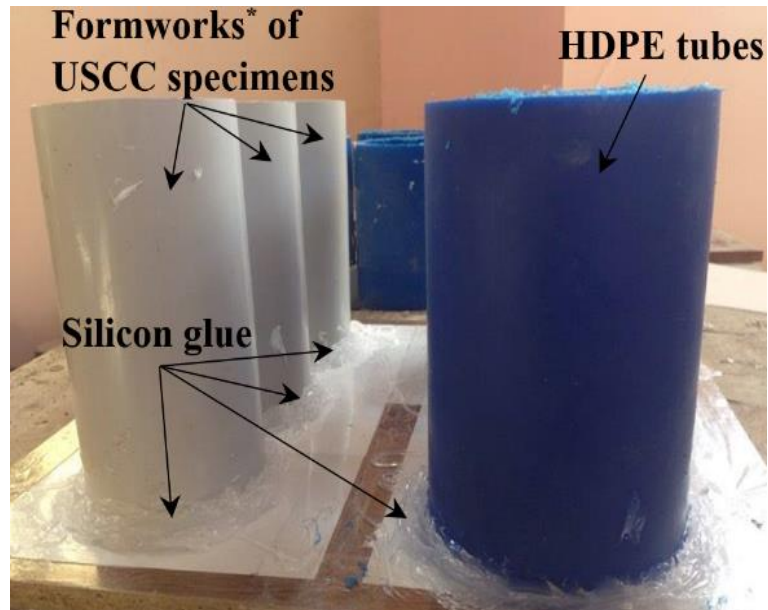

Figure 3.1 (a) Cutting of HDPE tube

Figure 3.1 (b) USCC formworks and HDPE tubes before casting*Removed after hardening of concrete

Figure 3.1 (c) Removal of formworks after hardening of SCC for unconfined specimens
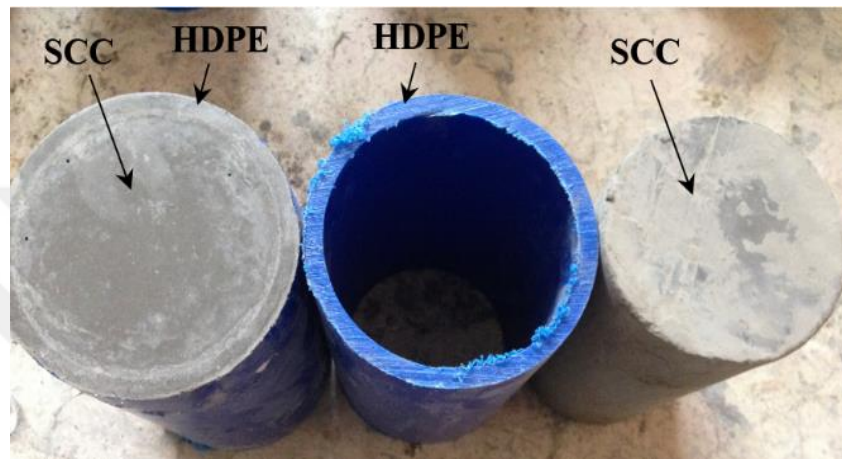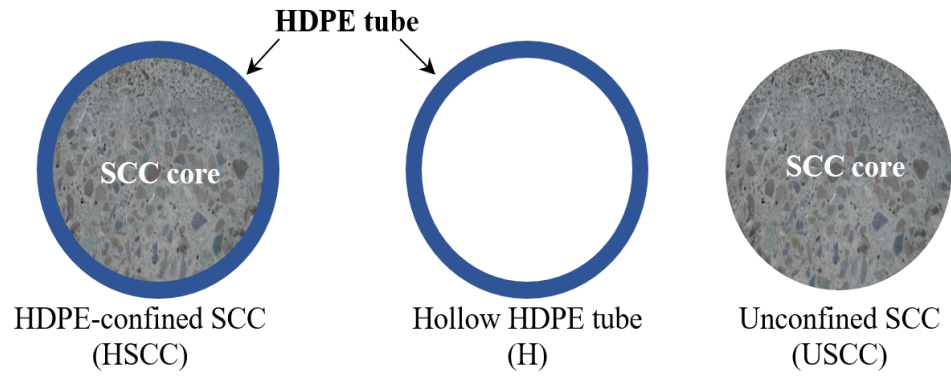
Figure 3.1 (d) Preparation of test specimens

3.3 Material properties

3.3.1 Self-compacting concrete (SCC)

Self-compacting concrete mix with an unconfined compressive strength of 32 MPa at 28 days was considered for the fabrication of all unconfined and confined cylinder specimens. Portland cement (ASTM type I) was used as binder. Local sand with a fineness modulus of 2.6 mm and dry crushed limestone with a maximum size of 12 mm was used as coarse aggregate. Three cubic and three cylinder samples were cast and cured under the same curing conditions. These samples were then tested as per ASTM standards to ensure the required compressive strength. Table 3.2 presents the concrete proportions used in the fabrication of fresh SCC with and without steel fibers. As stated in Table 3.3, all SCC requirements as per EFNARC standard were found satisfactory. The compressive and tensile strength results were obtained by averaging the outcomes of three tests for cylinder and cube samples. Quality control specimens were also cast from the same SCC mix.

Table 3.1 Test matrix and designation of specimens

	Group	Exposure type	Steel fiber ratio (%)	Specimen designation
HDPE-Confined SCC (HSCC)	G1	Water	0.0	HSCC-G1-0%-W
		Water	1.0	HSCC-G1-1%-W
		Acid	0.0	HSCC-G1-0%-A
		Acid	1.0	HSCC-G1-1%-A
		Sulfate	0.0	HSCC-G1-0%-S
		Sulfate	1.0	HSCC-G1-1%-S
	G2	Water	0.0	HSCC-G2-0%-W
		Water	1.0	HSCC-G2-1%-W
		Acid	0.0	HSCC-G2-0%-A
		Acid	1.0	HSCC-G2-1%-A
		Sulfate	0.0	HSCC-G2-0%-S
		Sulfate	1.0	HSCC-G2-1%-S
	G3	Water	0.0	HSCC-G3-0%-W
		Water	1.0	HSCC-G3-1%-W
		Acid	0.0	HSCC-G3-0%-A
		Acid	1.0	HSCC-G3-1%-A
		Sulfate	0.0	HSCC-G3-0%-S
		Sulfate	1.0	HSCC-G3-1%-S
Unconfined SCC (USCC)	G1	Water	0.0	USCC-G1-0%-W
		Water	1.0	USCC-G1-1%-W
		Acid	0.0	USCC-G1-0%-A
		Acid	1.0	USCC-G1-1%-A
		Sulfate	0.0	USCC-G1-0%-S
		Sulfate	1.0	USCC-G1-1%-S
	G2	Water	0.0	USCC-G2-0%-W
		Water	1.0	USCC-G2-1%-W
		Acid	0.0	USCC-G2-0%-A
		Acid	1.0	USCC-G2-1%-A
		Sulfate	0.0	USCC-G2-0%-S
		Sulfate	1.0	USCC-G2-1%-S
	G3	Water	0.0	USCC-G3-0%-W
		Water	1.0	USCC-G3-1%-W
		Acid	0.0	USCC-G3-0%-A
		Acid	1.0	USCC-G3-1%-A
		Sulfate	0.0	USCC-G3-0%-S
		Sulfate	1.0	USCC-G3-1%-S
	G1	Water	-	H-G1-W

		Acid	-	H-G1-A
		Sulfate	-	H-G1-S
	G2	Water	-	H-G2-W
Hollow HDPE tube (H)		Acid	-	H-G2-A
		Sulfate	-	H-G2-S
	G3	Water	-	H-G3-W
		Acid	-	H-G3-A
		Sulfate	-	H-G3-S

Table 3.2 SCC mix proportions

Material	Value (kg/m3)	
	without SF (0%)	with SF (1%)
Gravel	730	1005
Sand	900	1425
Portland cement	300	450
Fly Ash Admixture	250	412.5
Water	200	255
Super plasticizer	4	8.625
Steel Fiber	-	58.85

Table 3.3 Fresh and hardened SCC properties

Parameter	Value	Limits (EFNARC)
Air content (%)		
Slump (mm)	650	520-700
Unit weight (kg/m^3)		
V-funnel flow (s)	8	≤ 12
T-50 (s)	4	2-5
Blocking ratio (H$_2$/H$_1$)	0.9	0.8-1
Splitting tensile strength[*] (MPa)	3.21	-
Compressive strength[*] (MPa)	32	-

3.3.2 High-density polyethylene (HDPE) pipes

In this study, high-density polyethylene (HDPE) pipe was selected as confinement material. HDPE pipes demonstrate several advantages such as anti-corrosion characteristics, usability against mechanical damage caused by severe environment and long service life of more than 50 years. In addition, it can provide suitable curing

53

conditions for concrete due to low thermal conductivity. Table 3.4 shows the physical properties of HDPE pipes. Three types of HDPE pipe sizes were used as given in Table 3.5.

Table 3.4 Physical properties of HDPE

Parameter	Value
Class	PE 40
Density	0.945-0.965 g/cm3
Breaking elongation	min 350%
Elastic modulus	>600 MPa
Ultimate tensile strength	26 MPa
Working temperature	min. -80 °C, max. 100 °C
Thermal conductivity	0.29 kcal/m hr °C
Service life	>50 years

Table 3.5 Dimension of HDPE

Group	Inside diameter mm	Height mm	Thickness mm
G1	140	280	10
G2	120	240	10
G3	110	220	13

3.3.3 Steel fiber

The addition of steel fiber in concrete leads to a number of enhancements in the behavior of structural member. In compression, steel fibers do not significantly affect the ascending curve of the compressive stress-strain response. However, they cause the descending post-peak response curve to decline in a shallower fashion than the curve of plain concrete, resulting in an increased ductility and toughness. The researchers observed an enhancement of only 15% in compression. However, the peak strain increases significantly with the provision of steel fibers.

On the other hand, the addition of steel fibers induces a much more noticeable effect on the tensile behavior. The strain softening behavior is observed in the concrete with typical fiber volume content. This results in the composite having greater ductility and energy absorption capabilities than the plain concrete. In addition, because the fibers bridge the cracks in the composite and aid in the transfer of forces across the cracks, crack widths are less than those in plain concrete. If the reinforcing bars are present,

multiple cracks can form even for a strain-softening material. As compared to the plain concrete, there will be more cracks at shorter spacing and with smaller widths.

Steel hooked fibers (SF), shown in Fig. 3.2, were added in the self-compacting concrete mix to see the effect of SF on the load strain behavior of unconfined and HDPE-confined SCC cylinders under axial compression. Table 3.6 lists the properties of SF used in this study.

Figure 3.2 Steel fibers

Table 3.6 Steel fiber properties

Fiber type	Length mm	Diameter mm	Density (g/cm³)	Aspect ratio	Tensile strength MPa
Steel hooked fiber	50.3	0.75	7.8	67	1100

3.4 Testing procedure

Test specimens were submerged in water, acid or sulfate environments separately, in accordance with their corresponding group. Specimens were removed from the tanks and prepared for compression tests after 2 months of submergence in severe environment. Prior to axial compression tests, sulfur capping was applied to both ends of each confined and unconfined specimen to remove irregularities, unevenness, and to avoid direct contact of loading platens with the specimen.

Two linear variable displacement transducers (LVDTs) were mounted to measure the platen-to-platen displacement of the specimen, as illustrated in Fig. 3.3 Specimens were tested under axial compression using a 3000 kN-capacity universal testing machine at an approximate rate of 1 mm/min in displacement controlled mode. The load was applied to entire section, i.e. pipe wall section for H specimens, concrete section for USCC specimens and, concrete and pipe wall for HSCC specimens.
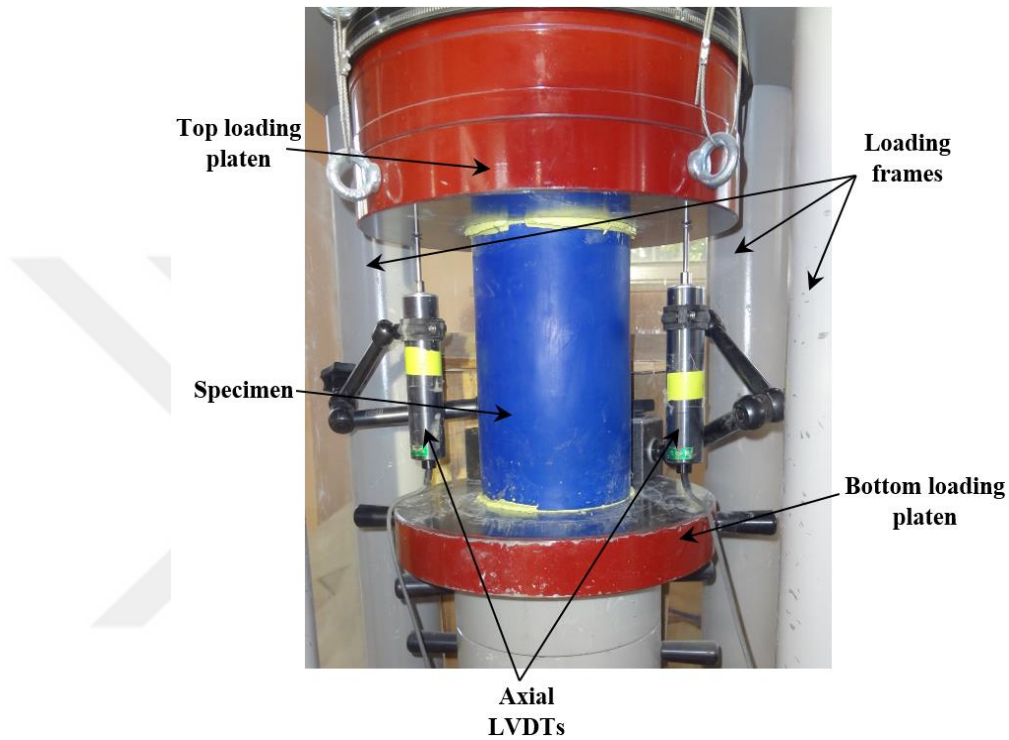

Figure 3.3 Test setup

A data acquisition system with a frequency capacity of 5 Hz was utilized to monitor the load values collected from load cell and the deflections received from LVDTs. Corresponding axial strain values were then calculated in accordance with the deflection values received from LVDTs. After the termination of experiments, a portion of HDPE tubes were cut in order to inspect the effect of chemicals on the inner face of HSCC specimens, as shown in Fig. 3.10.

3.5 Results and discussion

3.5.1 Failure modes

Two types of failure patterns (shear or drum type) was observed in HSCC specimens as illustrated in Fig. 3.4 (a) and Fig. 3.4 (b). In shear failure, core concrete was damaged with shear cracks whose direction can be judged by the appearance of failed specimen. By contrast, in drum type failure, cracks in core concrete were propagated towards all sections of specimen, which resulted in a drum type of appearance because of strong confinement effect. Besides, in both failure type, HSCC specimens exhibited significantly ductile behavior as the concrete core continued to push towards the HDPE wall, resulting in significant plastic deformation without disintegration. Non-uniform dilation of concrete core in shear type failure caused local bulging as shown in Fig. 3.4 (a). HSCC specimens with steel fibers showed a larger lateral dilation as compared to their counterparts without steel fibers. USCC specimens without steel fibers exhibited brittle type of failure as illustrated in Fig. 3.4 (c). Deep cracks with a thickness of up to 3 mm were observed in USCC specimens without steel fibers. By contrast, a relatively ductile failure type with thinner cracks was observed and the integrity was remained in USCC specimens with steel fibers, which can be attributed to the contribution of steel fibers in resisting the stress after the sudden failure of concrete core.

All hollow HDPE tube (H) specimens under axial compression showed an extremely plastic deformation with a non-regular elliptical shape as shown in Fig. 3.4 (d).

Figure 3.4 (a) Shear type failure (HSCC)

Figure 3.4 (b) Drum type failure (HSCC)

Figure 3.4 (c) Failure types of USCC specimens

Figure 3.4 (d) Failure type of hollow (H) specimens

3.5.2 Load – strain behavior

Typically, axial compression of confined concrete results in lateral expansion of concrete core due to Poisson's effect, followed by a gradual development of passive pressure on confining material. Hence, two main factors play significant roles in the behavior of confined concrete: (1) radial stiffness of confining material (i.e. FRP, PVC or HDPE), (2) lateral expansion of concrete core. Fig. 3.5 (a-j), shows load-strain curves for all cylinder specimens. Curves are categorized according to confinement type and group, i.e. HSCC, USCC, H in horizontal direction and G1, G2, G3 in vertical direction, respectively. Load-strain behavior of HSCC specimens is composed of three regions. The first region consists of linear ascending line and is similar to that of USCC specimens since the concrete core cracking is not reached to a level that allows the expansion of concrete. Hence, the confinement effect is not fully involved in the behavior in this region. In the second region, where nonlinear transition occurs around the peak load, an unstable expansion of concrete core is initiated due to significant cracking, resulted in an excessive drop in load. The behavior is similar for both confined and unconfined specimens in the first two regions. Finally, the contribution of confinement is fully engaged in the third region where a post-peak strain-softening was exhibited. In this region, slowly descending or ascending curve was observed depending on tube thickness. A smooth and consistent type of load-strain behavior was observed for all hollow section tubes, with a gradual post-peak reduction.
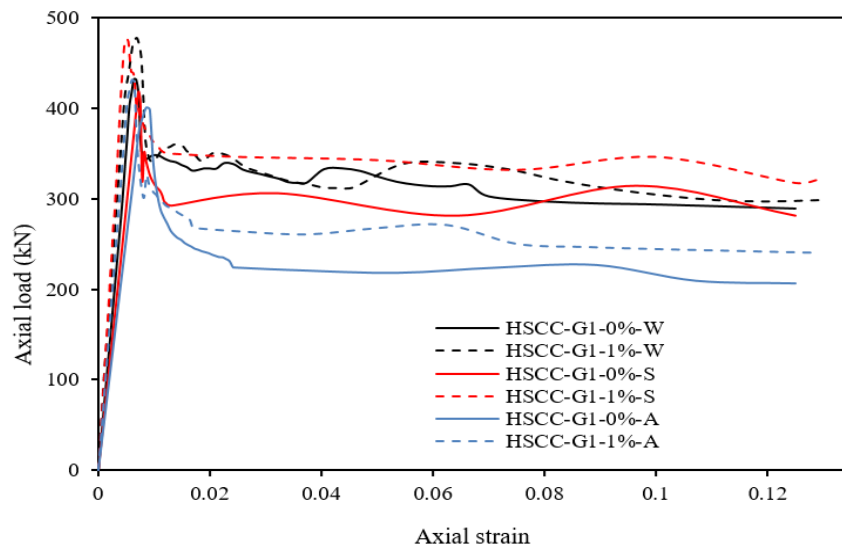

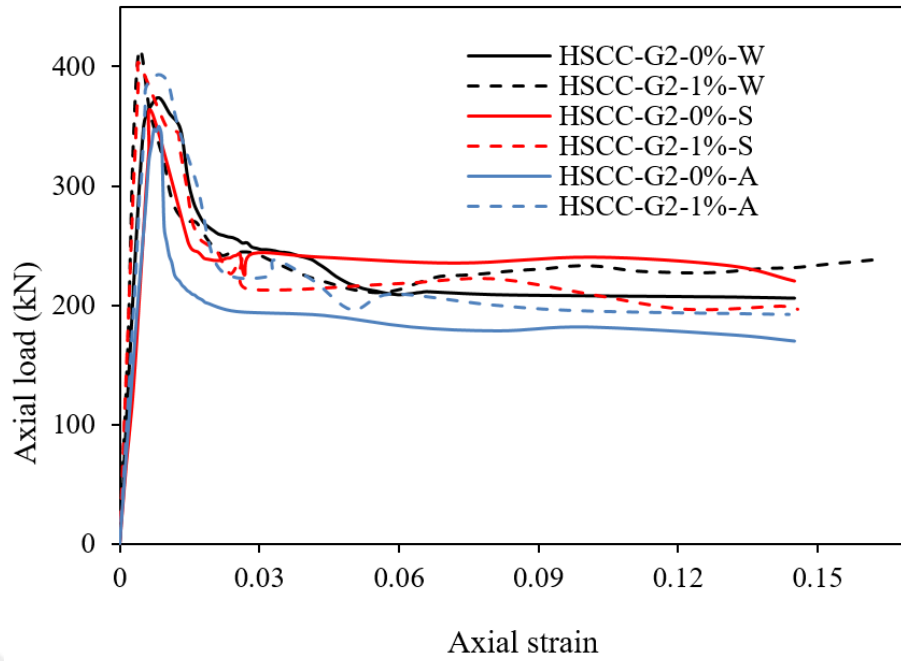**Figure 3.5 (a)** Load – strain graphs , Confined (HSCC) specimens , first geometric

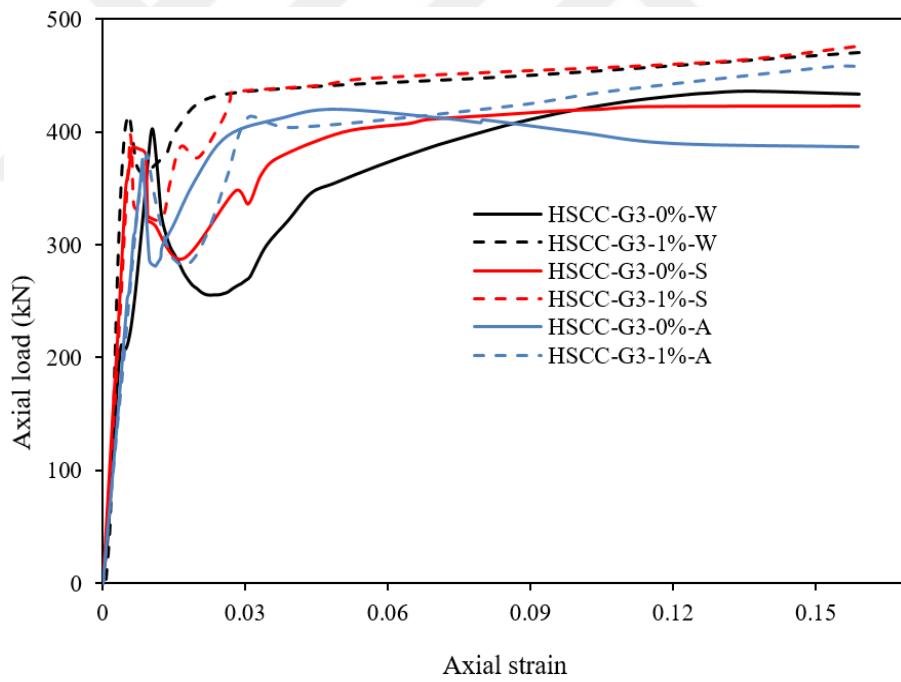**Figure 3.5 (b)** Load – strain graphs , Confined (HSCC) specimens , second geometric

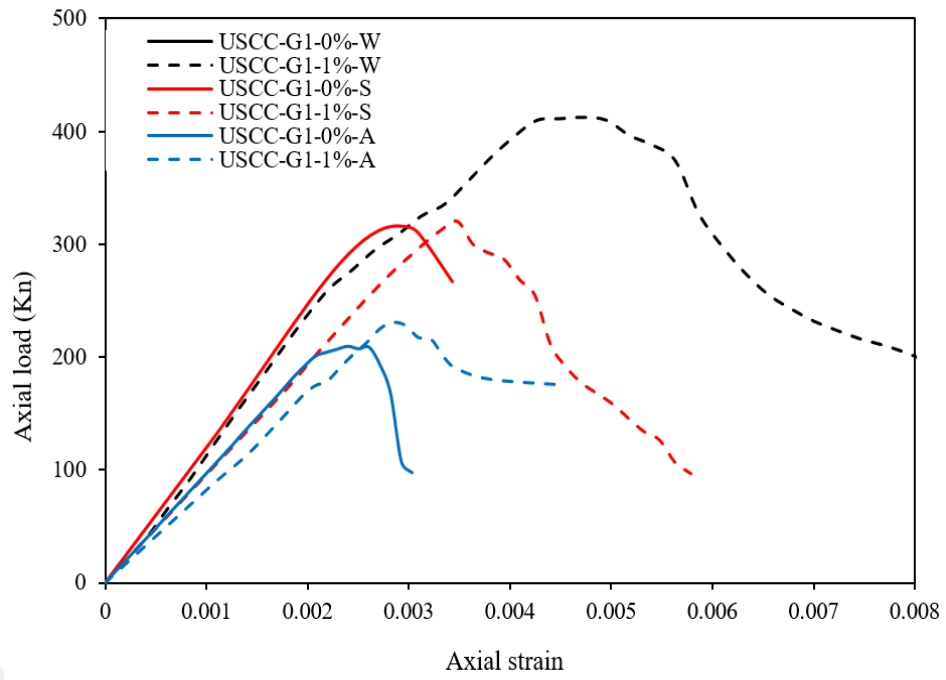**Figure 3.5 (c)** Load – strain graphs , Confined (HSCC) specimens , third geometric

61

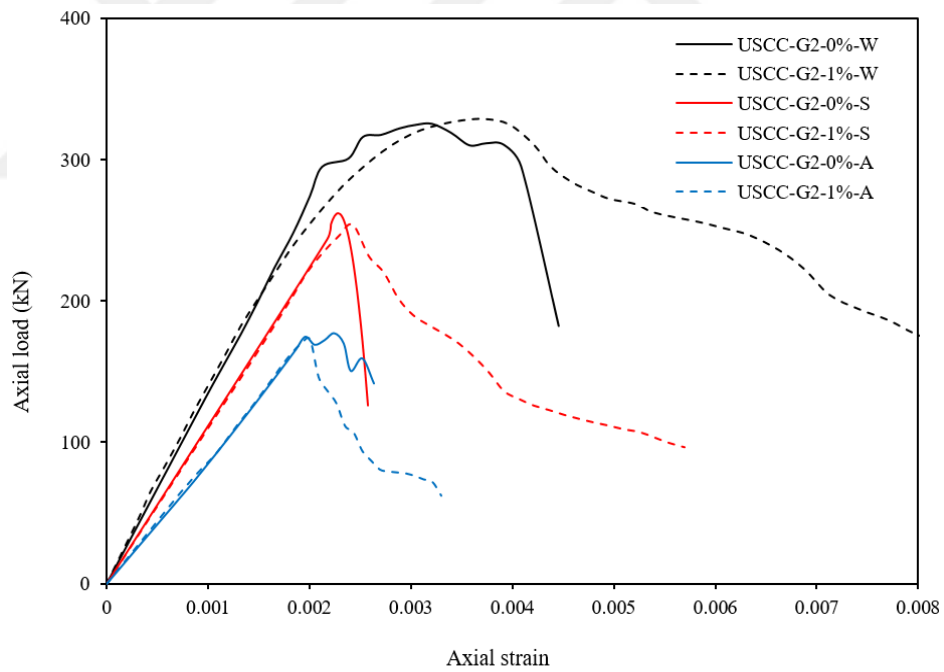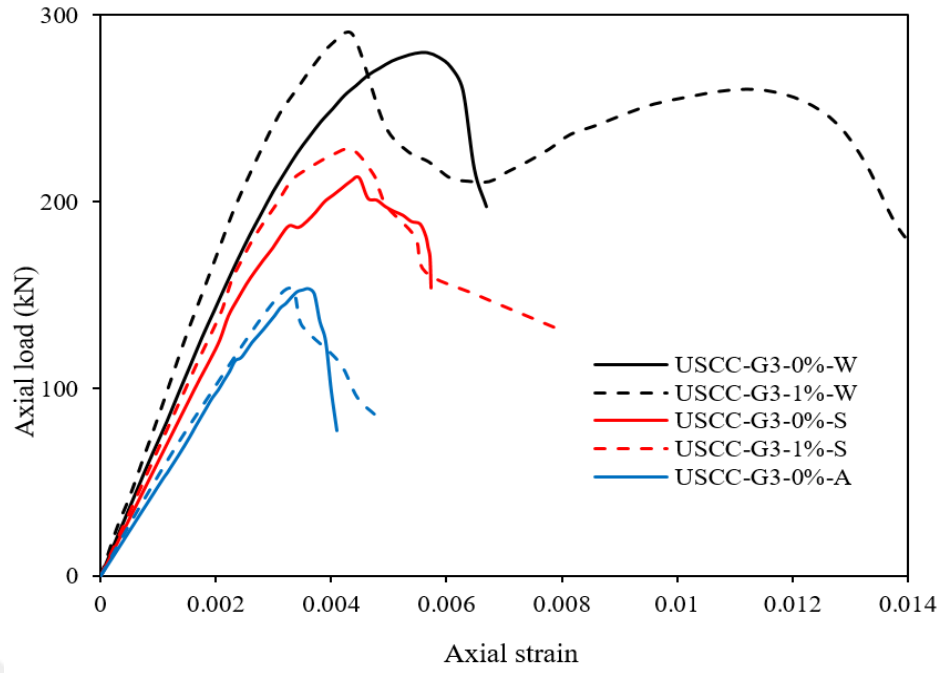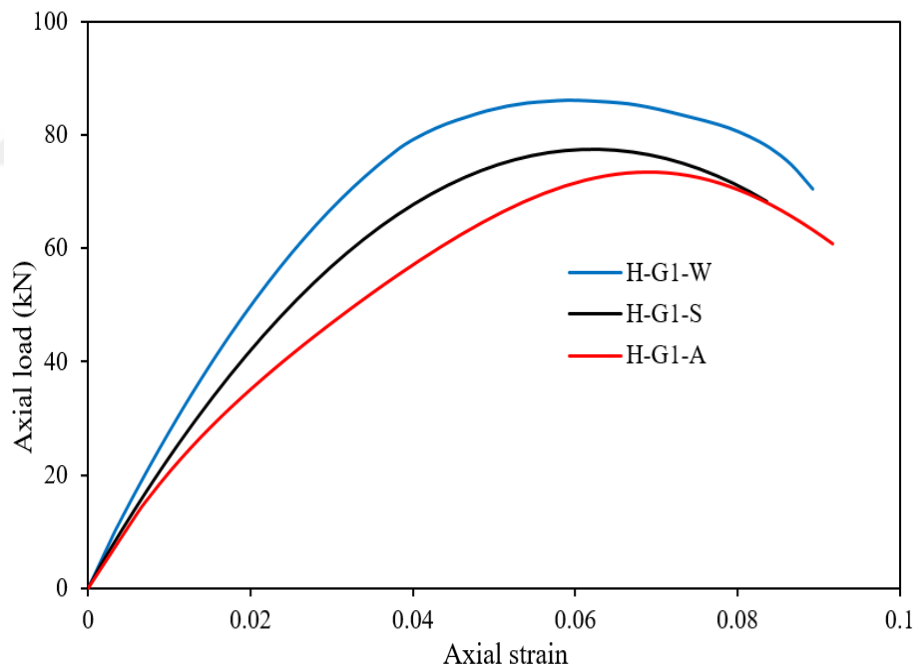**Figure 3.5 (d)** Load – strain graphs , Unconfined (USCC) specimens, first geometric

Figure 3.5 (e) Load – strain graphs , Unconfined (USCC) specimens, second geometric

Figure 3.5 (f) Load – strain graphs , Unconfined (USCC) specimens, third geometric

Figure 3.5 (g) Load – strain graphs , Hollow (H) specimens, first geometric

63
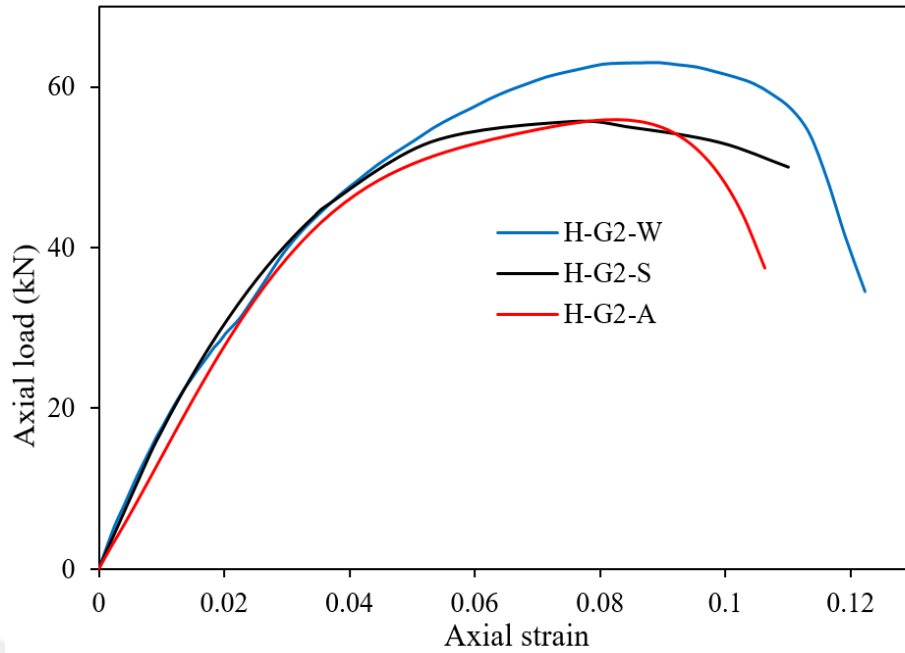
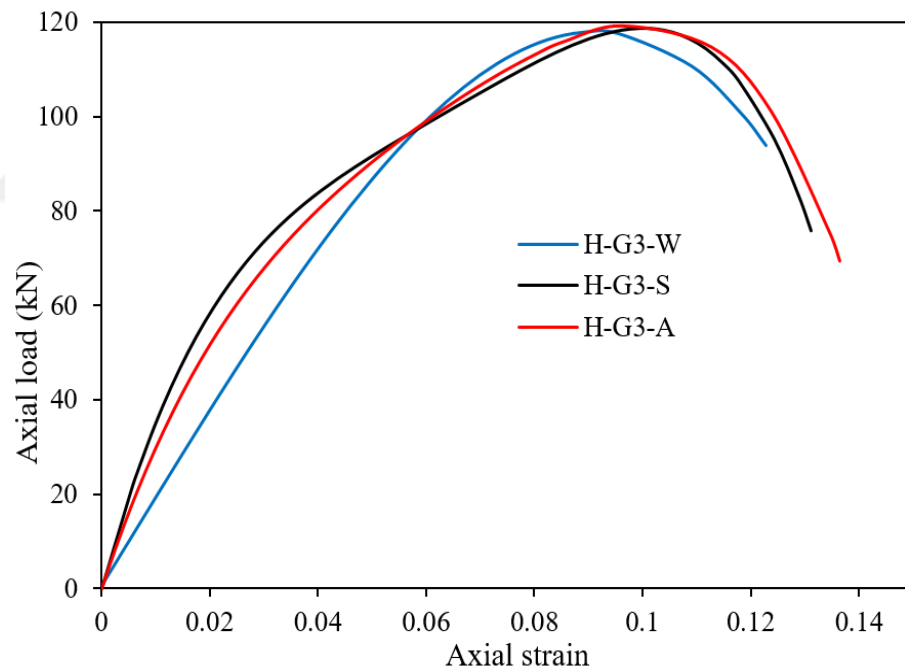**Figure 3.5 (h)** Load – strain graphs , Hollow (H) specimens, second geometric

Figure 3.5 (j) Load – strain graphs , Hollow (H) specimens, third geometric

3.5.3 Influence of confinement

Fig. 3.6 (a-c), compares the axial load-strain curves for HSCC, USCC and hollow specimens after exposure to water, sulfate or acid. Unconfined specimen exhibits a similar behavior up to peak load with a slightly higher slope and lower peak load. After the peak load, a sudden load reduction is observed in both HSCC and USCC specimens

due to the initiation of excessive cracking in concrete core. USCC specimens end up facing a brittle failure whereas the confinement effect starts to engage in HSCC specimens followed by a straight plateau region. Significant post-peak strain-softening behavior and ductility enhancement is observed in HSCC specimens as illustrated in Fig. 3.6 (a-c).
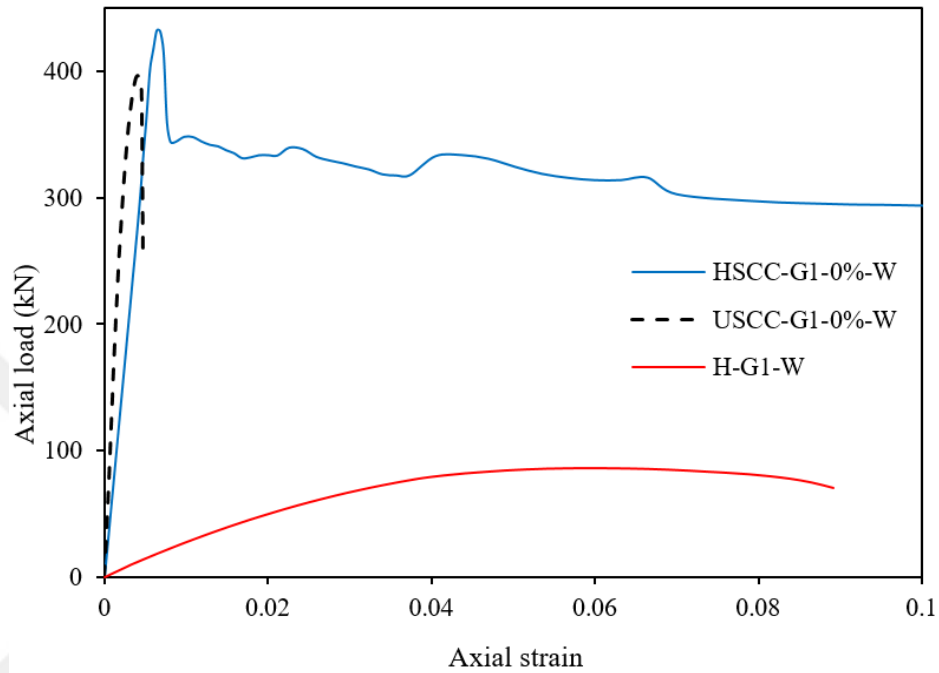

Figure 3.6 (a) Load-strain behavior of confined (HSCC), unconfined (USCC) and tube (H) specimens, after exposure to water
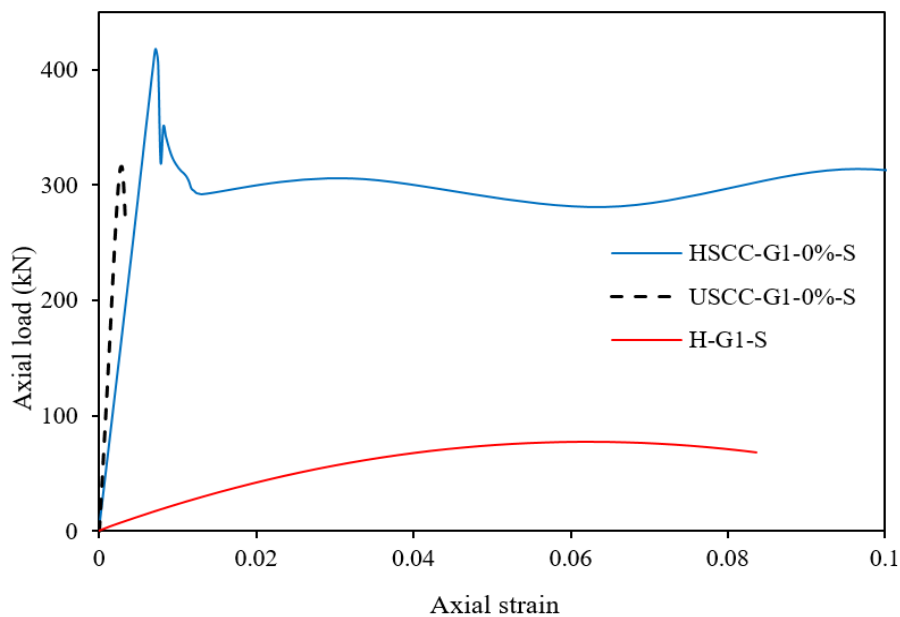

Figure 3.6 (b) Load-strain behavior of confined (HSCC), unconfined (USCC) and tube (H) specimens, after exposure to sulfate
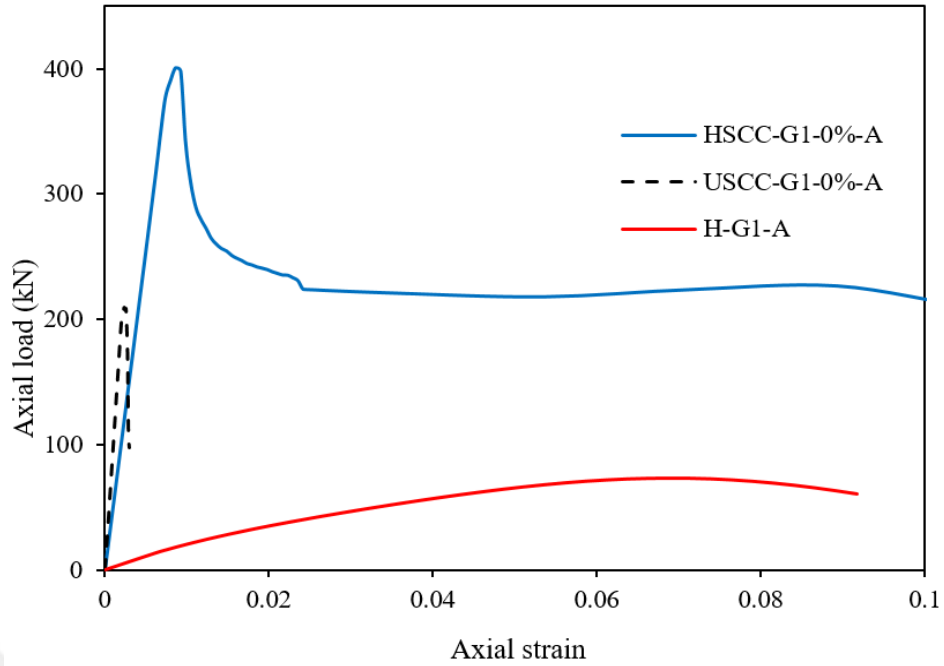
Figure 3.6 (c) Load-strain behavior of confined (HSCC), unconfined (USCC) and tube (H) specimens, after exposure to acid

3.5.4 Influence of thickness

As can be observed in Fig. 3.7 (a), post-peak curves for HSCC-G1-0%-W and HSCC-G2-0%-W specimens (both with a thickness of 10 mm) tend to decrease almost constantly up to a point after which the curves descend with approximately constant slope. HSCC-G3-0%-W specimen (with a thickness of 13 mm), on the other hand, demonstrate an entirely different post-peak behavior in which the curve starts ascending as opposed to the behavior of specimens with thinner tube.

Also, a significant effect of thickness was observed on the behavior of hollow tubes under axial compression as can be seen in Fig. 3.7 (b). H-G3-W specimen with a thickness of 13 mm demonstrated a higher load capacity as compared to its 10-mm-thick H-G2-W companion, despite both specimens have close inside diameter and height values. Hence, the higher axial load capacity of H-G3-W is attributable not only to size effect, but it is mainly dependent on larger thickness.
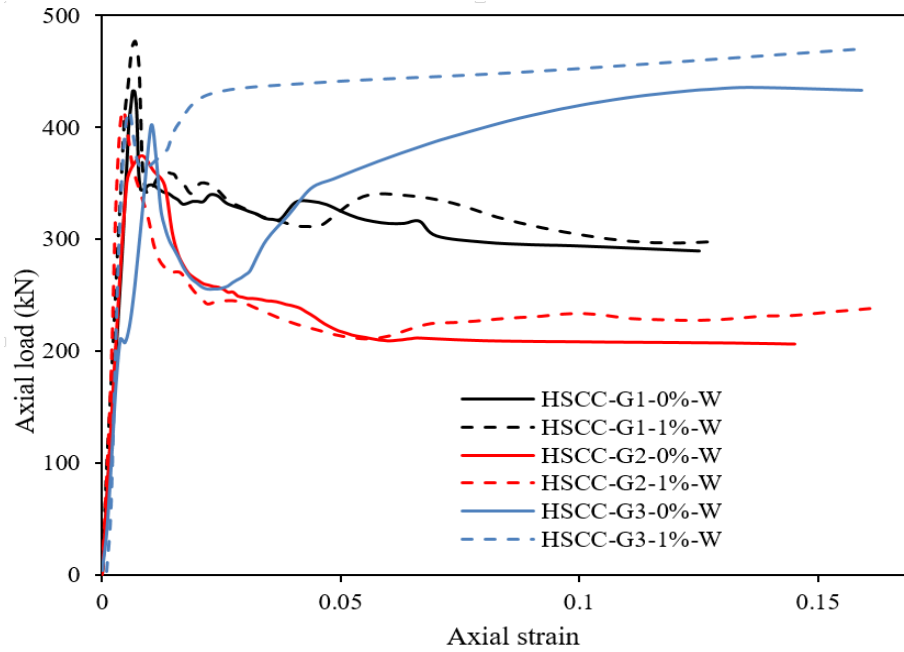
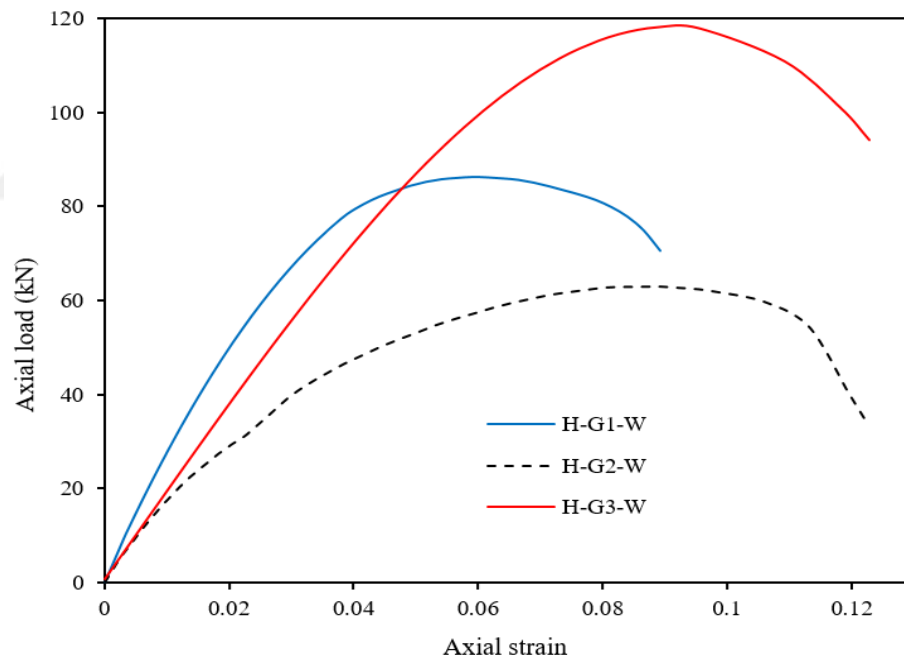**Figure 3.7 (a)** Influence of tube thickness, Confined specimens

Figure 3.7 (b) Influence of tube thickness, Hollow (H) specimens

3.5.5 Influence of steel fiber

Fig. 3.8 (a) is the narrowed version of Fig. 3.7 (a), in which the strain portion between $0 - 0.03$ is considered to see the effect of SF in more detail. Fig. 3.8 (a) shows that, considering the first region of load-strain curves, the provision of steel fibers in HSCC specimens led to an increased slope up to the peak load irrespective of geometry and

a slight increase in the peak load is also evident for specimens with steel fibers. For second and third regions, existence of steel fibers seems to have minor effect except for Group 3 HSCC specimen. As opposed to companion without SF, HSCC-G3-1%-W specimen demonstrates entirely different post-peak behavior (Fig. 3.7 (a)) in which the load started increasing up to a point where the slope was lowered yet continued constantly until failure. This can be the result of higher energy absorption caused by the combined effect of thicker confinement and steel fiber presence. Fig. 3.8 (b) compares the effect of steel fibers on unconfined specimens with various geometry. Provision of steel fibers appears to have a significant effect on the ductility of USCC specimens as the sudden rupture is prevented by steel fibers.
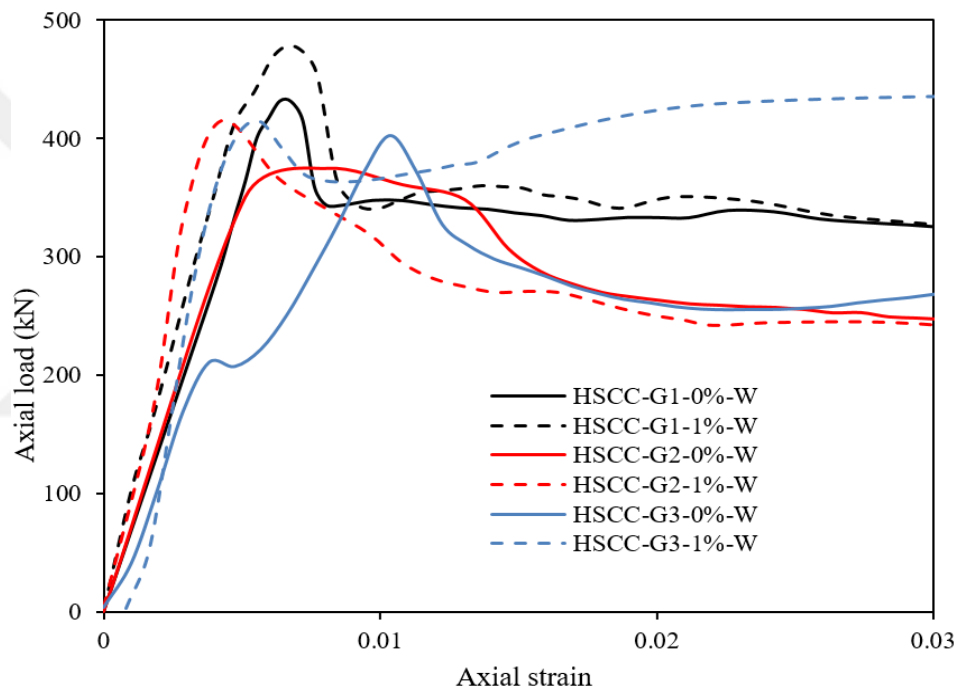

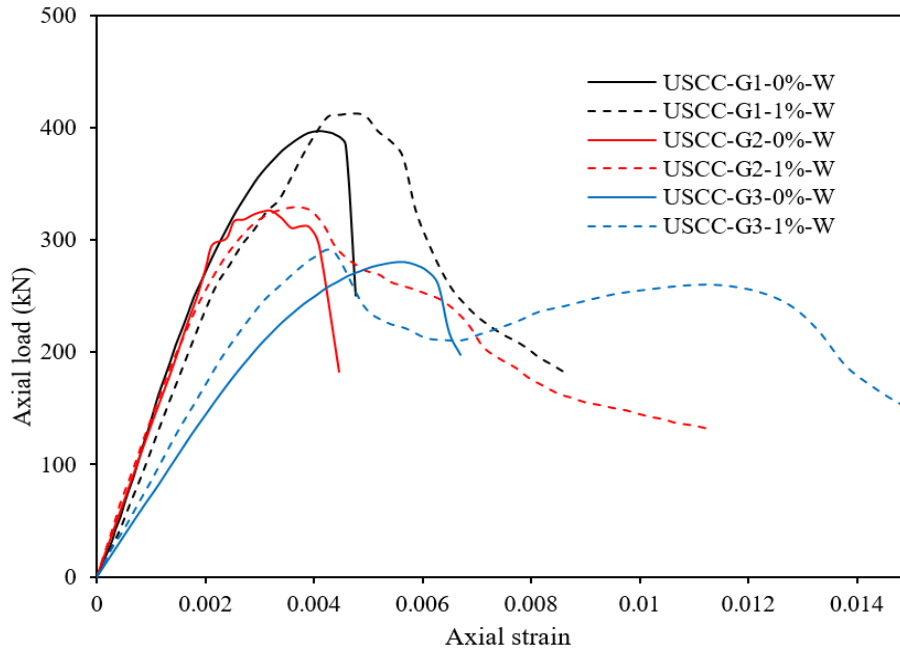**Figure 3.8 (a)** Influence of steel fiber, Confined specimens

Figure 3.8 (b) Influence of steel fiber, Unconfined specimens

3.5.6 Influence of chemical exposure

Fig. 3.9 shows the tested USCC specimens after submergence in water, sulfate and acid environment. No significant surface degradation was evident in USCC specimens submerged in water or sulfate beside these specimens during the test, visible cracks usually started from the top section of the cylinder. They spread with increased compressive load. No definite sign was noticed before the collapse, it happened in a twinkling, meanwhile cracks enlarged and spread downwards rapidly.

. Conversely, acid attack caused significant surface degradation of USCC specimens as shown in Fig. 3.9. HSCC specimens, however, suffered less from chemical environment as compared to unconfined counterparts owing to the protection provided by HDPE tube confinement as shown in Fig. 3.10. Top and bottom faces of confined and unconfined specimens were affected equally by chemical environment. Fig. 3.9 shows that there was no strong bond between sulfur and concrete and this was due to the models were not completely dry, which in turn led to a week connection between sulfur and concrete.

Fig. 3.11 (a) and Fig. 3.11 (b) compare the axial load-strain behavior of confined and unconfined specimens submerged in water, sulfate or acid. Since the Group 1 and Group 2 specimens had the same confinement thickness, Group 2 and Group 3

specimens were selected for comparison to see the effect of thickness in preventing the concrete core from acid or sulfate attack. It is evident from Fig. 3.11 that, irrespective of the concrete core geometry, USCC specimens largely effected by chemical solution. Load carrying performance of USCC specimens was exhibited the lowest by specimen subjected to acid exposure, and then the specimen subjected sulfate environment, and finally the water environment, respectively (Fig. 3.11 (b) and (d)). HSCC-G2-0%-W specimen submerged in water was found to have highest load carrying capacity. Sulfate attacked HSCC-G2-0%-S and acid attacked HSCC-G2-0%-A specimens, on the other hand, exhibited similar behavior up to peak load (Fig. 3.11 (b)). Group 3 HSCC specimens showed less complexity and similar behavior with higher peak load for all three types of exposure (Fig. 3.11 (c) and (d)). This is due to the fact that Group 3 HSCC specimens had thicker confining tube, thereby the higher protection capacity against chemical attack. Detailed photos of the experimental work are presented in Appendix B.
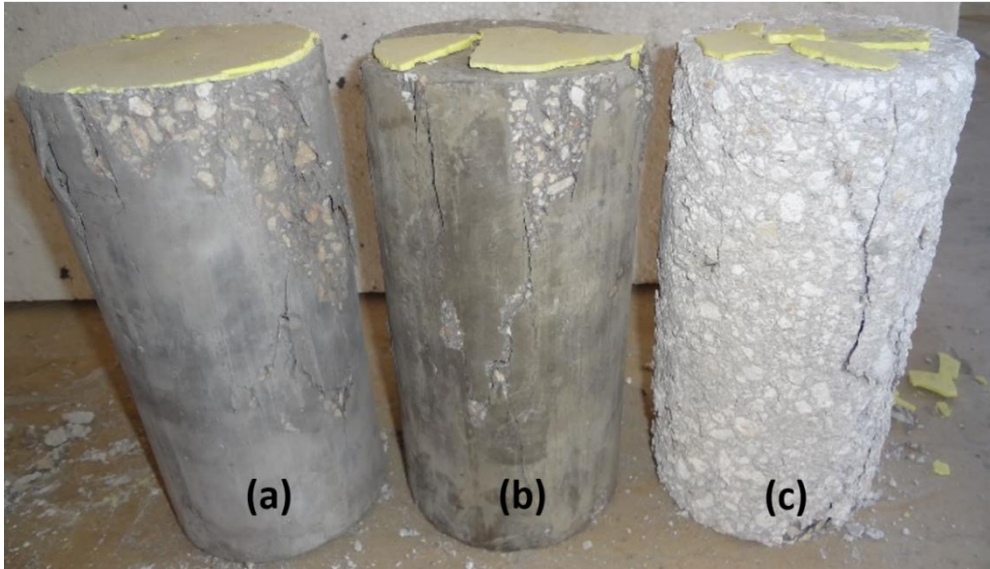
Figure 3.9 Unconfined specimens after exposure to (a) water, (b) sulfate and(c) acid

Figure 3.10 Confined and unconfined specimens after exposure to acid environment
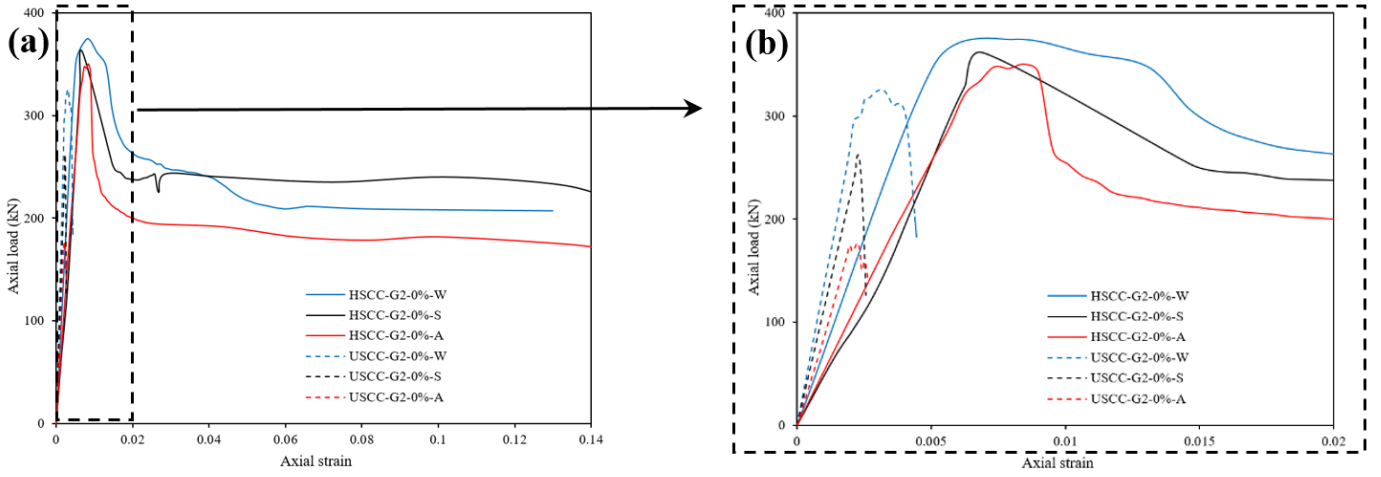
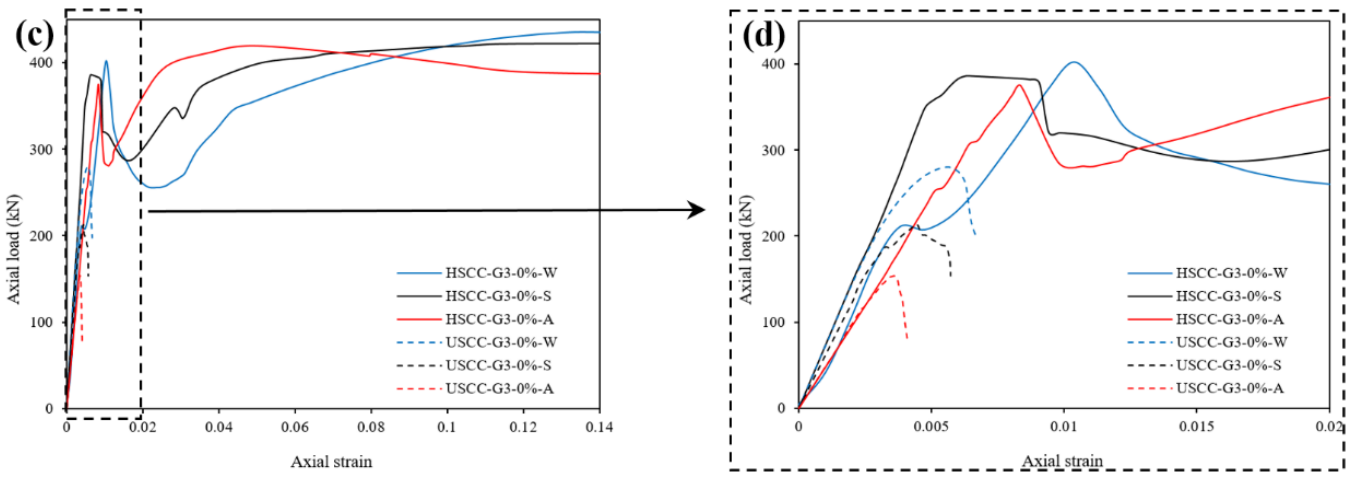**Figure 3.11 (a)** Influence of chemical exposure , second geometric

Figure 3.11 (b) Influence of chemical exposure , third geometric

CHAPTER 4

MECHANICAL PROPERTIES OF OF ULTRA-HIGH DUCTILE GEOPOLYMER FILLED HDPE TUBES

4.1 Introduction

Fiber reinforced polymer (FRP) and geopolymer concrete (GP) are engineering materials that have been inspired by the interest of many researchers and scholars in recent decades because of the strong advantages of owning (Ferdous, Manalo, Khennane, & Kayali, 2015). Many researchers have conducted recent examinations on the flexural behavior of CFFTs (Cole & Fam, 2006; A. Fam & Rizkalla, 2003) and reported large and growing body of experimental work for flexural behavior for CFFT beams reinforced with steel or strips through a number of recent quality studies (A. Fam, Cole, & Mandal, 2007; Wong, Yu, Teng, & Dong, 2008). More recent attention has focused on providing a different types of composite structure which has been generated by Ting et al through many modern research and studies on CFFTs. (Wong et al., 2008) in the composition of double-concrete-steel double-tubular (DST) column (DSTC). Eligibility criteria require this composite structure includes an internal hollow steel tube and an external FRP tube with the concrete sandwiched between the steel components and FRP tube. Through the collection of the benefits of the 3 materials consisting of composite column, it will be consist of superior than the specifications of its component material performance advantages. It has been conducting a number of tests and investigations of the axial compressive behavior of DSTCs (Tao Yu & Teng, 2012).

Concrete geopolymer are characterized by advantages which are appropriate for structural applications, and in addition to this contribute effectively to the development of fast and superior chemical, good compressive strength, remarkably durable and fire protection and drying shrinking and negligible thermal (Louk Fanggi & Ozbakkaloglu, 2013). The process of producing this type of concrete is through the use of alkaline waste materials such as ash fly ash and rice husk, which is

abundant with alumina and silica (Ozbakkaloglu & Fanggi, 2015)leading to 10% to 30% less costly compared to the OPC concrete relating to material cost (Anuradha, Sreevidya, Venkatasubramani, & Rangan, 2012; Davidovits, 1988; Sarker, 2008). As, to date, no research has submitted on the flexural behavior of Double-skin tubular HDPE (DST-HDPE) and HDPE beams filled by SCGP, for a deeper understanding that requires more study and the major issue is to be eligible for the model flexural response of the composite beams. To contribute shed light on this goal, the study of the flexural behavior of (DST-HDPE), HDPE, SCGP in this study considered as the first study of its kind. This research was aimed to examine the impact of key parameters on the flexural behavior of (DST-HDPE) and HDPE beams, with special emphasis placed on recovery and ductility behavior, Moreover the results will greatly contribute to the current technology of self-healing materials. Additionally, to create comparative performance of the above composite beams, the behavior of at SCGP beams with identical dimension to HDPE specimens was also experimentally inspected. The principle parameters of the research involved the thickness of HDPE tubes, cross- sectional shapes of interior steel tubular beams reinforcement, absence (or presence) of SCGP is filling inside the steel and HDPE tubes. Flexural behaviors of the composite beams were evaluated by utilizing recorded load-mid- span deflection relationships. In order to control the porous problem inside tubes after concrete hardening and the serviceability requirements such as (cracks) in case of using polymer covers there are few way to check the crack propagation monitoring of FRP-strengthened steel structures based on eddy current testing (ECT). (Li et al). showed that eddy current pulsed thermography (ECPT) could be used to detect impact damage on FRP-strengthened steel structures. (Yikuan et al). Used Lamb waves to monitor fatigue crack propagation and detect fatigue crack initiation in FRP-strengthened steel plates. Ma et al. Found that acoustic emission (AE) techniques were effective in revealing crack processes in FRP-strengthened reinforced concrete (RC) columns.

4.2 Experimental program

To date, various methods have been developed and introduced to measure, examine and investigate the behavior of Double-skin tubular HDPE (DST-HDPE) and HDPE beams filled by SCGP under flexural loading. Traditionally, this experiment included total number of 22 beams nominal length and diameter presented in Table 4.1. Twenty beams were cast by (SCGP) and the two left were tested empty to achieve the real

compressive strength of HDPE tubes. All 22 beams were divided into two groups of 12, and 11mm diameter with 10, and 13mm thickness respectively. For each HDPE tube one sample was cast as cylinder with the identical dimension to provide a pair-base logical comparison, (e.g. 12mm diameter HDPE was paired with a 12mm cylindrical specimen cast in normal plastic (PCV) formwork). Table 4.2, is showing the groups of samples based on their difference in parameters. The test instrumentation and setup are shown in Fig 4.1. The preparation process of a (DST-HDPE) and HDPE beams involved the Following steps:

Provide of the HDPE and steel tubes, which involved cutting the hollow tube to a desired length (Fig 4.2 a & b); (2) Turn the steel tubes to the vertical position and fix it with a circular plate with epoxy (Fig 4.2 b); (3) placing the FRP tube outside the steel tube (Fig 4.2 c); (4) casting (SCGP) the tubes and then the molds of PCV confined specimens were removed (Fig 4.2 d) ; (5) For each (DST-HDPE) and HDPE beams, one sample was cast as cylinder with the identical dimension to provide a pair-base logical comparison (Fig 4.2 e). Detailed photos of the experimental work are presented in Appendix C.

Table 4.1 Group HDPE & Inner steel tube details

Group FRP details				
NO OF Group	**Interior Demeter cm**	**Length cm**	**Thickness cm**	**Sample Designation**
1	12	120	1	G1
2	11	120	1.3	G2

Table 4.2 Specimen designation

Sample Designation	**Shape Designation**	**No of group**	**Filling or absence GP Inside HDPE**	**Filling or absence GP Inside HST**	**Shape of inner tube HST**
HDPE-1		G1	Filling	Filling	Circle

HDPE-2	⊙	G1	Filling	absence	Circle
HDPE-3	▢	G1	Filling	Filling	Square
HDPE-4	▢	G1	Filling	absence	Square
HDPE-5	●	G1	Filling	-	-
HDPE-6	○	G1	absence	-	-
HDPE-7	⊙	G2	Filling	Filling	Circle
HDPE-8	⊙	G2	Filling	absence	Circle
HDPE-9	▢	G2	Filling	Filling	Square
HDPE-10	▢	G2	Filling	absence	Square
HDPE-11	●	G2	Filling	-	-
HDPE-12	○	G2	absence	-	-
SCGP-13	⊙	G1	-	Filling	Circle
SCGP -14	⊙	G1	-	absence	Circle
SCGP -15	▢	G1	-	Filling	Square
SCGP -16	▢	G1	-	absence	Square
SCGP -17	●	G1	-	-	-

SCGP -18	○	G2	-	Filling	Circle
SCGP -19	○	G2	-	absence	Circle
SCGP -20	□	G2	-	Filling	Square
SCGP -21	□	G2	-	absence	Square
SCGP -22	⬤	G2	-	-	-
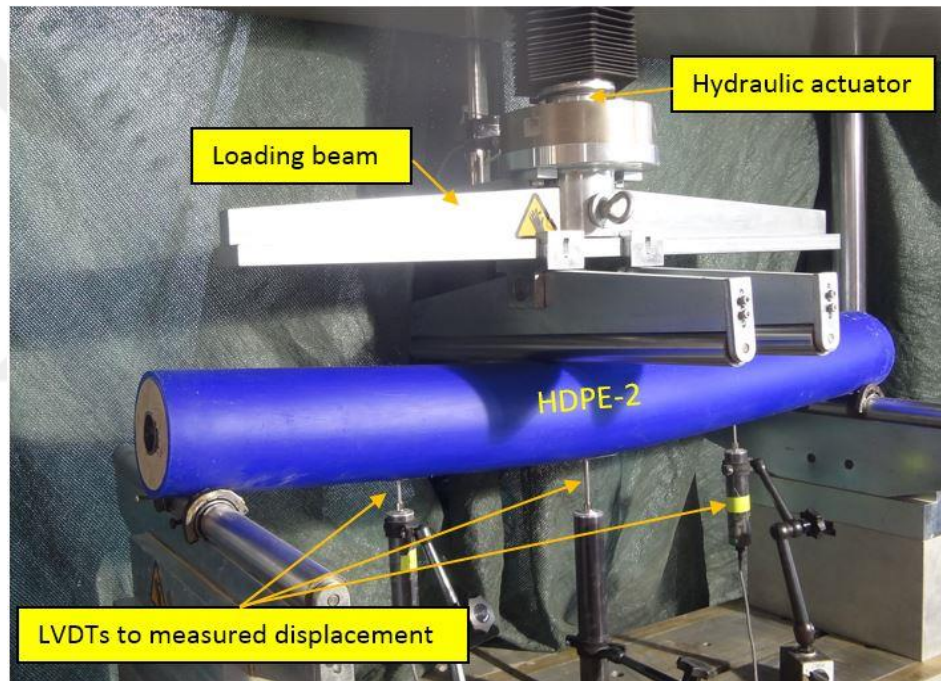
Figure 4.1 Test composite beams

Figure 4.2 (a) Manufacturing of FRP tubes

Figure 4.2 (b) Manufacturing process of steel tubes
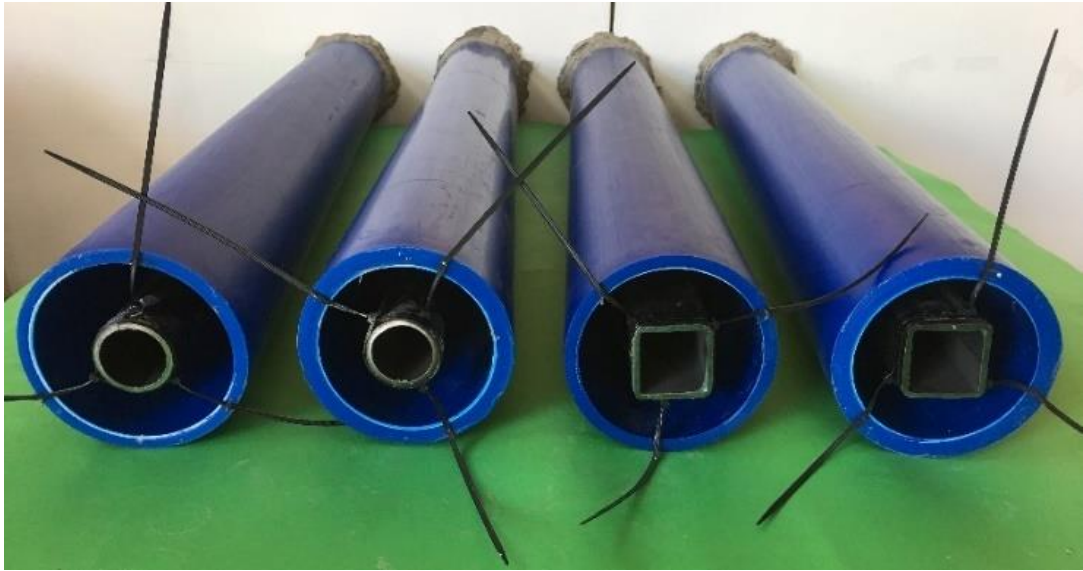
Figure 4.2 (c) Specimens before SCGP pouring
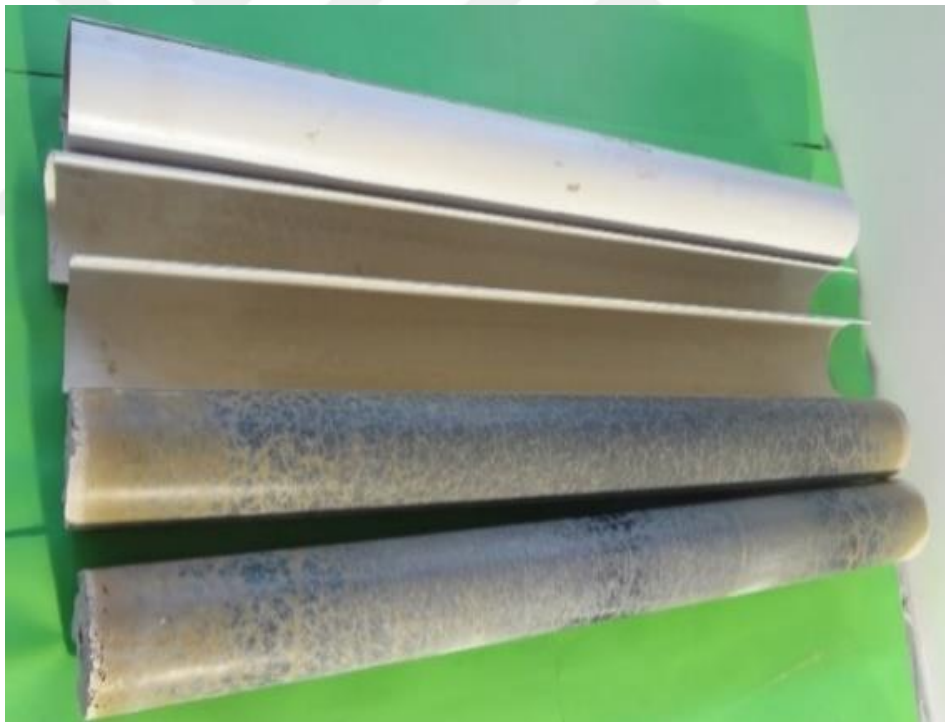
Figure 4.2 (d) Removal of formworks after hardening of SCGP for unconfined specimens

Figure 4.2 (e) Specimens after SCGP pouring

4.3 Material properties

4.3.1 Self-compacting geopolymers SCGP

4.3.1.1 Materials

Slag based self-compacting geopolymer mixture (SCGPC) were produced and corresponding fresh and mechanical performances of SCGPC were evaluated. Ground Granulated Blast Furnace Slag (GGBFS) were used in the research as binder materials. The crushed limestone as coarse aggregate with a maximum particle size of 11 mm, crushed limestone (smaller than 4 mm) as fine aggregate was utilized in the study. Alkali activator is a mix of both sodium silicate (Na_2SiO_3) and sodium hydroxide solutions (NaOH). The sodium silicate was taken from the regional source (Na_2O:13.7%, SiO_2: 29.4, water: 55.9% by mass). The sodium hydroxide was taken with 97%-98% purity and it was used as 12 molar concentration that was the better content for the mechanical performance of SCGC (Memon, Nuruddin, Khan, Shafiq, & Ayub, 2013). Table 4.3 shows the properties of GGBFS and Table 4.4 shows Mechanical properties of SCGC. The compressive and splitting tensile properties were measured on cylindrical concrete specimens of 150 mm diameter x 300 mm length at 28-days using a compression testing machine.

Table 4.3 Physical and chemical characteristics of GGBFS

Component	CaO	SiO2	Al2O3	Fe2O3	MgO	SO3	K2O	Na2O	LOI	SG	BF (m2/kg)
GGBFS (%)	34.12	36.40	11.39	1.69	10.30	0.49	3.63	0.35	1.64	2.79	418

A polycarboxylates ether based superplasticizer with a density of 1.095 g/cm3 was used to obtain high flowability without segregation and/or bleeding (Dubey & Kumar, 2012; Nuruddin et al., 2011)

Table 4.4 Mechanical properties of SCGC

Compressive strength MPa	78.6	79.8	81.2
Splitting tensile strength MPa	5.13	4.97	5.21

4.3.1.2 Concrete ingredients

SCGC mixture were produced with a constant total binder amount of 450 kg/m³. The mixture contains 100% slag by weight. Table 4.5 illustrates the mix ingredients.

Table 4.5 Mixture proportion of self-compacting geopolymer concrete

Mixture	Binder	Na_2SO_3 +NaOH	GGBFS	Fine Agg.	Coarse Agg.	Molarity	SP	Extra water
	kg/m³	kg/m³	kg/m³	kg/m³	kg/m³		%	%
SCGPC	450	225	450	865.61	742.88	12	7	15

Aggregate, binder and alkaline amount, maximum grain size (D_{max}) affect both fresh and mechanical performance of SCGPC specimens. The Na_2SiO_3/ NaOH ratio becomes in the range of 1.5 to 2.5 for economic reasons (Olivia & Nikraz, 2012) and it was utilized as 2.5 in the research.

For the mixing procedure, coarse and fine aggregates, GGBFS were included and blended for 2.5 minutes. The alkali activator, superplasticizer and extra water included in one minute and mixed additional 2 minutes. After that, fresh concrete was further mixed for 3 minutes to ensure homogeneity and uniformity.

4.3.1.3 Fresh state tests

After mixing procedure, fresh state tests were conducted on the SCGPC mixes since these mix should fulfill the flow-ability and passing ability requirements without segregation and/or bleeding. The flow-ability of geopolymer SCC specimens was measured via slump flow and V-funnel tests; passing ability was measured using L-Box test according to EFNARC committee (EFNARC, 2005). In the slump flow test, flow diameters in x and y direction were measured and t_{500} duration in which flow

diameter reaches up to 500 mm diameter were recorded in the tests. In the V-Funnel test, the section is totally filled with concrete, then concrete is let to discharge and discharge time is recorded. The viscosity can be measured indirectly via V-funnel and T_{500} slump flow time using the rate of flow. In the L-Box test, passing ability of the mixes (PL value) between narrower openings (41±1 mm) was estimated by dividing the concrete heights of the lateral section to the vertical section. Table 4.6 illustrates the upper and lower limits for fresh state performance of SCC mixes according to the EFNARC specification (EFNARC, 2005).

Table 4.6 Fresh state test evaluation with respect to EFNARC specification

Slump flow classes		
Class	Slump flow diameter [mm]	
Slump Flow 1	550-650	
Slump Flow 2	660-750	
Slump Flow 3	760-850	
Viscosity classes		
Class	T_{500} [sec]	V-funnel time [sec]
VS1/VF1	≤2	≤8
VS2/VF2	>2	9 to 25
Passing ability classes		
PA1	≥0.8 with two rebar	
PA2	≥0.8 with three rebar	

4.3.1.4 Curing method of the SCGC

After the production of concretes, specimens were covered for 24 hours by a plastic sheet to avoid the evaporation of the alkaline solution. Then specimens were put in room temperature for 24 hours at 23 °C. After the completion of curing period, samples were demoulded and put in an ambient laboratory environment until the 28-day of hardened state tests.

4.3.1.5 Hardened state tests

The hardened state tests were executed to analyze the ambient curing mechanical performance of the self-compacting geopolymer concretes. Compressive strength tests were realized on cubic specimens (100x100x100 mm) using ASTM C39 standard

(ASTM C39/C39M-01, 2003). Splitting tensile strength tests were done on 100x200 mm cylinder specimens in accordance with ASTM C496 (ASTM C496-96, 2003).

4.3.2 FRP and ınner steel tubes

In the current study, high-density polyethylene (HDPE) pipe was chosen such as confinement materials. HDPE pipes illustrate many merits for example, corrosion resistant properties, usability against physical damage due to serious environment and long service life in excess of 50 years. Additionally, it can offer suitable curing conditions for concrete because of low thermal conductivity. Table 4.7 displays the physical characteristics of HDPE pipes and moreover 16 of those composite beams had interior steel tubes with two varied shape (i.e. circle and square) and thicknesses (i.e. 3.5 and 2.9 mm), with same dimension, see Table 4.8.

Table 4.7 Physical properties of HDPE

Parameter	Value
Class	PE 40
Density	0.945-0.965 g/cm3
Breaking elongation	min 350%
Elastic modulus	>600 MPa
Ultimate tensile strength	26 MPa
Working temperature	min. -80 °C, max. 100 °C
Thermal conductivity	0.29 kcal/m hr °C
Service life	>50 years

Table 4.8 Properties of Inner steel tube

Shape	Dimension (mm)	Thickness (mm)	Yield strength (YS) (Mpa)	Ultimate tensile strength (UTS) (Mpa)
Circle	50	3.5	362	410
Square	50	2.9	362	410

4.4 Experımantal results

4.4.1 Mechanıcal behavıour of GP fılled HDPE tubes

High ductility of HDPE tubes causes excessive deformation of the specimens and this, in turn, may affect the calibration of the test specimens where at this point the test was stopped due to the inability of control similar load conditions. (Fig 4.3 b,c) Shows the

condition of both HDPE-8 and HDPE-10 after testing, to enable the exhibit of the most damaged region of the SCGP, the HDPE tube shell was removed and to determine the state of the steel tube reinforcement, both the HDPE tube shell and SCGP was removed. There was no sign of rupture of the FRP tube for each (DST-HDPE) and HDPE beams. Of the initial cohort of composite beams 22, 12 were HDPE (DST-HDPE) and HDPE beams suffered significant ultra-deformation along their mid – span regions and this caused an opening gap occurs along the longitudinal axis of the HDPE tubes. The HDPE tubes exhibit the efficiency of the proposed self-healing system based on the recovery of technical characteristics (deflection capacity, flexural strength and energy absorption capacity), the four HDPE beams (inside the blue box. Fig 4.3 a) returned to their original shape after being examined whereas the eight (DST-HDPE) beams (inside the black box. Fig 4.3 a) revealed opening gap along their mid span regions, due to the status of the steel tube reinforcement prevented the HDPE tubes from reverting to its original shape. Removal of the HDPE shell tube along the specimen's length throughout the tension area to be able to exhibit the SCGP within the numerous collapse areas which were cracked in varied regions, as seen in (Fig 4.3 b, c). The number and spacing of SCGP cracks generated for both HDPE-8 and HDPE-10, seemed slightly convergent. (Fig 4.3 b, c) Illustrates the state of the interior steel reinforcements after removals of the surrounding SCGP and FRP shell. As obvious through the figure, it shown considerable plastic deformation over the constant moment areas of the interior steel reinforcements of all composite beams (Fig 4.3 b, c). The dominant failure mode of all the examined SCGP beams of this research, it was Flexural-tension failure (Fig 4.3 d).

4.4.2 Load–deflection relationships

A smooth transition region with nearly bi-linear load-deflection relationship was dominant behavior for DST-HDPE and HDPE beams, as shown in (Fig 4.7). The majority behavior of the (DST-HDPE) and HDPE beams was a nearly flat second branch with a gradual decline and ascent significant on their flexural strengths. Further, throughout loading history the (DST-HDPE) and HDPE beams demonstrated a monotonically ascending load-deflection relationship. The key points of the load-deflection relationships have been recording data, as shown table 4.10, specifically the peak load (P_{peak}), recorded mid-span deflection at the peak load (Δ peak), mid-span deflection at ultimate (Δ_{ult}) where tests was stopped. Moment of ultimate (M_{ult}) and

Peak moment (M_{peak}), which were investigated from the recorded loads, as well as presented in Table 4.10. A detailed examination on the effect of test variables in the trends of the load-deflection relationships of the composite beams is developed after in this research, beside the modulus of rupture in case of SCCG was 4 (kN.M).

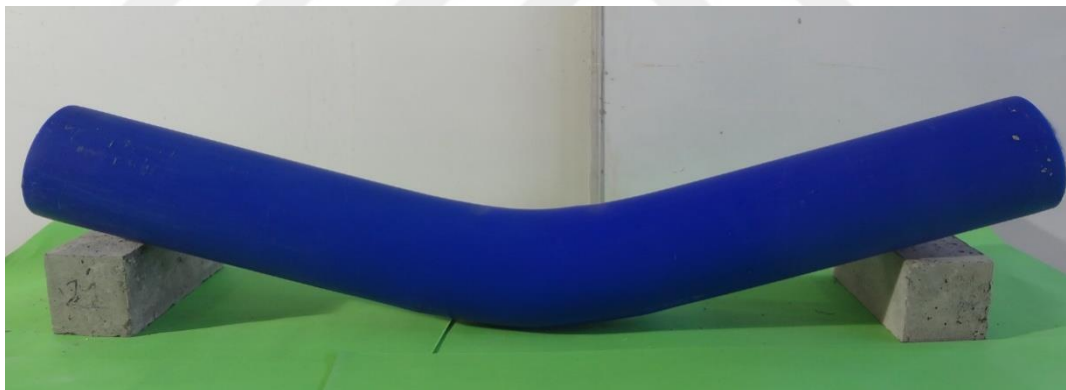**Figure 4.3 (a)** All the HDPE tubes after examined the test

Figure 4.3 (b1) Composite beams HDPE-10 after tested

Figure 4.3 (b2) Composite beams HDPE-10 after remove the shell of HDPE tube

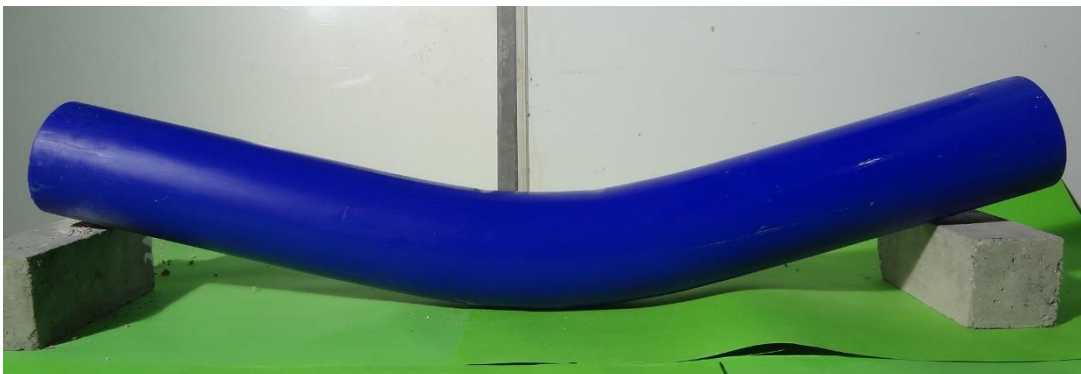**Figure 4.3 (b3)** Composite beams HDPE-10 after remove the SCGP

Figure 4.3 (c1) Composite beams HDPE-8 after tested

Figure 4.3 (c2) Composite beams HDPE-8 after remove the shell of HDPE tube

Figure 4.3 (c3) Composite beams HDPE-8 after remove the SCGP

Figure 4.3 (d) Composite beams SCGP -14 after tested

4.5 Evaluation of test results

4.5.1 Recovery behavior

The effect recovery behavior of the HDPE-6 and HDPE-12 on the flexural behavior was inspected by testing each model five times, (fig 4.4 a, b) and table 4.9 presents the summary statistics for these specimens. The findings of the reloading of the HDPE-6 with thickness 10 mm showed a decrease in flexural strength with an approximate rate 12% of the total strength at each test, while HDPE-12 with thickness 130 mm exhibit decreased rate (.i.e. 13 %) less than HDPE-6 and this is due to the effect of thickening.

4.5.2 FRP tube's thickness

The impact of the thickness of the HDPE tube on the flexural behavior of the (DST-HDPE) and HDPE beams was investigated by comparing HDPE-1 and HDPE-7. The sample with 1.3 cm thick HDPE-7 tube developed a peak load (P_{peak}) of 52.69 kN at 227.26 mm mid-span deflection, while the sample with 1 cm thick HDPE-1 was eligible to tolerate a peak load (P_{peak}) of just 42.525 kN at 230.433 mm mid-span deflection. HDPE-7 showed an ascending second branch significantly in its load-deflection curve, while HDPE-1 had a curve with a gradual ascending second branch, as can be seen in Fig 4.5 (a-e).

4.5.3 Influence of fillin interior steel tube beam with SCGP.

It could be determined for the influence of filling the interior steel tube with SCGP by evaluating the behaviour of HDPE-7, which had at SCGP-filled interior steel tube beam with this of HDPE-8, with a hollow interior steel tube beam. In an identical path, both composite beams exhibited a nearly ascending second branch on their load-deflection curves. As a result of improved area of SCGP. A greater peak load was recorded for HDPE-7 (52.79 kN at 229.28 mm mid-span deflection) than HDPE-8 (49.83 kN at 230.84 mm of mid-span deflection). It could improve the flexural capability of (DST-HDPE) without influencing their ductility .These observations have been achieved through that SCGP filling of the inner steel tubular beam, as can be seen in Fig 4.5 (a-e).

4.5.4 Confinement effect

The effects of the confinement of the composite beams was researched by evaluating HDPE-7, HDPE-12 with SCGP -18, and HDPE-7. It has showed load-deflection curve with the ascending second branches, whereas HDPE-12 showed a load -deflection curve with flat and gradual descending second branches. SCGP-18 revealed load - deflection curve with strong descending second branches. The peak load of HDPE-7 was 52.79 KN and recorded at 229.29 mm mid-span deflection while HDPE-12 reached 13.53 KN of peak load at 140.95 mm mid-span deflection. SCGP-18 showed a tolerability until 24.93 KN of peak load at 19.105 mm mid-span deification obviously. SCGP core confinement by HDPE tube has shown better ductile behavior as result, the ultimate load carry capacity increased as shown in Fig 4.6 (a-j).

4.5.5 Influence of cross-sectional shape of interior steel tube beam

The influence of cross-sectional shape of the interior steel tubular beam was scrutinized by evaluating the behaviours of HDPE-1 (circular inner steel tubular beam) and HDPE-3 (square interior steel tube beam). Thickness and cross section of the inner steel tubular beam for this work were similar, as expected, this led to similar reinforcement ratios (As / AC) as seen in Table 4.1. As can be shown in Fig 4.7 (a,b), the load-deflection curve of HDPE-1 started revealing as ascending conduct in the second branch until reaching the peak load of 43.52 kN at 230 mm mid-span deflection. As shown in Table 4.10, the peak load of HDPE-3 (i.e. 35.9 kN) was less than those of HDPE-1, but it was achieved at a nearly the same mid-span deflection (i.e.228.2 mm). This could be related to its more effective interior steel tube beam reinforcement position, which is the most likely evidence of the higher flexural capacity of HDPE-1.

Table 4.9 Reloading results

	HDPE-6		
No of reloading	**Ultimate Force(kN)**	**% Decrease of Ultimate load**	**Sample Designation**
1	7.16	-	T 1-G1
2	6.34	11.45	T 2-G1
3	5.65	10.88	T 3-G1
4	4.9	13.27	T 4-G1
5	4.11	16.12	T 5-G1
	HDPE-12		
No of reloading	**Ultimate Force(kN)**	**% Decrease of Ultimate load**	**Sample Designation**
1	7.16	-	T 1-G2
2	6.34	5.25	T 2-G2
3	5.64	5.238	T 3-G2
4	4.9	7.508	T 4-G2
5	4.11	5.53	T 5-G2

Table 4.10 Summary of Result

Specimens	P_{peak} (kN)	Δ_{peak} (mm)
HDPE-1	42.52	230.48
HDPE-2	39.76	230.94
HDPE-3	35.95	228.36
HDPE-4	33.06	228.66
HDPE-5	24.16	220.805
HDPE-6	6.5	230.54
HDPE-7	52.79	229.28
HDPE-8	49.18	228.19
HDPE-9	48.25	226.29
HDPE-10	48	229.303
HDPE-11	36.54	233
HDPE-12	13.5	224.68
SCGP-13	25.8	47.53
SCGP -14	24.7	49.51
SCGP -15	23.76	52.2

SCGP -16	22.63	50.77
SCGP -17	6.96	2.02
SCGP -18	24.9	50.62
SCGP -19	24.32	51.055
SCGP -20	23.7	45.46
SCGP -21	22.6	37.63
SCGP -22	5.16	2.06
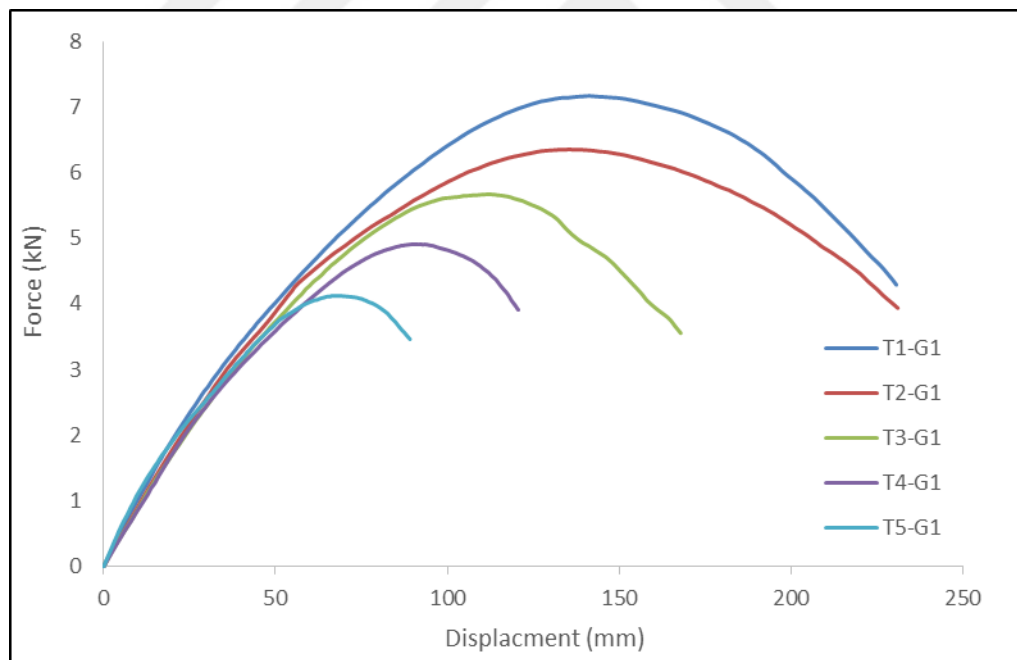
Figure 4.4 (a) Effect of recovery behavior for HDPE-6
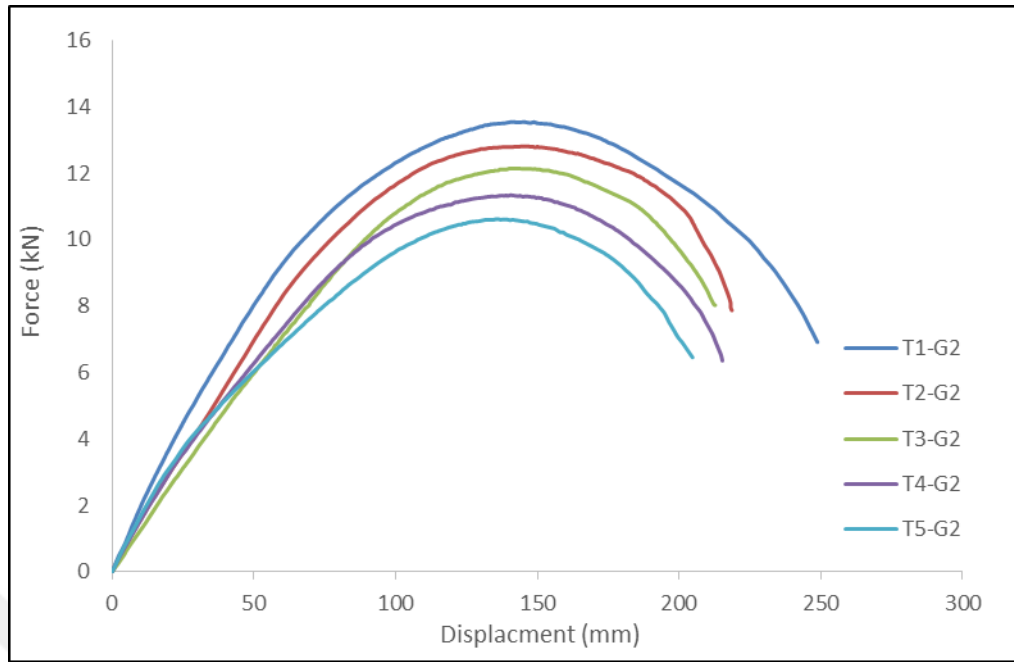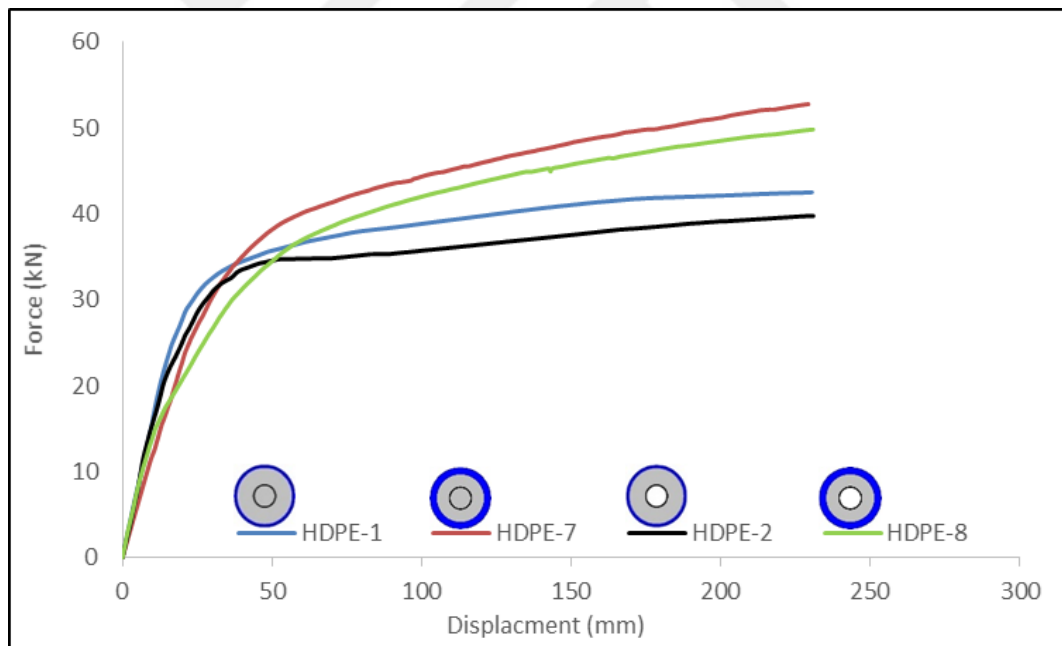
Figure 4.4 (b) Effect of recovery behavior for HDPE-12

Figure 4.5 (a) Effect of the (thickness and filling or absence the SCGP inside inerr tube) for the HDPE-1, HDPE-7, HDPE-2 and HDPE-8
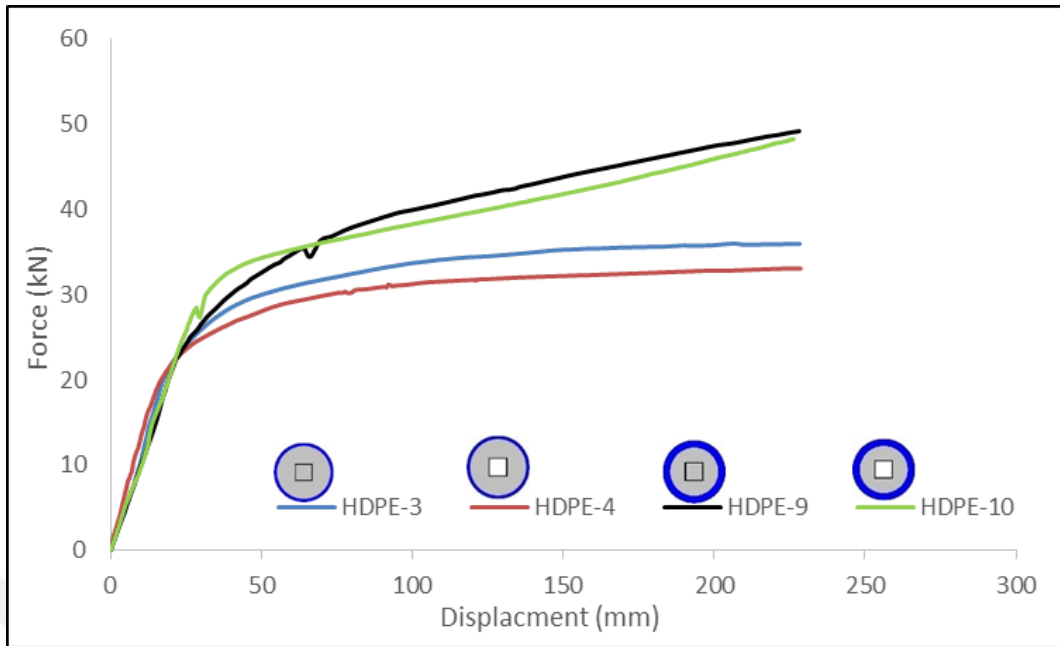
Figure 4.5 (b) Effect of the (thickness and filling or absence the SCGP inside inerr tube) for the HDPE-3, HDPE-4, HDPE-9 and HDPE-10
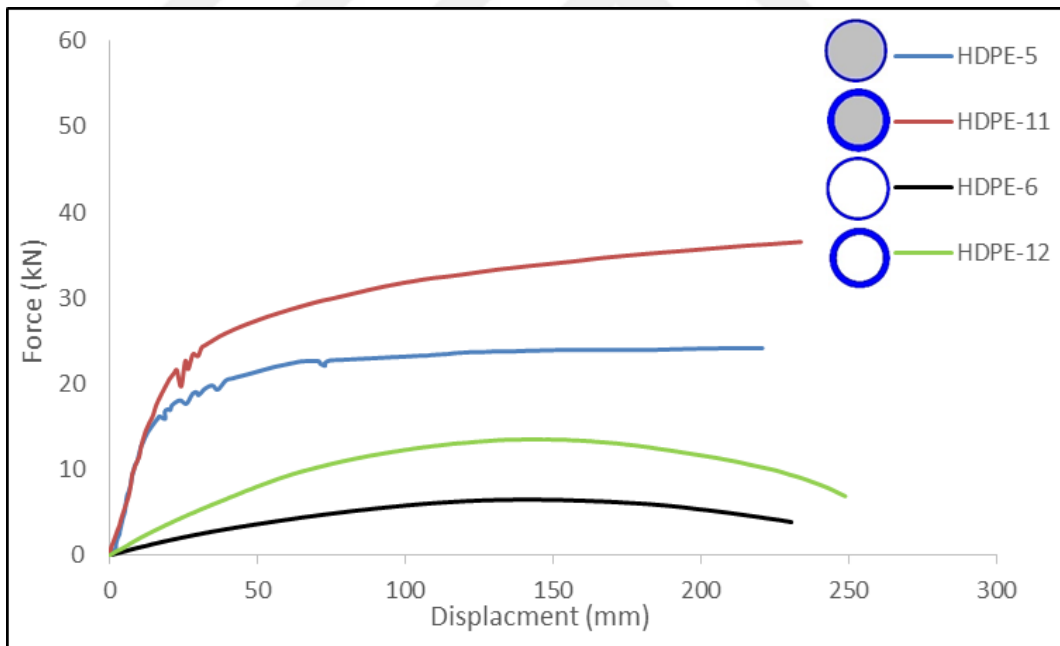

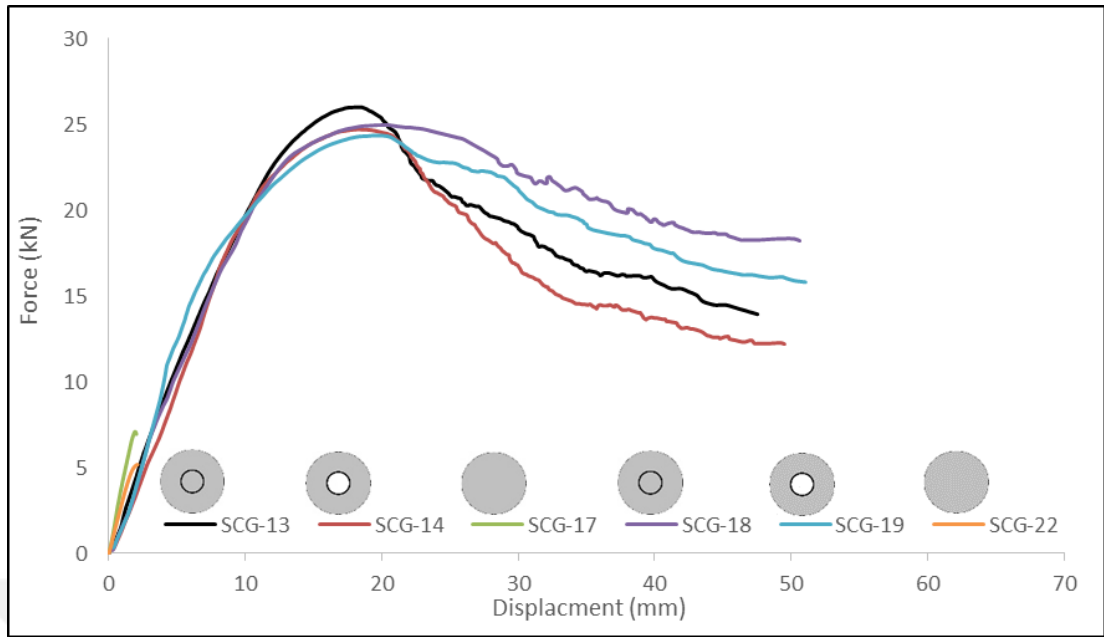**Figure 4.5 (c)** Effect of the thickness for the HDPE-5, HDPE-11, HDPE-6 and HDPE-12

Figure 4.5 (d) Effect of the (different geometric and filling or absence SCGP inside inerr tube) for the SCG-13, SCG-14, SCG-17, SCG-18, SCG-19 and SCG-22
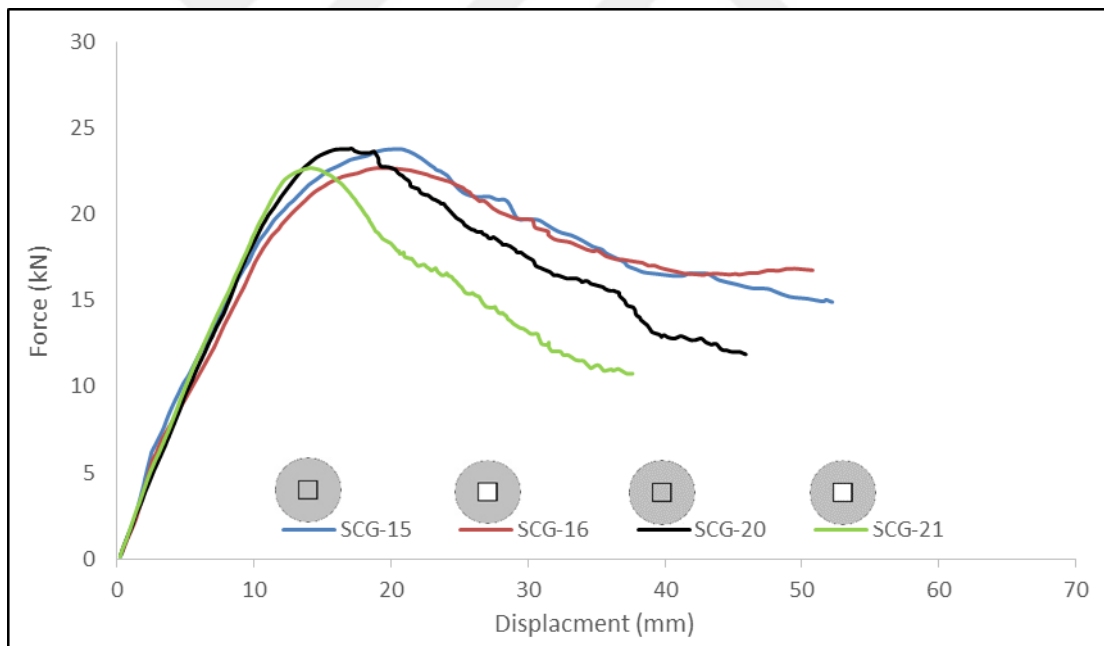

Figure 4.5 (e) Effect of the (different geometric and filling or absence SCGP inside inerr tube) for the SCG-15, SCG-16, SCG-20 and SCG-21
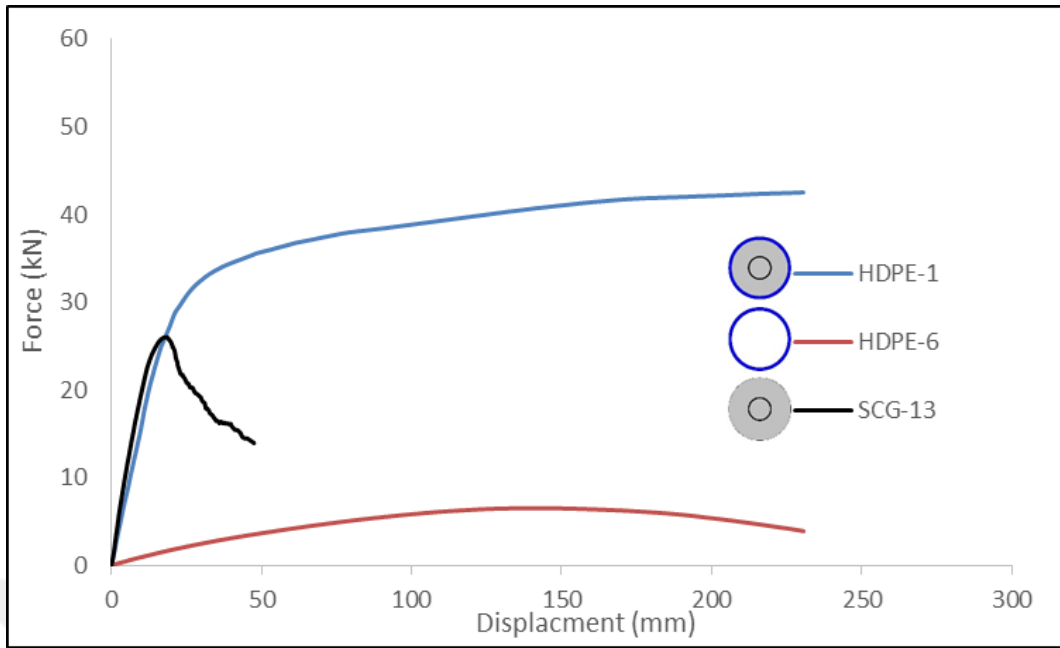
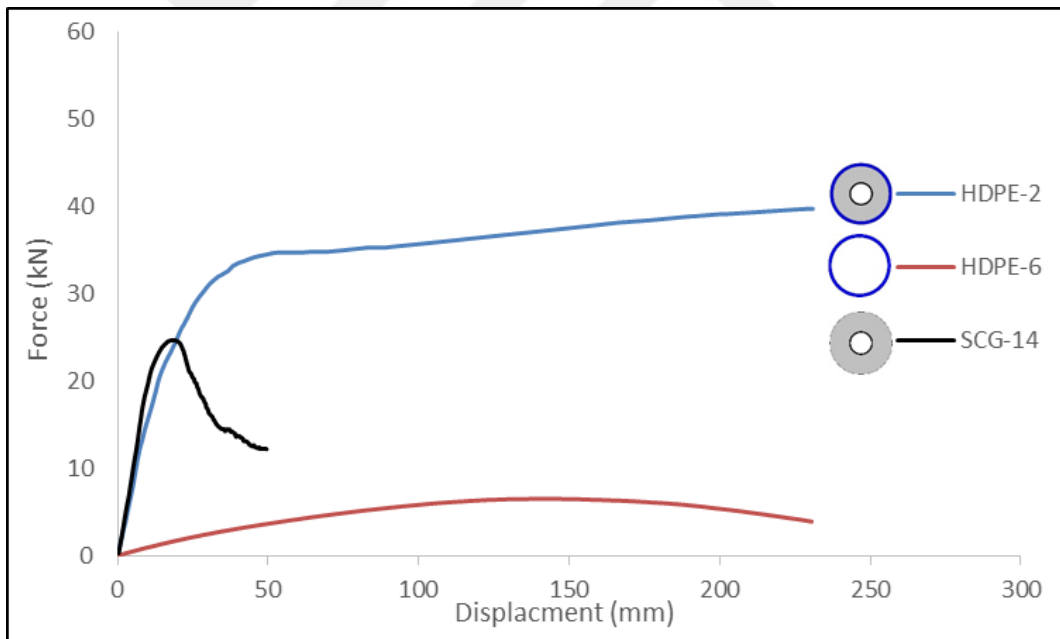**Figure 4.6 (a)** Confinement effect for HDPE-1, HDPE-6 and SCG-13

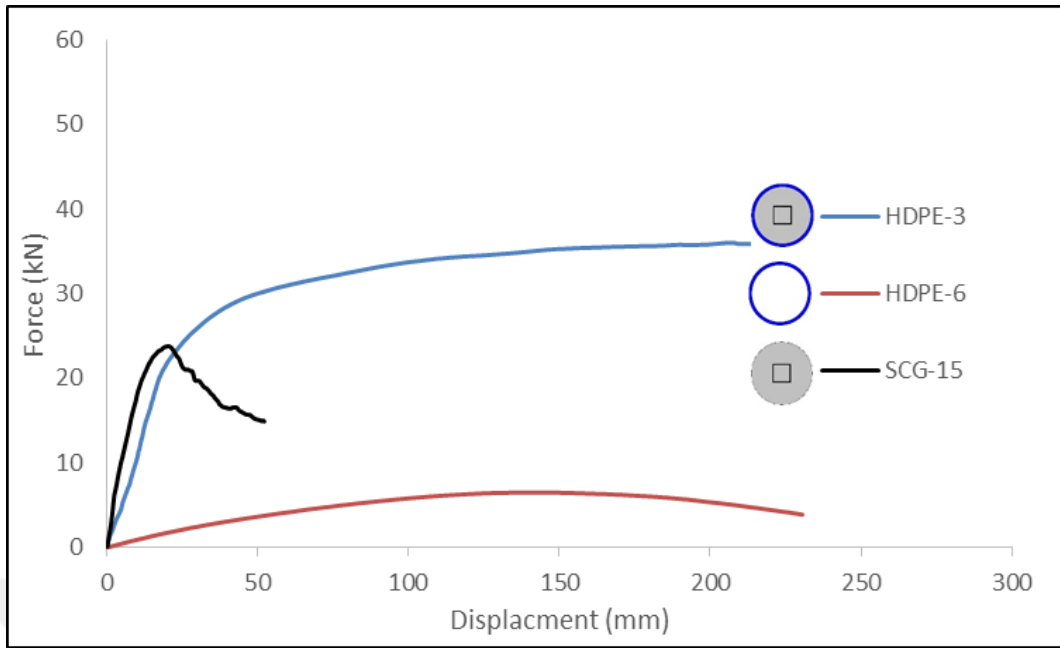**Figure 4.6 (b)** Confinement effect for HDPE-2, HDPE-6 and SCG-14

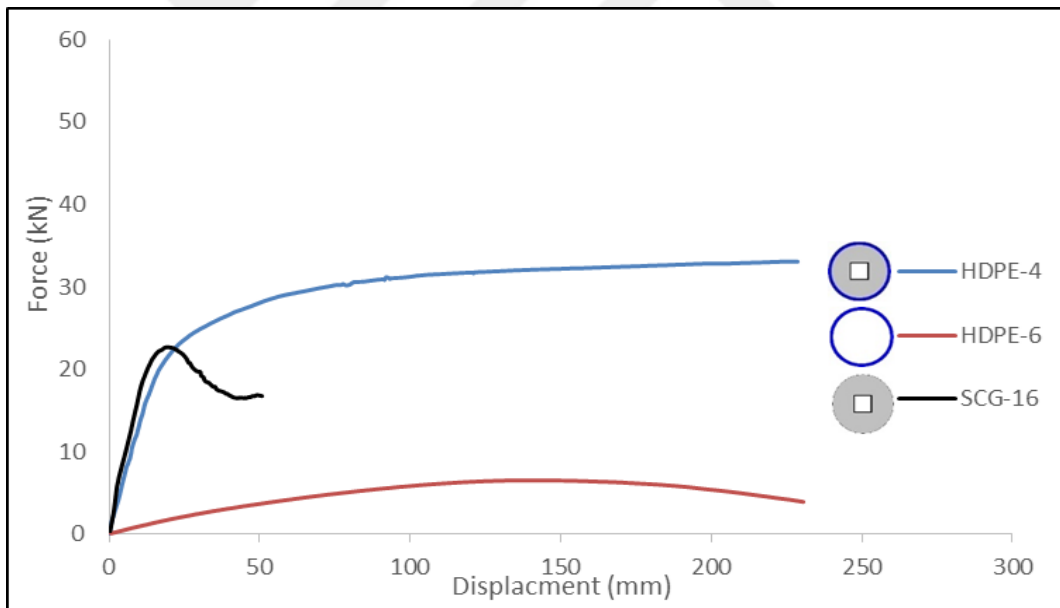**Figure 4.6 (c)** Confinement effect for HDPE-3, HDPE-6 and SCG-15

Figure 4.6 (d) Confinement effect for HDPE-4, HDPE-6 and SCG-16
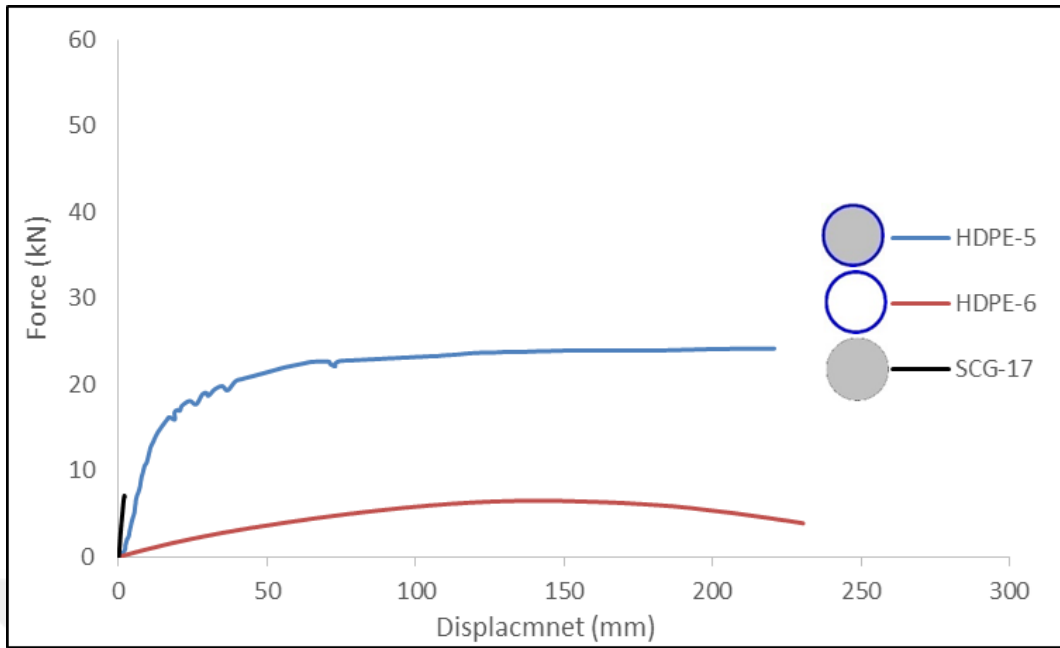
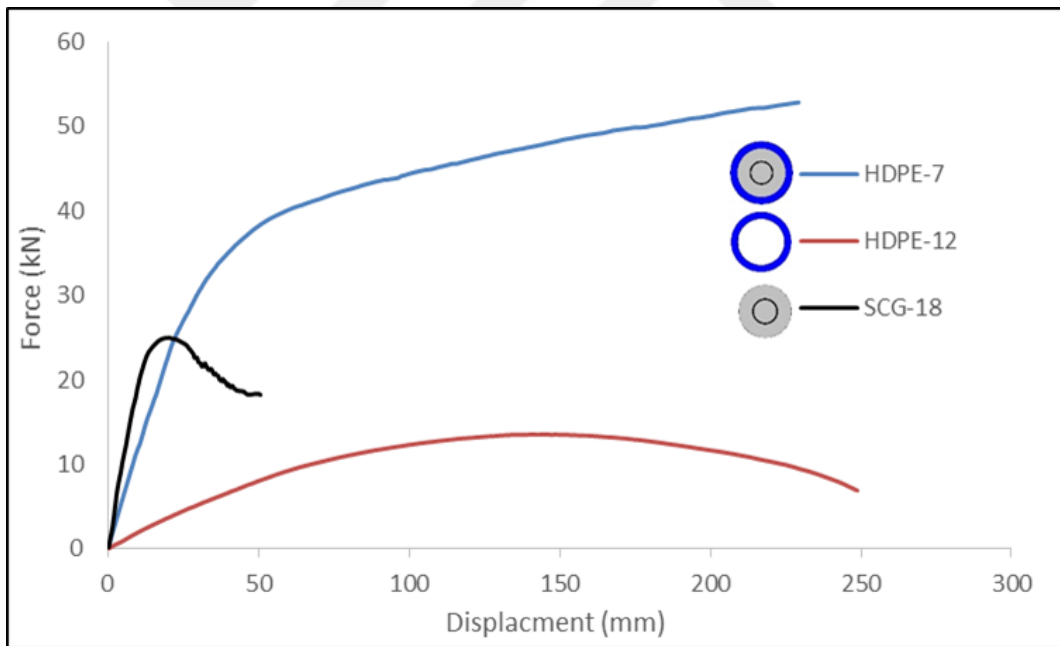**Figure 4.6 (e)** Confinement effect for HDPE-5, HDPE-6 and SCG-17

Figure 4.6 (f) Confinement effect for HDPE-7, HDPE-12 and SCG-18

Figure 4.6 (g) Confinement effect for HDPE-8, HDPE-12 and SCG-19

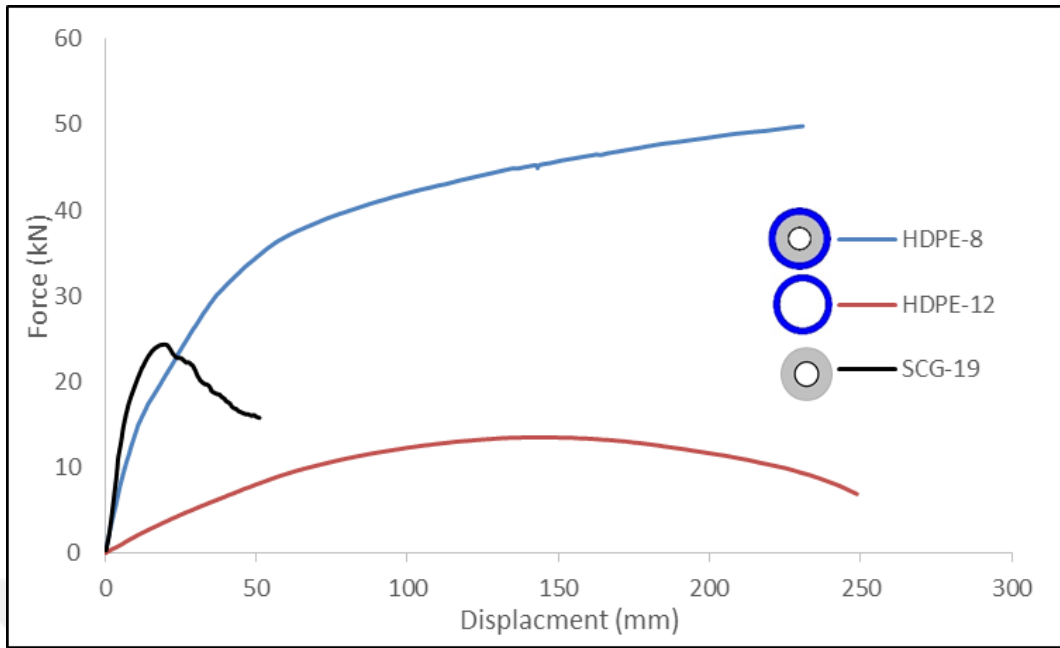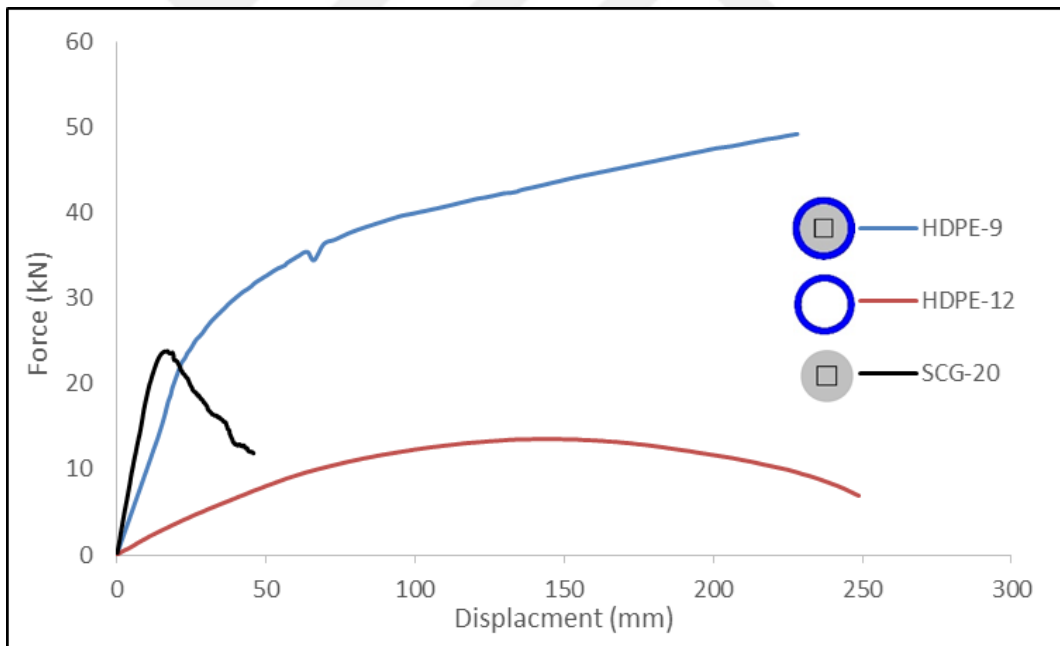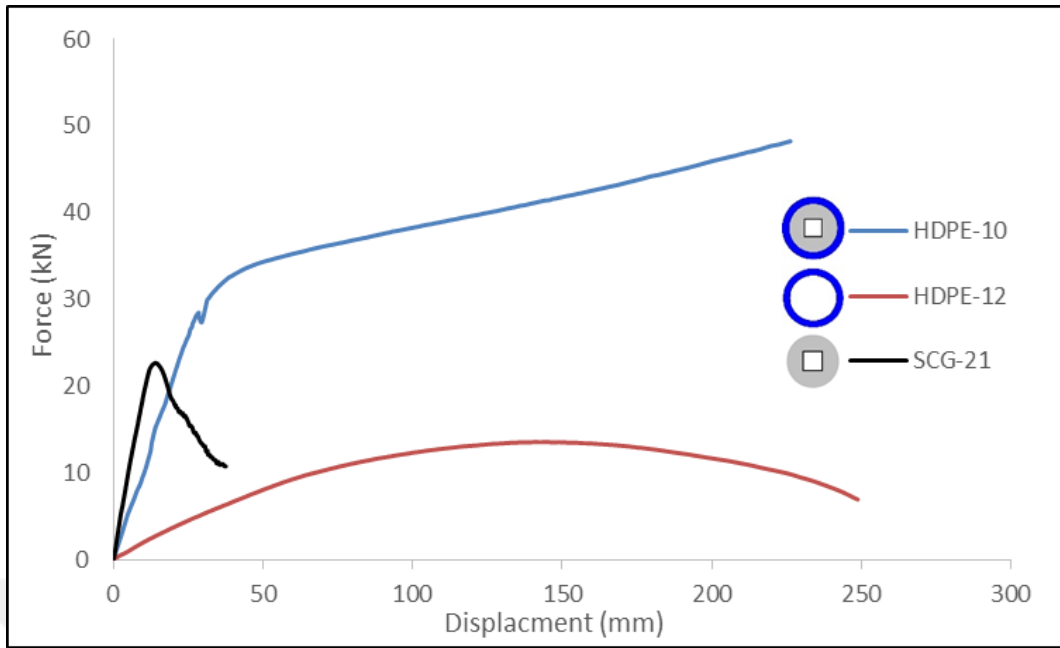**Figure 4.6 (h)** Confinement effect for HDPE-9, HDPE-12 and SCG-20

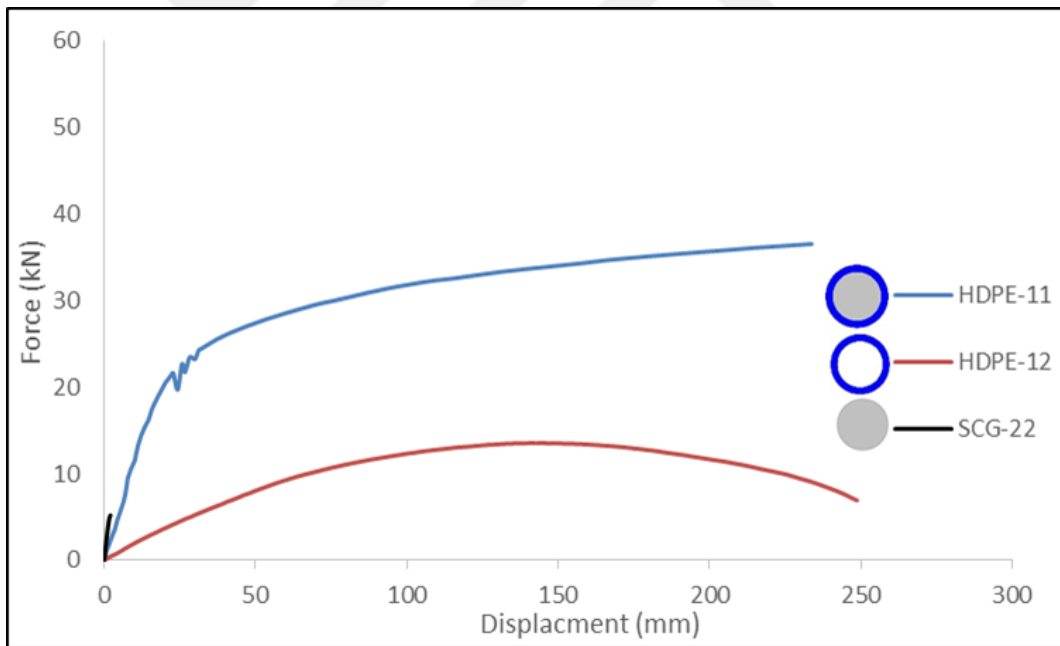**Figure 4.6 (i)** Confinement effect for HDPE-10, HDPE-12 and SCG-21

Figure 4.6 (j) Confinement effect for HDPE-11, HDPE-12 and SCG-22
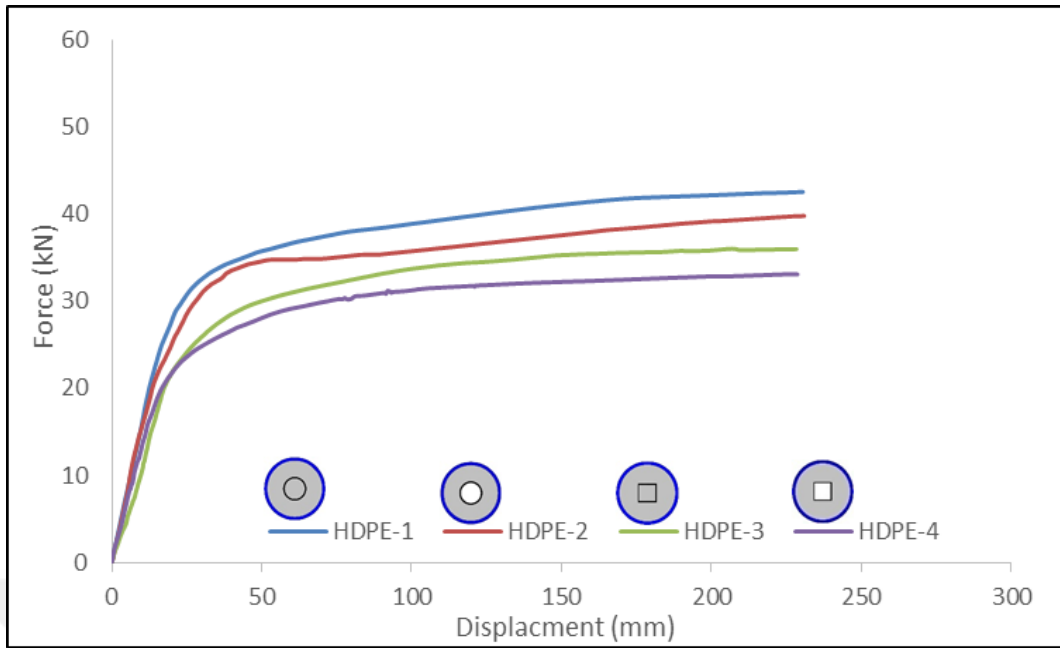
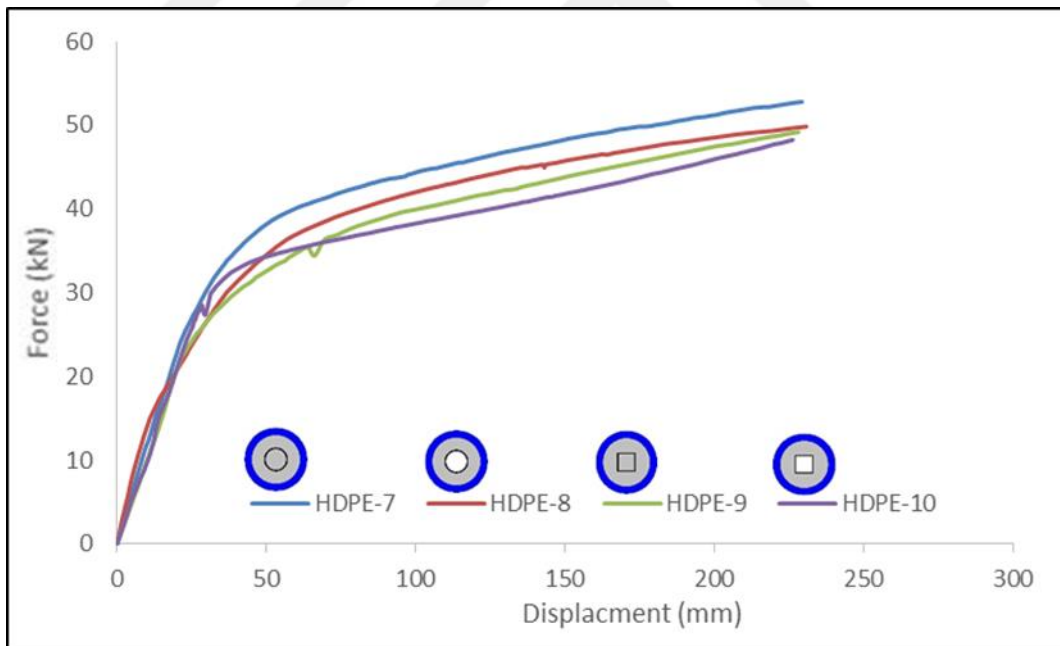**Figure 4.7 (a)** Effect of the shape inner tube for the HDPE-1, HDPE-2, HDPE-3 and HDPE-4

Figure 4.7 (b) Effect of the shape inner tube for the HDPE-7, HDPE-8, HDPE-9 and HDPE-10

CHAPTER 5

CONCLUSIONS AND RECOMMENDATIONS

5.1 Conclusions

This thesis investigates the mechanical behavior of self compacting concrete and geopolymer concrete filled by (glass reinforced polymer (GRP), high density polyethylene (HDPE)) tubes which consists of three parts.

The first part investigates the durability characteristics of self-compacting concrete confined with square GRP pipes with varying geometry. A total of 40 specimens were prepared and exposed to water or acid environments. The parameters considered for investigation were the presence of confinement, geometry, steel fiber presence and exposure type (water or acid). Following conclusions can be drawn:

1. In a composite system such as GCSCC, GRP pipe can function as a wall between concrete and outer environment e.g., salt water, sulfate and acid. Cost-effective GRP pipe confinement can protect the concrete and rebars in columns/beams against the chemicals present in the sea water or underground water. Additionally, GRP pipes may also work as a weather-proof jacket for the core concrete and rebar's.

2. GRP hollow tubes do not suffer from extreme environmental conditions significantly. They demonstrate high residual load-strain behavior after exposure to acid environment.

3. Specimens with GRP confinement do not show significant reduction in load capacity after exposure to aggressive environments owing to the high protection capacity of GRP pipes. Load capacity is reduced nearly by half for unconfined SCC columns exposed to acid.

4. Confinement of SCC with GRP pipes had substantial contribution in axial load carrying capacity of GCSCC specimens. This contribution is pronounced

5. More for samples with larger interior dimensions and thicker pipe wall. Post peak region under load-strain curve has increased significantly, which depicts the large enhancement in energy absorption capacity, thereby the ductility, of confined SCC columns.

6. Change in the tube height did not have a substantial effect on the peak load for confined specimens. However, reducing the height of unconfined specimens resulted in lower peak load. Steel fibers have moderate contribution in ductility of unconfined specimens under axial compression. This effect is pronounced more with the contribution of confinement

7. In general, results confirmed that the load carrying capacity of unconfined samples exposed to acid was significantly reduced whereas GRP-confined specimens exposed acid solution maintained their load carrying capacity. GRP confinement have also improved the post peak behavior and ductility.

8. The results showed that the addition of steel fiber gave an insignificant effect in stress and strain. In addition, a limited effect was observed when adding this hooked steel fiber.

The second part investigates the residual mechanical characteristics of SCC-filled HDPE tubes with and without steel fibers, after exposure to chemical environment. Influences of HDPE confinement, tube thickness, steel fiber addition in SCC, and chemical attacks (i.e., sulfate or acid exposure) were key parameters. Following conclusions are drawn based on test results:

1. SCC-filled HDPE tubes can withstand excessive dilation of concrete under compression and make the concrete more ductile with a significant post-peak strain hardening behavior. Fracture energy of confined specimens exposed to water is significantly higher (up to 55 times) as compared to unconfined counterparts. In addition, the specimens can maintain integrity, as a result of excessive plastic deformation capacity of HDPE confinement.

2. HDPE hollow tubes do not suffer from extreme environmental conditions significantly. They can demonstrate high residual load-strain behavior even after exposure to various type of chemicals.

3. Presence of steel fibers has little contribution to maximum load capacity, i.e., 0.3-1 % increase in load capacity. However, steel fiber inclusion increases the fracture energy for up to 20%.

4. Confinement of SCC with HDPE pipes has little contribution in peak load for specimens exposed to water, due to low elastic modulus and yield strength of HDPE pipes. After peak load, however, a strain-softening post-peak behavior is observed with an excessively higher energy absorption capacity, hence the ductility is increased significantly, i.e. after acid exposure, 174 times higher fracture energy as compared unconfined counterpart in the same environment.

5. Pipe thickness has a substantial effect on the post-peak behavior of HDPE-confined SCC tubes. Energy absorption capacity of specimens with thicker confinement is improved significantly, owing to the enhanced plastic deformation capacity of tubes with larger thickness, i.e., increasing tube thickness by 30% results in up to 50% higher fracture energy.

The third part investigates the flexural performance of (DST-HDPE) and HDPE composite beams depending on the findings that provided in the study, the subsequent conclusions can be shown: After flexural test of HDPE-6 and HDPE-12 specimens, it can be seen that almost similar strain and compressive strength are recovered.

1. The HDPE tube high tensile strength prevents the completing rupture of the tube while the final collapse stage is yielded and deformed accordingly with showing any crack on the surface.

2. HDPE confinement of SCGP is significantly enhanced the ductility of beams which as result, ultimating axial strain under flexural loading that significantly increased. The enhancement of axial displacement up to 23 cm showed that the ductility of such as composite beams is far beyond the brittle range of plain concrete strain which is roughly 5 cm.

3. The HDPE tube thickness effect on mechanical performance of composite beam was significant. The thicker (1.3cm) tubes almost showed a behavior alike the full HDPE-confined ideal model, while the 1.0cm HDPE tubes also showed a similar range of ductility and energy absorption, but it was noticed that the thicker the thickness of HDPE tubes, the higher is the energy absorption of beam.

4. Flexural capabilities of DST-HDPE could be increased improved by using SCGP-filling of their interior steel tubes .No detrimental effect of SCGP - filling was noticed on the ductility of DST-HDPE.

5. In general, The findings indicate that (HDPE) tubes are able to enhancing ultra-high ductile performance and besides its exhibiting to recovery behavior in (deflection capacity and flexural strength), however; tubes confinement has also improved the post peak behavior and ductility.

5.2 Recommendations for future work

Based on the findings and conclusions of the current study, the followingrecommendations are made for future research:

1. More research is needed to study the effect of internal steeltube on thebehaviour of composite (beams and columns).

2. Research is needed to systematically investigate the size effect on the flexuralstrength of composite beams.

3. Additional experimental works on large scale composite beamsare needed toinvestigating the applicability of the proposed equations of this study to predict the effective moment of inertia.

4. Research is needed to quantify the compressive strength of short and slendercomposite columns reinforced with basalt or carbon FRP bars.

5. More experiments works on large scale composite columns are needed to investigatethe applicability of the proposed equations of this study to predict the yield andultimate compressive strength of composite columns.

6. More research is needed to study the construction joints of the FRP.

7. More research is needed to study the control of the porous problem inside tubes after concrete hardening.

8. More research is needed to study the check and monitor the serviceability requirements such as (cracks) in case of using polymer covers.

References

440, A. C. I. C. (1996). State-of-the-art Report on Fiber Reinforced Plastic (FRP) Reinforcement for Concrete Structures: ACI 440R-96. American Concrete Institute.

Abdulla, N. A. (2017). Concrete filled PVC tube: A review. *Construction and Building Materials*, *156*, 321–329.

Alsubari, B., Shafigh, P., & Jumaat, M. Z. (2015). Development of self-consolidating high strength concrete incorporating treated palm oil fuel ash. *Materials*, *8***(5)**, 2154–2173.

Altun, F., Haktanir, T., & Ari, K. (2007). Effects of steel fiber addition on mechanical properties of concrete and RC beams. *Construction and Building Materials*, *21***(3)**, 654–661.

Alwan, J. M., Naaman, A. E., & Guerrero, P. (1999). Effect of mechanical clamping on the pull-out response of hooked steel fibers embedded in cementitious matrices. *Concrete Science and Engineering*, *1***(1)**, 15–25.

Andini, S., Cioffi, R., Colangelo, F., Grieco, T., Montagnaro, F., & Santoro, L. (2008). Coal fly ash as raw material for the manufacture of geopolymer-based products. *Waste Management*, *28***(2)**, 416–423.

Anuradha, R., Sreevidya, V., Venkatasubramani, R., & Rangan, B. V. (2012). Modified guidelines for geopolymer concrete mix design using Indian standard.

Anuradha, R., Sreevidya, V., Venkatasubramani, R., Rangan, B. V, Ozbakkaloglu, T., Fanggi, B. L., … Dong, S. L. (2013). Composite tubes as an alternative to steel spirals for concrete members in bending and shear. *Journal of Composites for Construction*, *17***(2)**, 961–974. https://doi.org/10.1016/j.compositesb.2007.04.001

ASTM C39/C39M-01. (2003). Standard test method for compressive strength of

cylindrical concrete specimens. *American Society for Testing and Materials, West Conshohocken, USA*.

ASTM C496-96. (2003). Standard test method for splitting tensile strength of cylindrical concrete specimens. *American Society for Testing and Materials, West Conshohocken, USA*.

Barris, C., Torres, L., Comas, J., & Mias, C. (2013). Cracking and deflections in GFRP RC beams: an experimental study. *Composites Part B: Engineering*, **55**, 580–590.

Behr, M., Rosentritt, M., Regnet, T., Lang, R., & Handel, G. (2004). Marginal adaptation in dentin of a self-adhesive universal resin cement compared with well-tried systems. *Dental Materials*, **20(2)**, 191–197.

Benmokrane, B., El-Salakawy, E., El-Ragaby, A., & Lackey, T. (2006). Designing and testing of concrete bridge decks reinforced with glass FRP bars. *Journal of Bridge Engineering*, **11(2)**, 217–229.

Celik, K., Meral, C., Gursel, A. P., Mehta, P. K., Horvath, A., & Monteiro, P. J. M. (2015). Mechanical properties, durability, and life-cycle assessment of self-consolidating concrete mixtures made with blended portland cements containing fly ash and limestone powder. *Cement and Concrete Composites*, **56**, 59–72.

Choi, E., Kim, J.-W., Rhee, I., & Kang, J.-W. (2014). Behavior and modeling of confined concrete cylinders in axial compression using FRP rings. *Composites Part B: Engineering*, **58**, 175–184.

Chun, S. S., & Park, H. C. (2002). Load carrying capacity and ductility of RC columns confined by carbon fiber reinforced polymer. In *Proc., 3rd Int. Conf. on Composites in Infrastructure*. Univ. of Arizona San Francisco.

Cole, B., & Fam, A. (2006). Flexural load testing of concrete-filled FRP tubes with longitudinal steel and FRP rebar. *Journal of Composites for Construction*, **10(2)**, 161–171.

Dai, J.-G., Bai, Y.-L., & Teng, J. G. (2011). Behavior and modeling of concrete confined with FRP composites of large deformability. *Journal of Composites for Construction*, **15(6)**, 963–973.

Davidovits, J. (1988). Geopolymer chemistry and properties. In *Geopolymer* (Vol. **88**, pp. 25–48).

De Lorenzis, L., & Teng, J. G. (2007). Near-surface mounted FRP reinforcement: An emerging technique for strengthening structures. *Composites Part B: Engineering*, *38***(2)**, 119–143.

Deluce, J. R., & Vecchio, F. J. (2013). Cracking Behavior of Steel Fiber-Reinforced Concrete Members Containing Conventional Reinforcement. *ACI Structural Journal*, *110*(3).

Dubey, R., & Kumar, P. (2012). Effect of superplasticizer dosages on compressive strength of self compacting concrete. *International Journal of Civil and Structural Engineering*, *3***(2)**, 360.

EFNARC. (2005). The European Guidelines for Self-Compacting Concrete: Specification, Production and Use. *The European Guidelines for Self Compacting Concrete*, (May), 68.

El Chabib, H., Nehdi, M., & El Naggar, M.-H. (2005). Behavior of SCC confined in short GFRP tubes. *Cement and Concrete Composites*, *27***(1)**, 55–64.

Ernst, S., Bridge, R. Q., & Wheeler, A. (2010). Correlation of beam tests with pushout tests in steel-concrete composite beams. *Journal of Structural Engineering*, *136***(2)**, 183–192.

Fakharifar, M., & Chen, G. (2016). Compressive behavior of FRP-confined concrete-filled PVC tubular columns. *Composite Structures*, *141*, 91–109.

Fam, A., Cole, B., & Mandal, S. (2007). Composite tubes as an alternative to steel spirals for concrete members in bending and shear. *Construction and Building Materials*, *21***(2)**, 347–355. https://doi.org/10.1016/j.conbuildmat.2005.08.016

Fam, A., & Rizkalla, S. (2003). Large scale testing and analysis of hybrid concrete/composite tubes for circular beam-column applications. *Construction and Building Materials*, *17***(6–7)**, 507–516.

Fam, A. Z., & Rizkalla, S. H. (2001). Confinement model for axially loaded concrete confined by circular fiber-reinforced polymer tubes. *Structural Journal*, *98***(4)**, 451–461.

Fanella, D. A., & Naaman, A. E. (1985). Stress-strain properties of fiber reinforced mortar in compression. *Journal of the American Concrete Institute*, *82***(4)**, 475–483.

Feng, P., Cheng, S., Bai, Y., & Ye, L. (2015). Mechanical behavior of concrete-filled square steel tube with FRP-confined concrete core subjected to axial compression. *Composite Structures*, *123*, 312–324.

Ferdous, W., Manalo, A., Khennane, A., & Kayali, O. (2015). Geopolymer concrete-filled pultruded composite beams–concrete mix design and application. *Cement and Concrete Composites*, *58*, 1–13.

Grdic, Z. J., Toplicic-Curcic, G. A., Despotovic, I. M., & Ristic, N. S. (2010). Properties of self-compacting concrete prepared with coarse recycled concrete aggregate. *Construction and Building Materials*, *24***(7)**, 1129–1133.

Gupta, P. K., & Verma, V. K. (2016). Study of concrete-filled unplasticized poly-vinyl chloride tubes in marine environment. *Proceedings of the Institution of Mechanical Engineers, Part M: Journal of Engineering for the Maritime Environment*, *230***(2)**, 229–240.

Hollaway, L. C., & Teng, J.-G. (2008). *Strengthening and rehabilitation of civil infrastructures using fibre-reinforced polymer (FRP) composites*. Elsevier.

Huang, L., Yu, T., Zhang, S. S., & Wang, Z. Y. (2017). FRP-confined concrete-encased cross-shaped steel columns: Concept and behaviour. *Engineering Structures*, *152*, 348–358. https://doi.org/10.1016/j.engstruct.2017.09.011

Idris, Y., & Ozbakkaloglu, T. (2015). Flexural behavior of FRP-HSC-steel double skin tubular beams under reversed-cyclic loading. *Thin-Walled Structures*, *87*, 89–101. https://doi.org/10.1016/j.tws.2014.11.003

Jamaluddin, N., Azeez, A. A., Rahman, N. A., Attiyah, A. N., Ibrahim, M. H. W., Mohamad, N., & Adnan, S. H. (2017). Experimental Investigation of Concrete Filled PVC Tube Columns Confined By Plain PVC Socket. In *MATEC Web of Conferences* (Vol. **103**, p. 2006). EDP Sciences.

Jiang, S.-F., Ma, S.-L., & Wu, Z.-Q. (2014). Experimental study and theoretical analysis on slender concrete-filled CFRP–PVC tubular columns. *Construction*

and Building Materials, *53*, 475–487.

Karimi, K., Tait, M. J., & El-Dakhakhni, W. W. (2011a). Influence of slenderness on the behavior of a FRP-encased steel-concrete composite column. *Journal of Composites for Construction*, *16*(**1**), 100–109.

Karimi, K., Tait, M. J., & El-Dakhakhni, W. W. (2011b). Testing and modeling of a novel FRP-encased steel–concrete composite column. *Composite Structures*, *93*(**5**), 1463–1473.

Khalifa, M. A., Hodhod, O. A., & Zaki, M. A. (1996). Analysis and design methodology for an FRP cable-stayed pedestrian bridge. *Composites Part B: Engineering*, *27*(**3–4**), 307–317.

Lam, L., & Teng, J. G. (2003). Design-oriented stress–strain model for FRP-confined concrete. *Construction and Building Materials*, *17*(**6–7**), 471–489.

Louk Fanggi, B. A., & Ozbakkaloglu, T. (2013). Compressive behavior of aramid FRP-HSC-steel double-skin tubular columns. *Construction and Building Materials*, *48*, 554–565. https://doi.org/10.1016/j.conbuildmat.2013.07.029

Manalo, A., Benmokrane, B., Park, K.-T., & Lutze, D. (2014). Recent developments on FRP bars as internal reinforcement in concrete structures. *Concrete in Australia*, *40*(**2**), 46–56.

Mander, J. B., Priestley, M. J. N., & Park, R. (1988). Theoretical stress-strain model for confined concrete. *Journal of Structural Engineering*, *114*(**8**), 1804–1826.

Matthys, S., Toutanji, H., & Taerwe, L. (2006). Stress–strain behavior of large-scale circular columns confined with FRP composites. *Journal of Structural Engineering*, *132*(**1**), 123–133.

Memon, F. A., Nuruddin, M. F., Khan, S., Shafiq, N., & Ayub, T. (2013). Effect of sodium hydroxide concentration on fresh properties and compressive strength of self-compacting geopolymer concrete. *Journal of Engineering Science and Technology*, *8*(**1**), 44–56.

Mirmiran, A. (2003). Stay-in-place FRP form for concrete columns. *Advances in Structural Engineering*, *6*(**3**), 231–241.

Mirmiran, A., & Shahawy, M. (1995). A novel FRP-concrete composite construction for the infrastructure. In *Restructuring: America and Beyond* (pp. 1663–1666). ASCE.

Hakimi, A. (2017). Concrete filled glass fiber reinforced polymer (GFRP) short column (Master dissertation). Gaziantep University.

Mirmiran, A., Shahawy, M., & Beitleman, T. (2001). Slenderness limit for hybrid FRP-concrete columns. *Journal of Composites for Construction*, *5*(**1**), 26–34.

Nanni, A., & Bradford, N. M. (1995). FRP jacketed concrete under uniaxial compression. *Construction and Building Materials*, *9*(**2**), 115–124.

Nanni, A., Norris, M. S., & Bradford, N. M. (1993). Lateral confinement of concrete using FRP reinforcement. *Special Publication*, *138*, 193–210.

Nuruddin, M. F., Demie, S., Ahmed, M. F., Shafiq, N., Fareed Ahmed, M., & Fadhil Nuruddin, M. (2011). Effect of Superplasticizer and NaOH Molarity on Workability, Compressive Strength and Microstructure Properties of Self-Compacting Geopolymer Concrete. *World Academy of Science, Engineering and Technology*, *74*(**3**), 8–14. https://doi.org/10.1139/l11-077

Okamura, H., & Ouchi, M. (1999). SCC Development, present use and future. In *Int. Symp. RILEM, Sztokholm, wrzesień* (Vol. *3*).

Olivia, M., & Nikraz, H. (2012). Properties of fly ash geopolymer concrete designed by Taguchi method. *Materials & Design (1980-2015)*, *36*, 191–198.

Ouchi, M., Nakamura, S.-A., Osterberg, T., Hallberg, S., & Lwin, M. (2003). Applications of self-compacting concrete in Japan, Europe and the United States. *Kochi University of Technology, Kochi, Japan*.

Ozbakkaloglu, T. (2013). Behavior of square and rectangular ultra high-strength concrete-filled FRP tubes under axial compression. *Composites Part B: Engineering*, *54*, 97–111.

Ozbakkaloglu, T., & Fanggi, B. A. L. (2015). FRP–HSC–steel composite columns: behavior under monotonic and cyclic axial compression. *Materials and Structures*, *48*(**4**), 1075–1093.

Ozbakkaloglu, T., & Lim, J. C. (2013). Axial compressive behavior of FRP-confined

concrete: Experimental test database and a new design-oriented model. *Composites Part B: Engineering*, **55**, 607–634.

Pan, Y., Guo, R., Li, H., Tang, H., & Huang, J. (2017). Analysis-oriented stress–strain model for FRP-confined concrete with preload. *Composite Structures*, **166**, 57–67.

Persson, B. (2001). A comparison between mechanical properties of self-compacting concrete and the corresponding properties of normal concrete. *Cement and Concrete Research*, **31**(**2**), 193–198.

Qian, J. R., & Liu, M. X. (2006). Experiment of FRP-concrete-steel double-skin tubular long columns under axial compressive load. *Concrete*, **9**, 31–34.

Rovero, L., Focacci, F., & Stipo, G. (2012). Structural behavior of arch models strengthened using fiber-reinforced polymer strips of different lengths. *Journal of Composites for Construction*, **17**(**2**), 249–258.

Saafi, M., Toutanji, H. A., & Li, Z. (1999). Behavior of concrete columns confined with fiber reinforced polymer tubes. *ACI Materials Journal*, **96**(**4**), 500–509.

Sarker, P. (2008). *A constitutive model for fly ash-based geopolymer concrete*. *Archit Civil Eng Environ* (Vol. **1**).

Sciolti, M. S., Frigione, M., & Aiello, M. A. (2010). Wet lay-up manufactured FRPs for concrete and masonry repair: influence of water on the properties of composites and on their epoxy components. *Journal of Composites for Construction*, **14**(**6**), 823–833.

Song, P. S., & Hwang, S. (2004). Mechanical properties of high-strength steel fiber-reinforced concrete. *Construction and Building Materials*, **18**(**9**), 669–673.

Teng, J. G., & Lam, L. (2002). Compressive behavior of carbon fiber reinforced polymer-confined concrete in elliptical columns. *Journal of Structural Engineering*, **128**(**12**), 1535–1543.

Teng, J. G., Yu, T., & Fernando, D. (2012). Strengthening of steel structures with fiber-reinforced polymer composites. *Journal of Constructional Steel Research*, **78**, 131–143.

Teng, J. G., Yu, T., & Wong, Y. L. (2011). Hybrid FRP-concrete-steel double-skin tubular structural members. In *Advances in FRP Composites in Civil Engineering* (pp. 26–32). Springer.

Teng, J. G., Yu, T., Wong, Y. L., & Dong, S. L. (2007). Hybrid FRP–concrete–steel tubular columns: concept and behavior. *Construction and Building Materials*, *21*(**4**), 846–854.

Thériault, M., & Neale, K. W. (2000). Design equations for axially loaded reinforced concrete columns strengthened with fibre reinforced polymer wraps. *Canadian Journal of Civil Engineering*, *27*(**5**), 1011–1020.

Tiberti, G., Minelli, F., & Plizzari, G. (2015). Cracking behavior in reinforced concrete members with steel fibers: a comprehensive experimental study. *Cement and Concrete Research*, *68*, 24–34.

Topcu, I. B., Bilir, T., & Uygunoğlu, T. (2009). Effect of waste marble dust content as filler on properties of self-compacting concrete. *Construction and Building Materials*, *23*(**5**), 1947–1953.

Vejmelková, E., Keppert, M., Grzeszczyk, S., Skaliński, B., & Černý, R. (2011). Properties of self-compacting concrete mixtures containing metakaolin and blast furnace slag. *Construction and Building Materials*, *25*(**3**), 1325–1331.

Villa, C., Pecina, E. T., Torres, R., & Gómez, L. (2010). Geopolymer synthesis using alkaline activation of natural zeolite. *Construction and Building Materials*, *24*(**11**), 2084–2090.

Vincent, T., & Ozbakkaloglu, T. (2013). Influence of concrete strength and confinement method on axial compressive behavior of FRP confined high-and ultra high-strength concrete. *Composites Part B: Engineering*, *50*, 413–428.

Wang, B., Teng, J.-G., De Lorenzis, L., Zhou, L.-M., Ou, J., Jin, W., & Lau, K. T. (2009). Strain monitoring of RC members strengthened with smart NSM FRP bars. *Construction and Building Materials*, *23*(**4**), 1698–1711.

Wang, R., Han, L. H., & Tao, Z. (2015). Behavior of FRP-concrete-steel double skin tubular members under lateral impact: Experimental study. *Thin-Walled Structures*, *95*, 363–373. https://doi.org/10.1016/j.tws.2015.06.022

Wang, X., & Wu, Z. (2011). Vibration control of different FRP cables in long-span cable-stayed bridge under indirect excitations. *Journal of Earthquake and Tsunami*, *5*(**2**), 167–188.

Wong, Y. L., Yu, T., Teng, J. G., & Dong, S. L. (2008). Behavior of FRP-confined concrete in annular section columns. *Composites Part B: Engineering*, *39*(**3**), 451–466.

Xu, H., & Van Deventer, J. S. J. (2000). The geopolymerisation of alumino-silicate minerals. *International Journal of Mineral Processing*, *59*(**3**), 247–266.

Yoo, D.-Y., Shin, H.-O., Yang, J.-M., & Yoon, Y.-S. (2014). Material and bond properties of ultra high performance fiber reinforced concrete with micro steel fibers. *Composites Part B: Engineering*, *58*, 122–133.

Yoo, D.-Y., Yoon, Y.-S., & Banthia, N. (2015). Flexural response of steel-fiber-reinforced concrete beams: Effects of strength, fiber content, and strain-rate. *Cement and Concrete Composites*, *64*, 84–92.

Yu, T., & Remennikov, A. M. (2013). Hybrid double-skin tubular members for sustainable mining infrastructure.

Yu, T., & Teng, J. G. (2012). Behavior of hybrid FRP-concrete-steel double-skin tubular columns with a square outer tube and a circular inner tube subjected to axial compression. *Journal of Composites for Construction*, *17*(**2**), 271–279.

Yu, T., Wong, Y. L., Teng, J. G., Dong, S. L., & Lam, E. S. (2006). Flexural behavior of hybrid FRP-concrete-steel double-skin tubular members. *Journal of Composites for Construction*, *10*(**5**), 443–452.

Zaghi, A. E., Saiidi, M. S., & Mirmiran, A. (2012). Shake table response and analysis of a concrete-filled FRP tube bridge column. *Composite Structures*, *94*(**5**), 1564–1574.

Zaman, A., Gutub, S. A., & Wafa, M. A. (2013). A review on FRP composites applications and durability concerns in the construction sector. *Journal of Reinforced Plastics and Composites*, *32*(**24**), 1966–1988.

Zhao, J. (2017). Behaviour and modelling of large-scale hybrid FRP-concrete-steel double-skin tubular beams with shear connectors. The Hong Kong Polytechnic

University.

Zhu, Z., Ahmad, I., & Mirmiran, A. (2005). Effect of column parameters on axial compression behavior of concrete-filled FRP tubes. *Advances in Structural Engineering*, *8***(4)**, 443–449.

Appendix A.

The title of first part: Experimental investigation on the short-term durability of self-compacting concrete-filled GRP tubular columns

Figure (A1) cutting of GRP tube
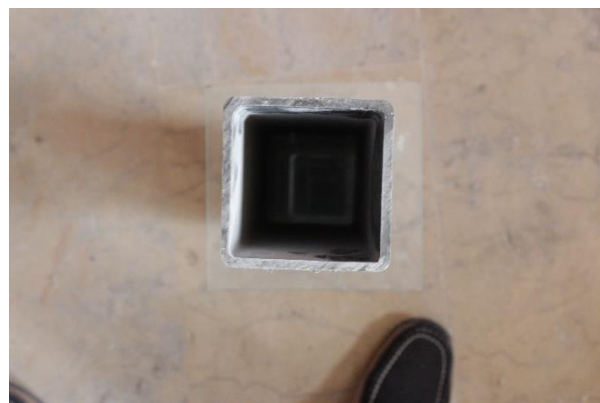
Figure (A2) GRP tubes before the casting

Figure (A3) GRP tube during curing

Figure (A4) GRP tube prepare to test

Figure (A5) GRP tube (GC-SCC-G1-0%-W) step1 for the test

Figure (A6) GRP tube (GC-SCC-G1-0%-W) step 2 for the test

Figure (A7) GRP tube (GC-SCC-G1-0%-W) step 3 for the test
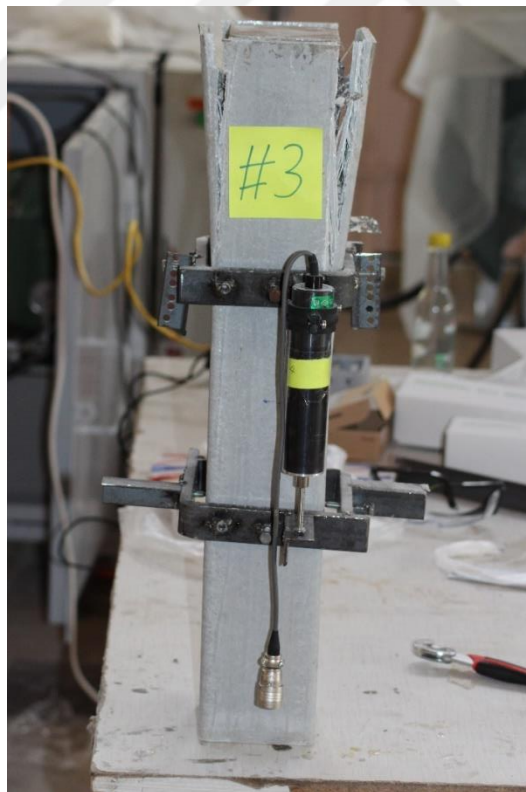
Figure (A8) GRP tube (GC-SCC-G1-0%-W) after test

Figure (A9) GRP tube (GC-SCC-G1-0%-W) after test

Figure (A10) GRP tube (GC-SCC-G1-1%-W) after test

Figure (A11) GRP tube (GC-SCC-G1-1%-W) after test

Figure (A12) GRP tube (GC-SCC-G1-1%-W) after test

Figure (A13) GRP tube (GC-SCC-G3-0%-W) step 1 for the test

Figure (A14) GRP tube (GC-SCC-G3-0%-W) step 2 for the test

Figure (A15) GRP tube (GC-SCC-G3-0%-W) after test

Figure (A16) GRP tube (GC-SCC-G3-1%-W) after test

Figure (A17) GRP tube (GC-SCC-G2-0%-W) step 1 for the test

Figure (A18) GRP tube (GC-SCC-G2-0%-W) step 2 for the test

Figure (A19) GRP tube (GC-SCC-G2-1%-W) step 1 for the test

Figure (A20) GRP tube (GC-SCC-G2-1%-W) after testing

Figure (A21) GRP tube (GC-SCC-G2-1%-W) after test

Figure (A22) GRP tube (GC-SCC-G4-0%-W) step 1 for the test
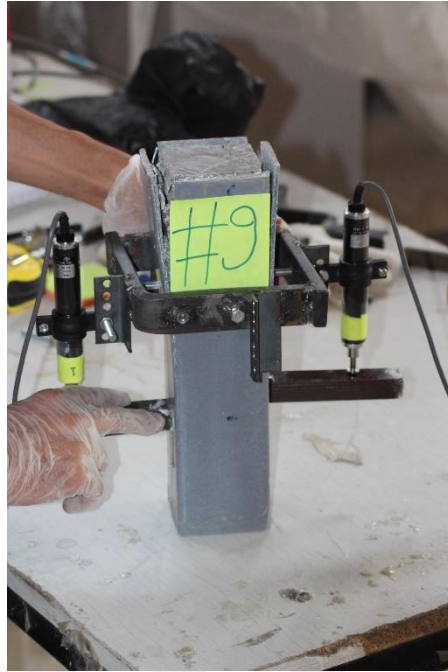
Figure (A23) GRP tube (GC-SCC-G4-0%-W) after test

Figure (A24) GRP tube (GC-SCC-G4-0%-W) after test

Figure (A25) GRP tube (GC-SCC-G4-1%-A) and (GC-SCC-G4-0%-A) after test

Figure (A26) GRP tube (GC-SCC-G2-1%-W) during test
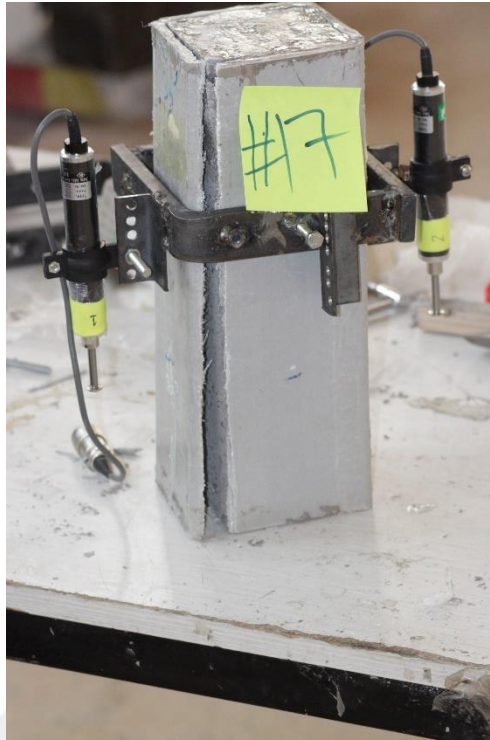
Figure (A27) GRP tube (GC-SCC-G2-1%-W) after test

Figure (A28) GRP tube (GC-SCC-G3-0%-W) after test
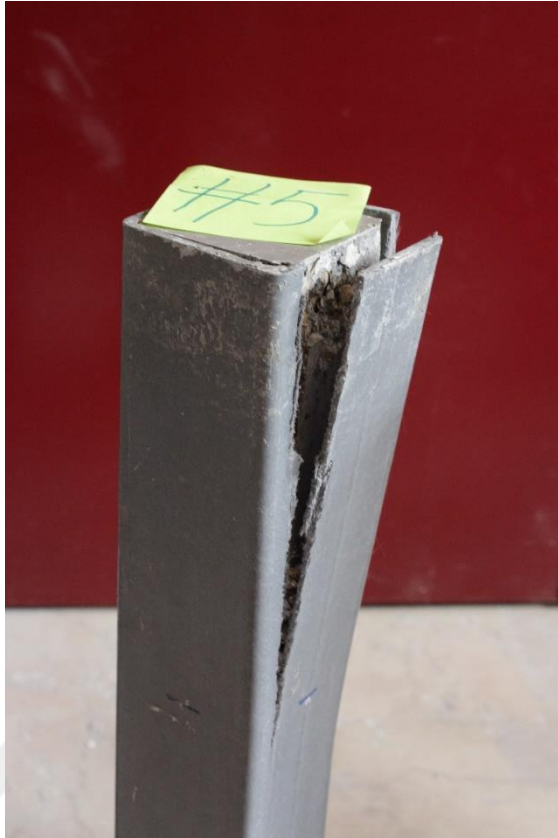
Figure (A29) GRP tube (GC-SCC-G3-0%-W) after test

Figure (A30) GRP tube (GC-SCC-G3-0%-W) after test

Figure (A31) GRP tube (GC-SCC-G3-1%-W) after test

Figure (A32) GRP tube (GC-SCC-G3-1%-W) after test

Figure (A33) GRP tube (GC-SCC-G1-1%-W) after test

Figure (A34) GRP tube (GC-SCC-G1-1%-W) after test
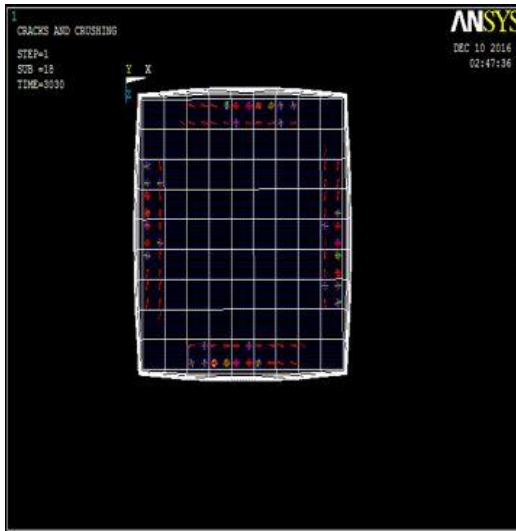
Figure (A35) Perimeter crush of concrete, ANSYS and Experimental sample
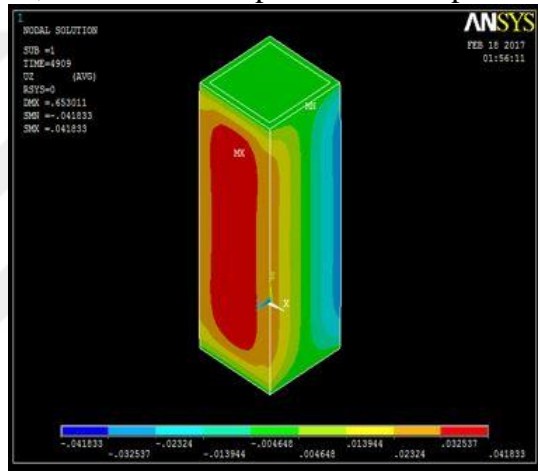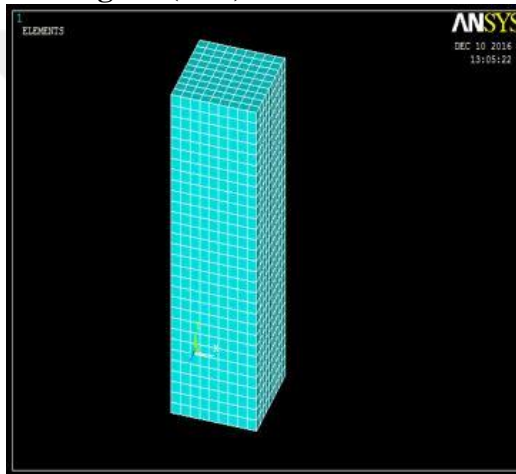
Figure (A36) ANSYS Model representing lateral displacement
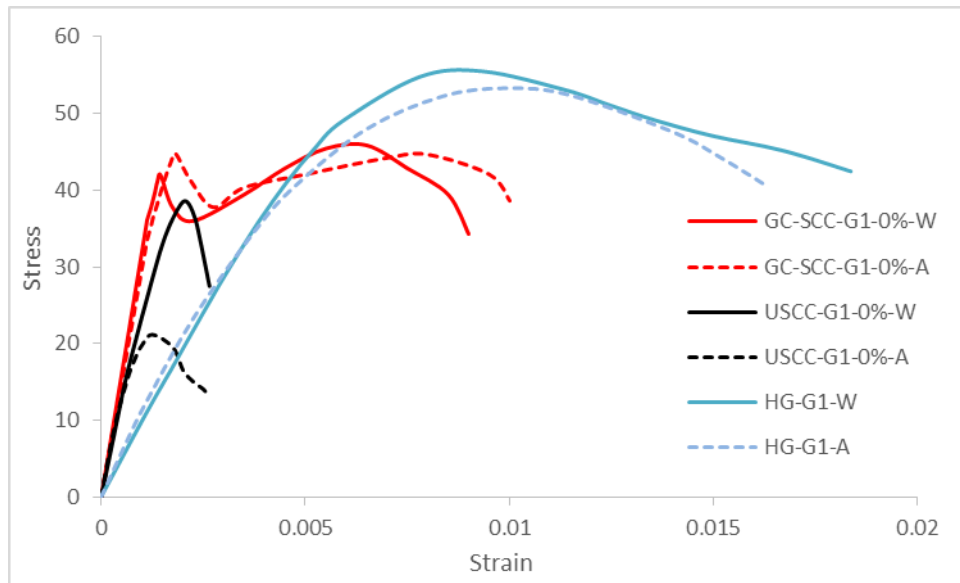
Figure (A37) stress – strain curves for Group 1, with out steel fibers
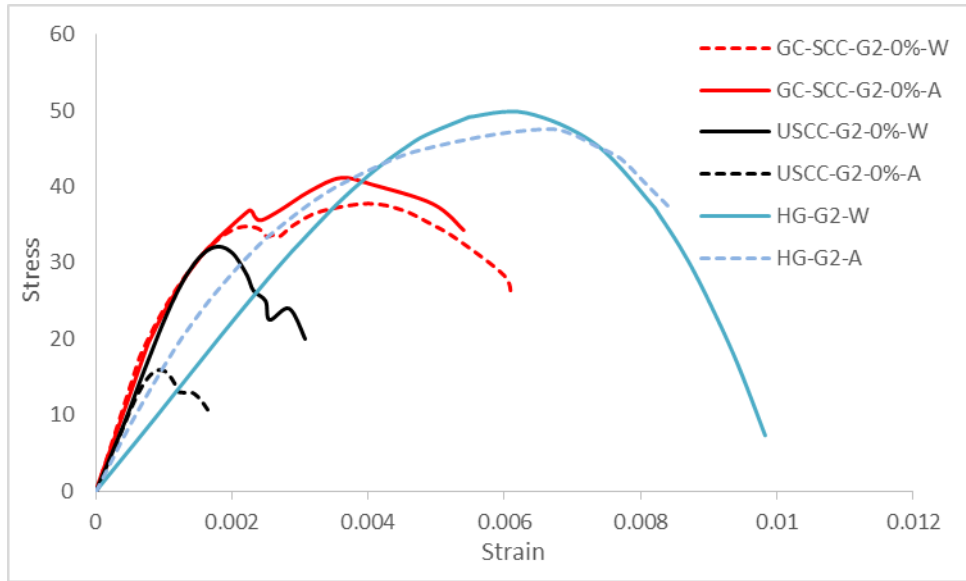
Figure (A38) stress – strain curves for Group 2, with out steel fibers
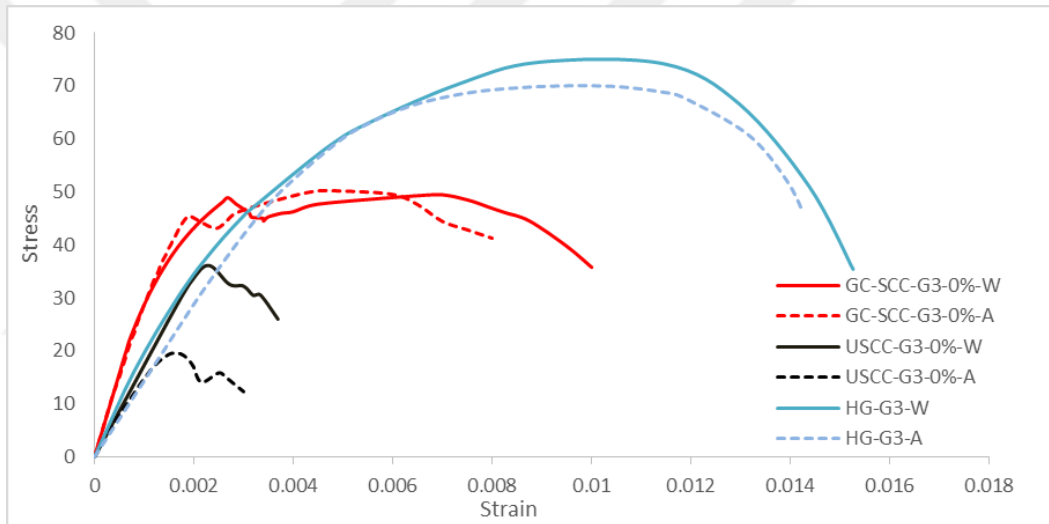
Figure (A39) stress – strain curves for Group 3, with out steel fibers
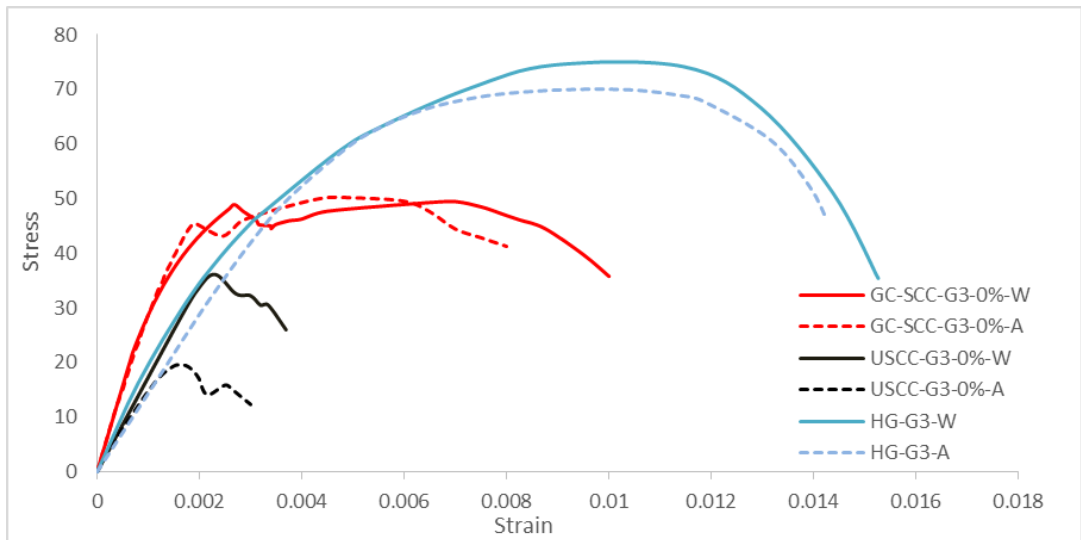
Figure (A40) stress – strain curves for Group 4, with out steel fibers
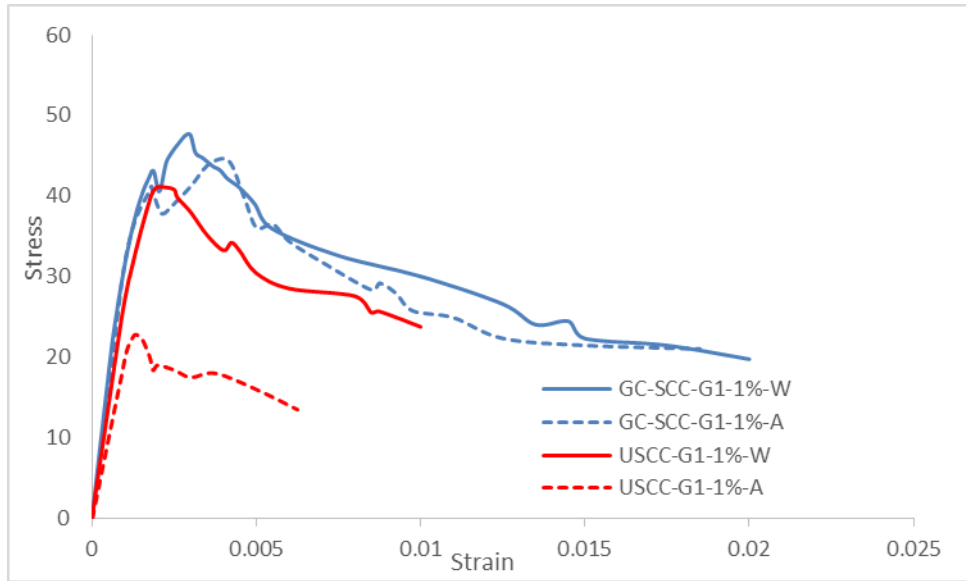
Figure (A41) stress – strain curves for Group 1, with steel fibers
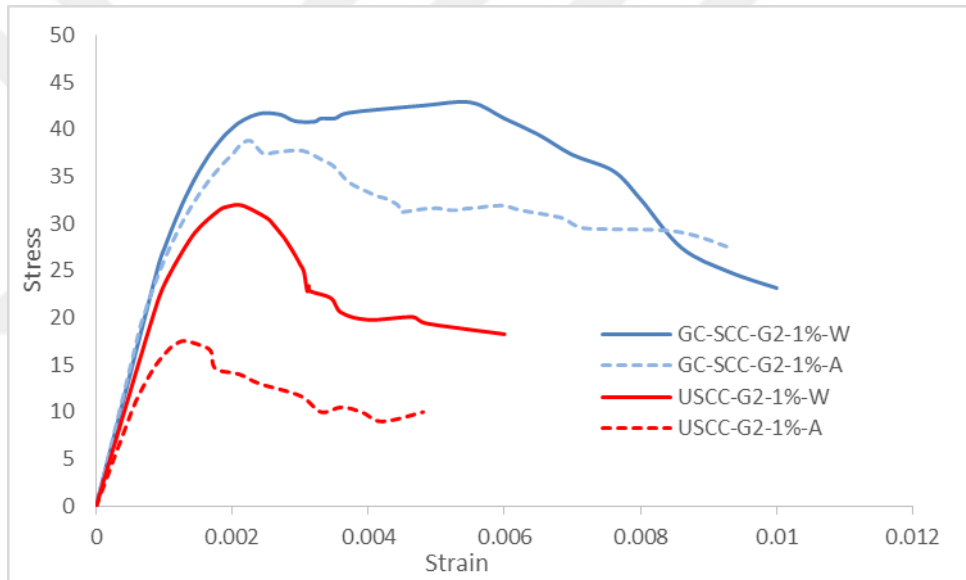
Figure (A42) stress – strain curves for Group 2, with steel fibers
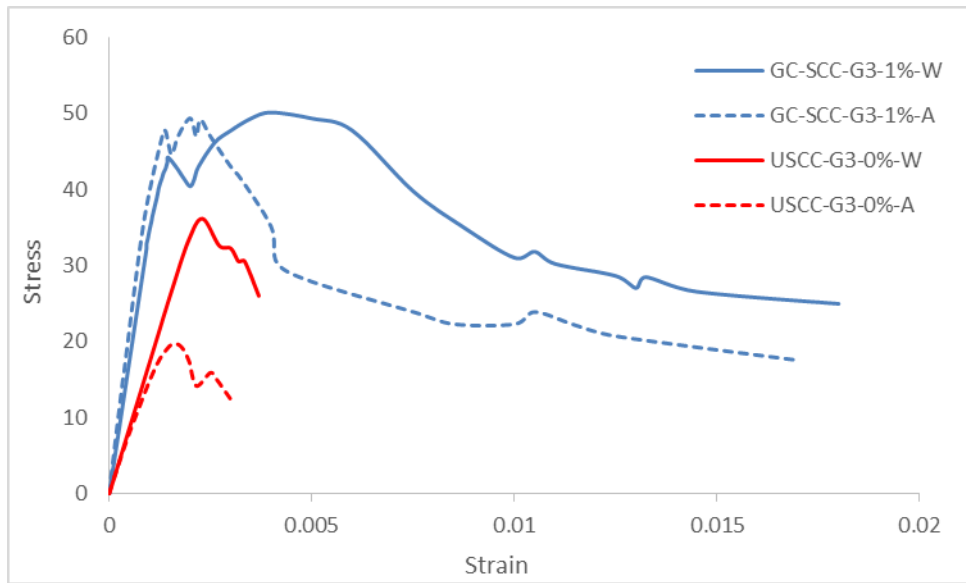
Figure (A43) stress – strain curves for Group 3, with steel fibers
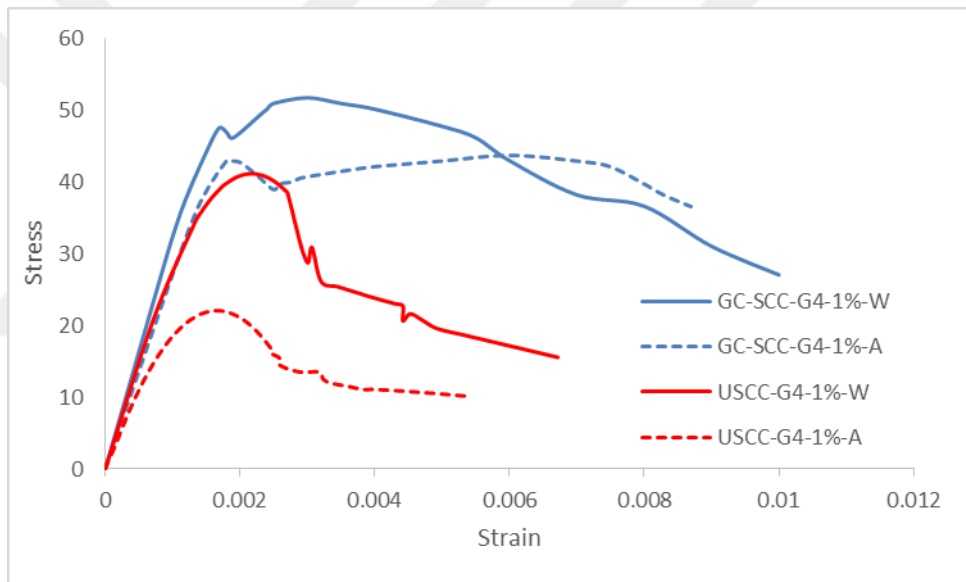
Figure (A44) stress – strain curves for Group 4, with steel fibers

Appendix B.

The title of second part: Mechanical investigation and durability of HDPE-confined SCC columns exposed to severe environment

Figure (B1) first step of cutting HDPE tubes

Figure (B2) second step of cutting HDPE tubes

Figure (B3) HDPE tubes before the casting

Figure (B4) HDPE tubes after the casting
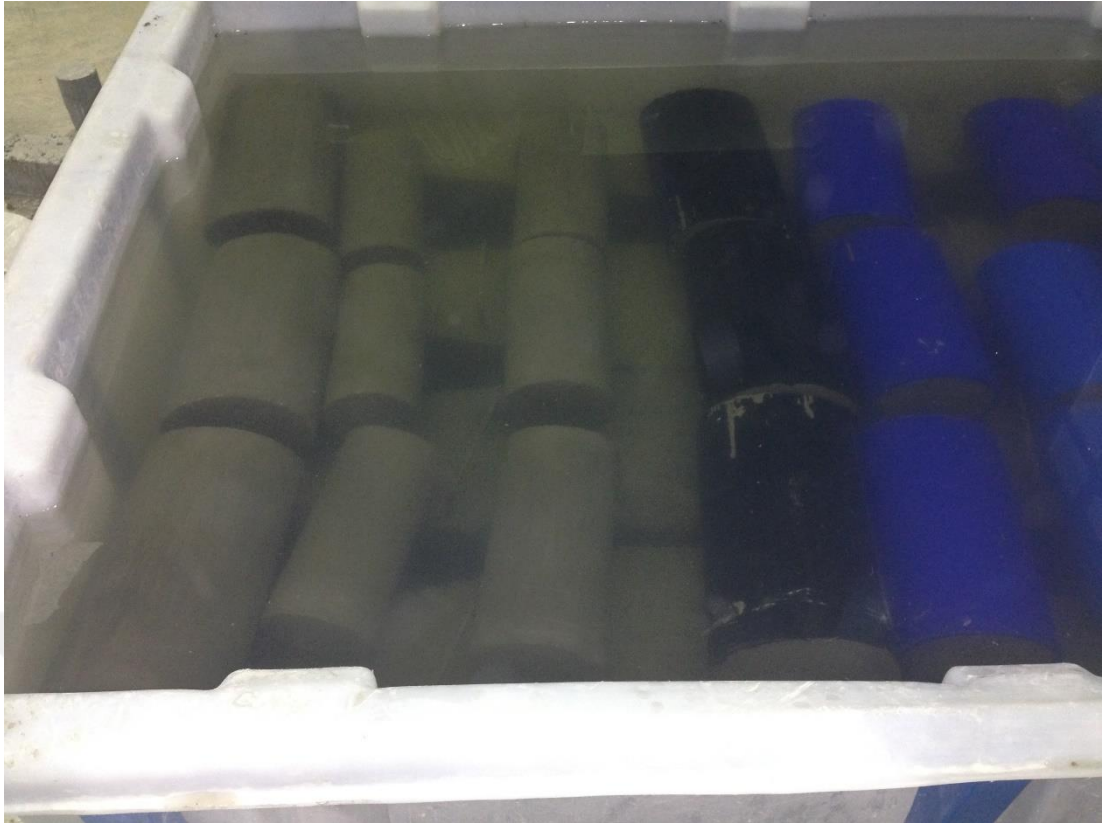
Figure (B5) HDPE tubes during curing

Figure (B6) The acid and sulfate solution were prepared mechanically to insure
the uniform concentration of particles in solution

Figure (B7) HDPE tube (H-G1-W) step 1 for the test

Figure (B8) HDPE tube (H-G1-W) step 2 for the test

Figure (B9) HDPE tube (H-G1-W) step 3 for the test
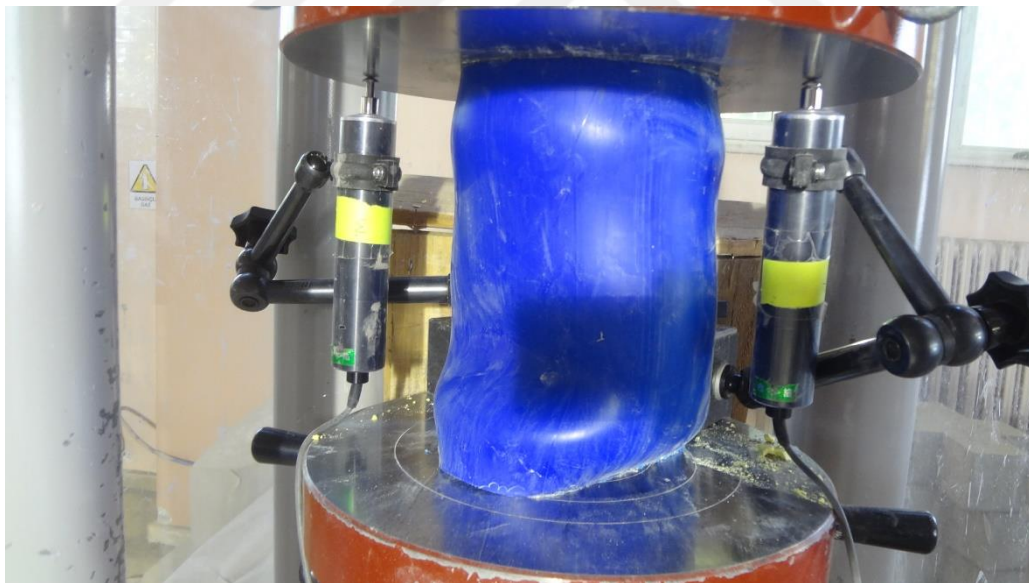
Figure (B10) HDPE tube (H-G1-W) step 4 for the test

Figure (B11) unconfined SCC (USCC-G1-W) step 1 for the test

Figure (B12) unconfined SCC (USCC-G1-W) after test

Figure (B13) HDPE tube (HSCC-G1-1%-S) step 1 for the test

Figure (B14) HDPE tube (HSCC-G1-1%-S) after test

Figure (B15) HDPE tube (HSCC-G2-0%-W) step 1 for the test

Figure (B16) HDPE tube (HSCC-G2-0%-W) step 2 for the test

Figure (B17) HDPE tube (HSCC-G2-0%-W) after test

Figure (B18) HDPE tube (HSCC-G2-0%-W) after test

Figure (B19) HDPE tube (HSCC-G1-1%-A) after test

Figure (B20) HDPE tube (HSCC-G1-1%-A) after test

Figure (B21) HDPE tube (HSCC-G1-1%-A) and (USCC-G1-1%-A) after test

Figure (B22) HDPE tube (USCC-G1-1%-W) , (USCC-G1-1%-S) and (USCC-G1-1%-A) after test
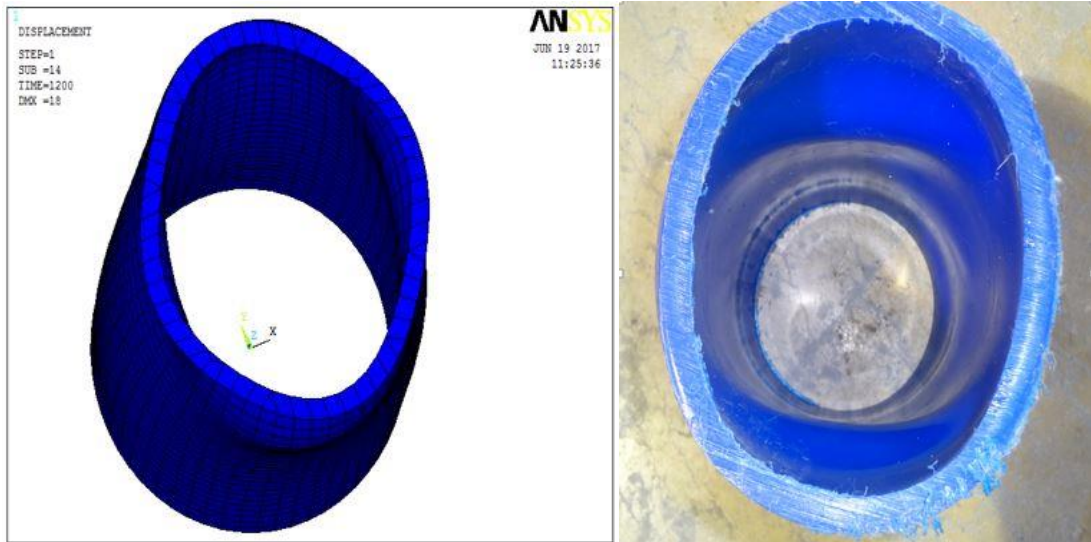
Figure (B23) deformation shape in the ANSYS & Experimental work

Figure (B24) Perimeter crush of concrete, ANSYS and Experimental sample

Appendix C.

The title of third part: Flexural behavior of ultra-high ductile geopolymer HDPE tubes
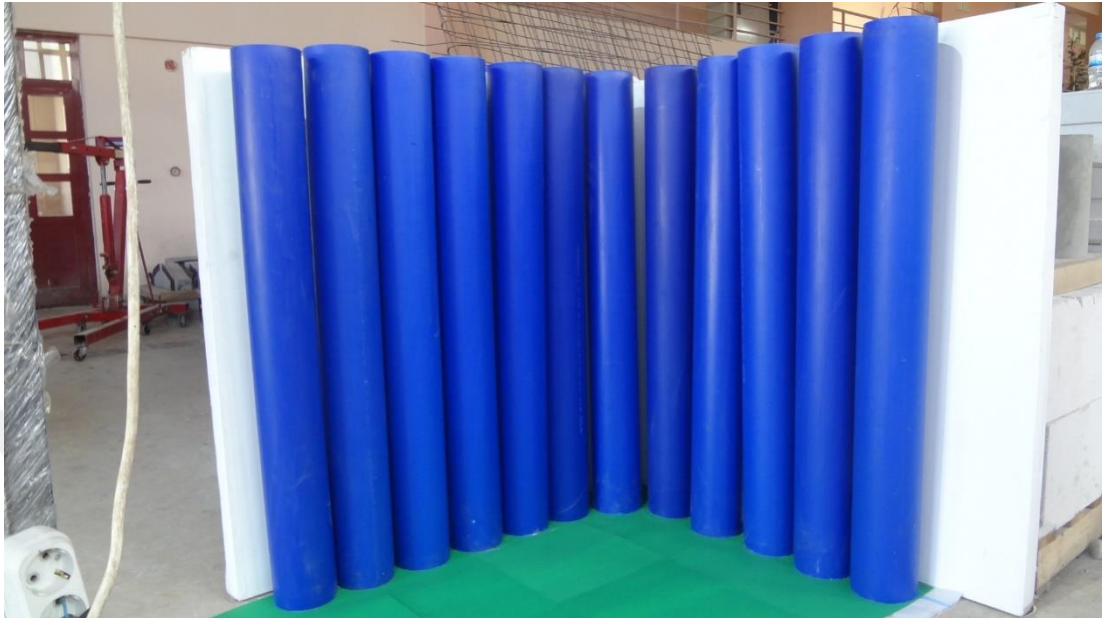
Figure (C1) prepare the HDPE tubes

Figure (C2) prepare the inner steel tubes

Figure (C3) groups of inner steel tubes
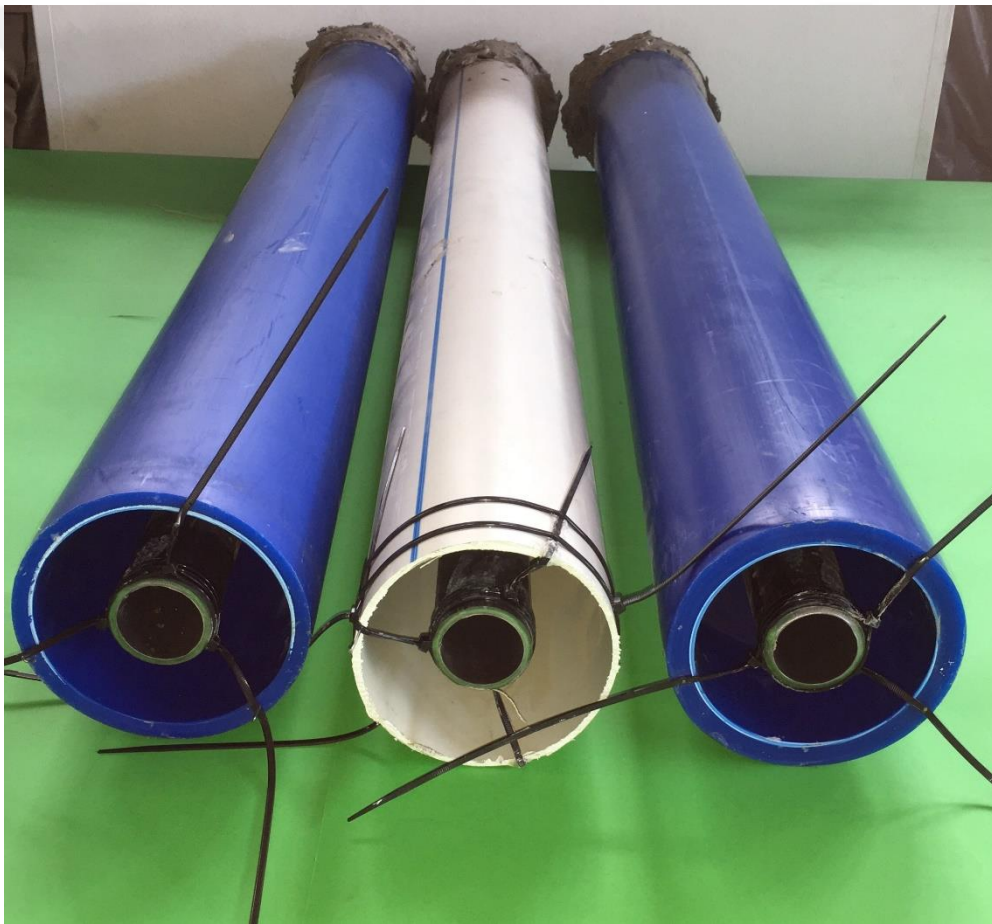
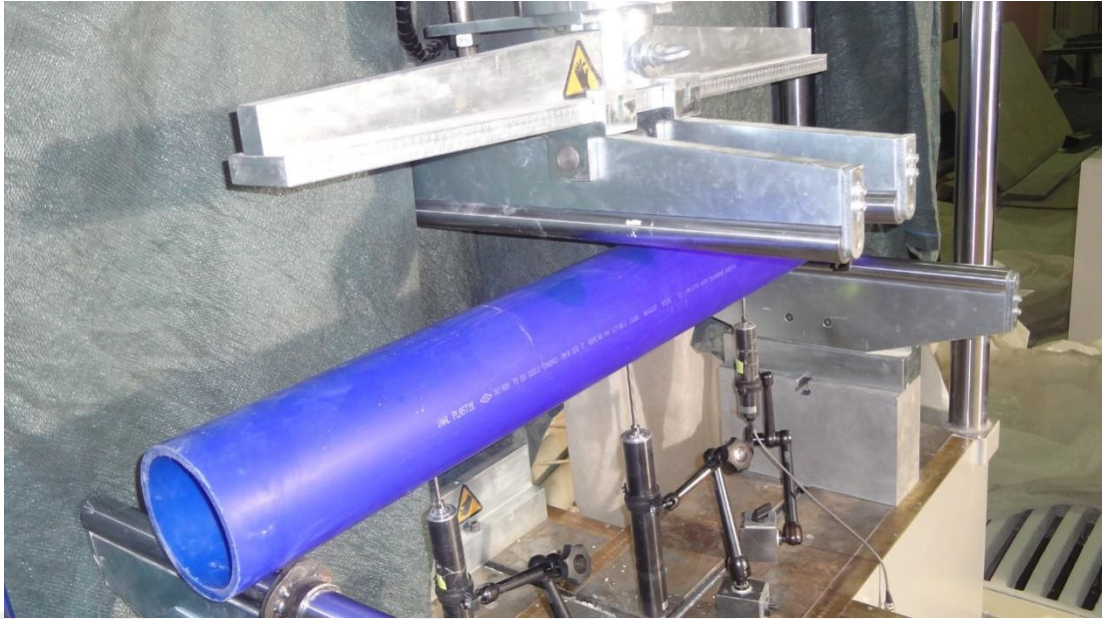**Figure (C4)** process of prepare the composite beams

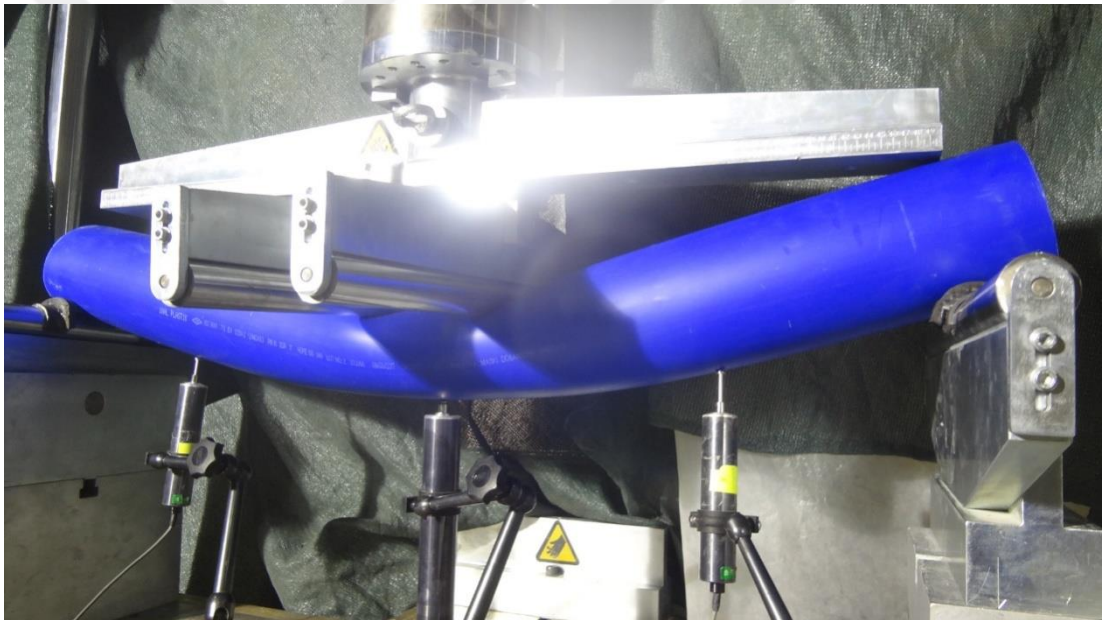**Figure (C5)** HDPE-6 ,step 1 for the test

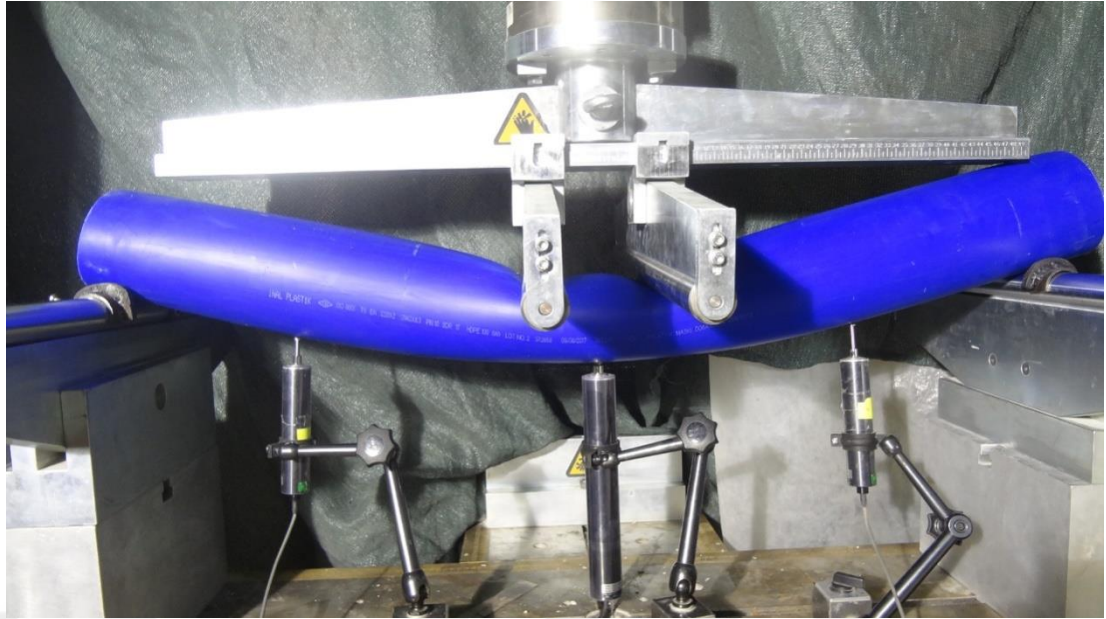**Figure (C6)** HDPE-6 step 2 for the test

Figure (C7) HDPE-6 step 3 for the test

Figure (C8) HDPE-2 step 1 for the test

Figure (C9) HDPE-2 step 2 for the test

Figure (C10) HDPE-2 step 3 for the test
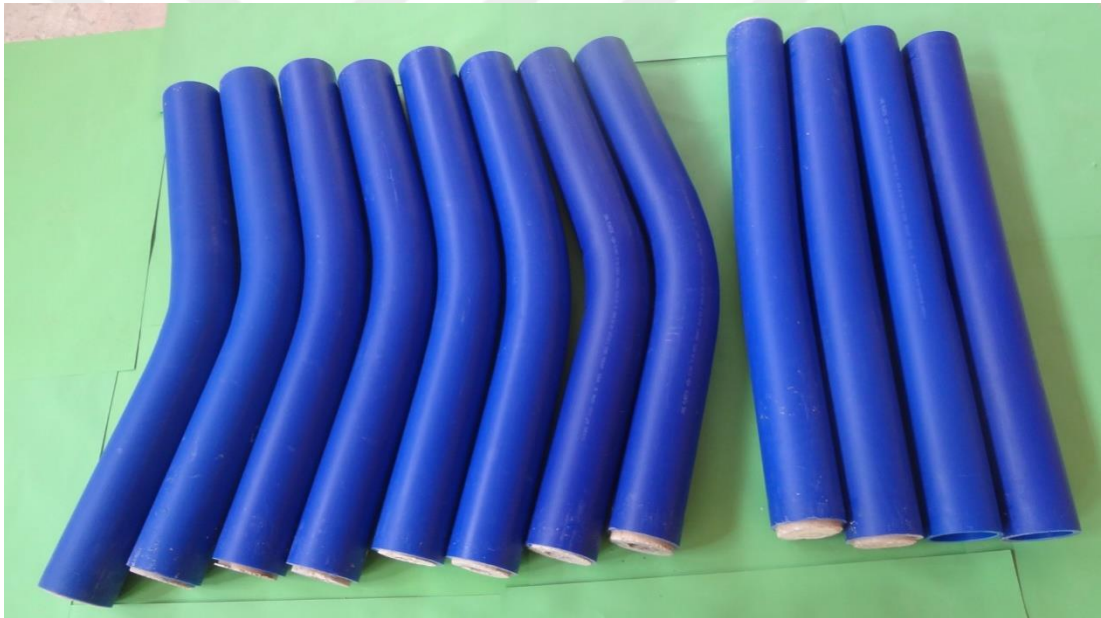
Figure (C11) HDPE-2 step 4 for the test

Figure (C12) all HDPE tubes after test
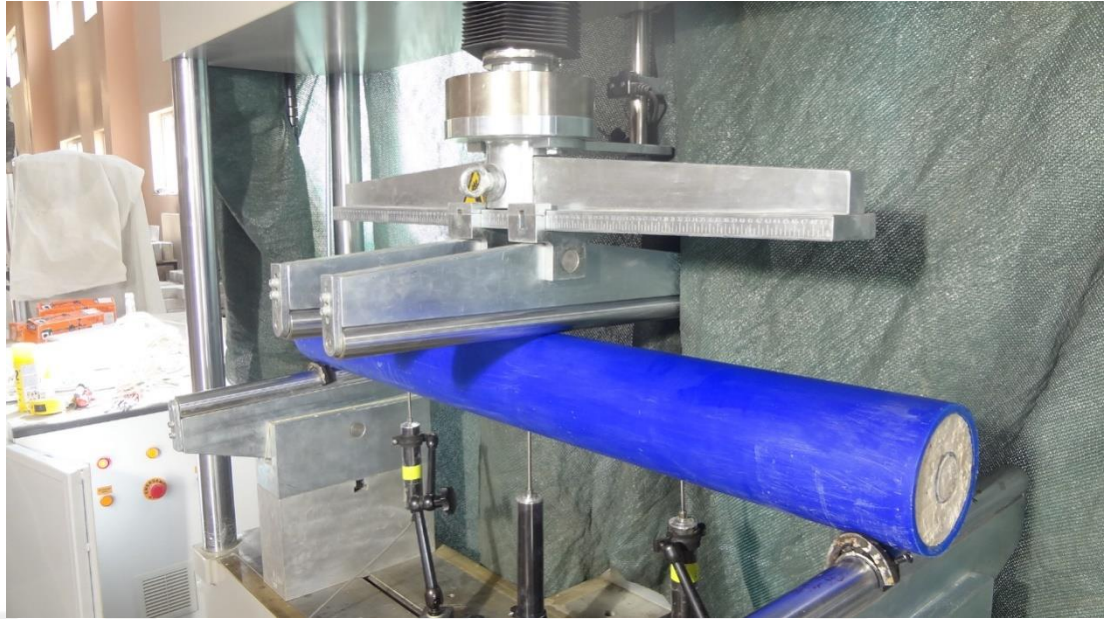
Figure (C13) HDPE-1 step 1 for the test
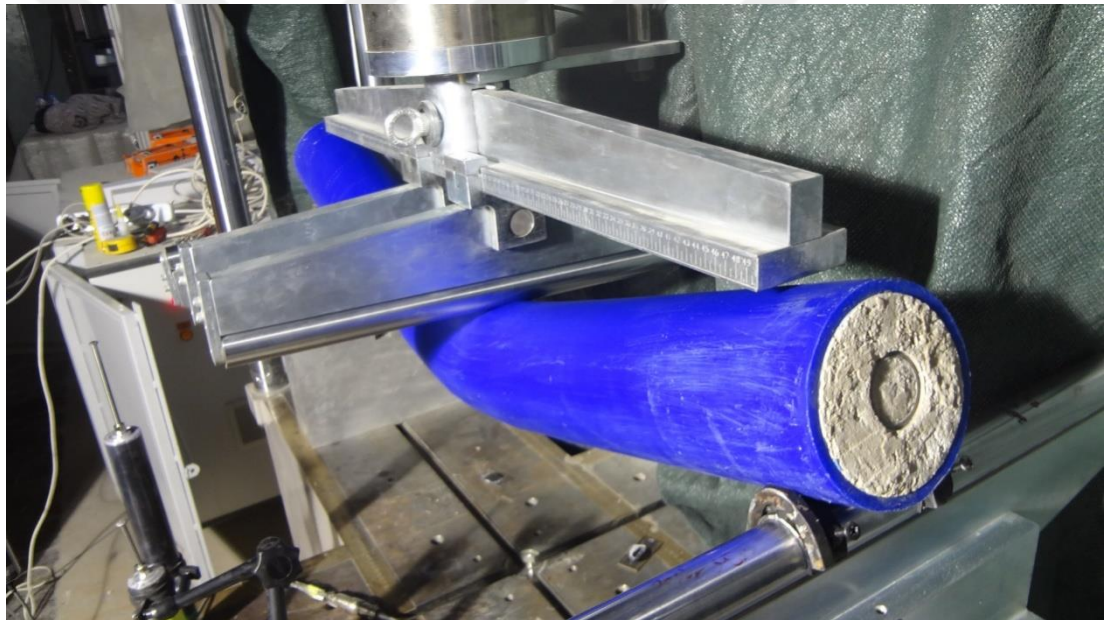

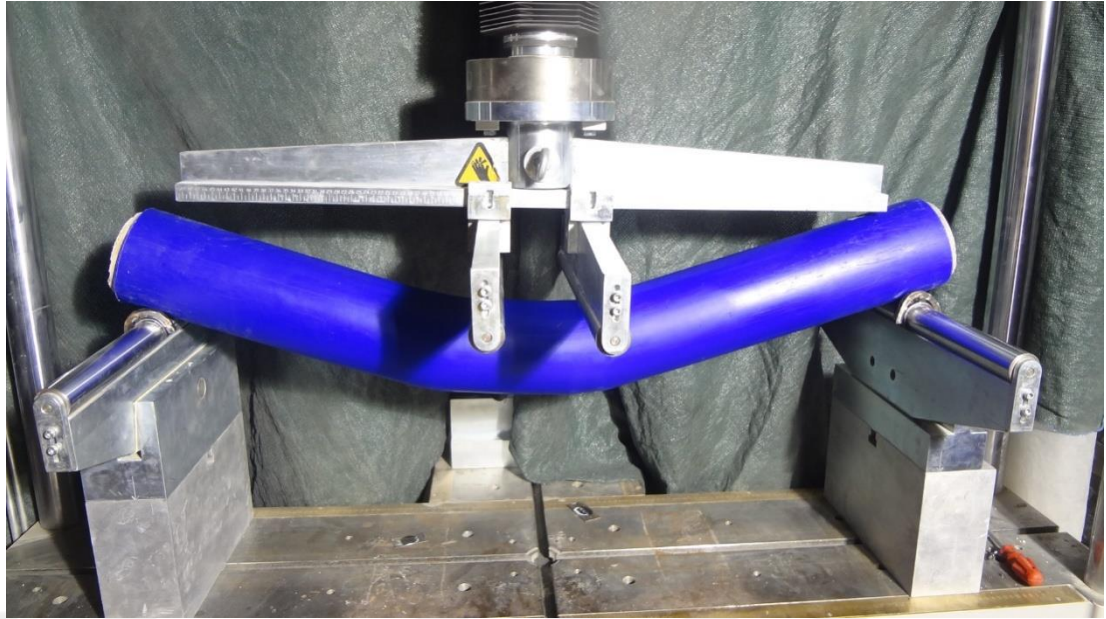**Figure (C14)** HDPE-2 step 2 for the test

Figure (C15) HDPE-2 step 3 for the test

Figure (C16) SCGP-13 step 1 for the test

Figure (C17) SCGP-13 step 2 for the test

Figure (C18) SCGP-13 step 3 for the test

Figure (C19) SCGP-13 step 4 for the test

Figure (C20) HDPE-6 and HDPE-12after the test

Figure (C21) HDPE-7 and HDPE-11after the test

Currıculum Vıtae (CV)

Date and Place of Birth	:	July / 1987- Iraq
Marital Status	:	single
Nationality	:	Iraq
Languages	:	Arabic (very good)-English (very good)-Turkish
		English Certificate: TOEFL-CBT, TOEFL-IBT, GRE
Home Address	:	Gaziantep – Turkey
Mobile No.	:	00905315709098
E-mail Address	:	civilh143@gmail.com

EDUCATION:

- Doctorate of Philosophy (Ph.D.) (2018-2019): "Self-Compacting Geopolymer & Concrete Filled Polymer Tubes", Department of Civil Engineering, University of Gaziantep, Gaziantep, Turkey.
- MSc (2014-2015): "Comparative Analysis of High-Rise RC Structures According to International Seismic Design Codes", Department of Civil Engineering, Hasan Kalyoncu University, Gaziantep, Turkey.
- BSc (2009-2010): university of diyala, Faculty of Civil Engineering, diyala, Iraq.

PUBLICATIONS:

Journals

1. Mohammed, A. H., Nassani. D. E., Tayşi, N., Hussein. A. K., (2018). "Nonlinear Finite Element Model for the Optimization of Post-Tensioned One-Way Concrete Slab". KSCE Journal of Civil Engineering, Vol. 22, No. 7, pp 2519–2527 (SCI-E).

2. Nassani. D. E., Hussein. A. K., Mohammed, A. H. (2017). "Comparative Response Assessment of Steel Frames with different Bracing Systems under Seismic Effect". Structures, 11, pp. 229-242 (E-SCI).

3. Nassani. D. E., Hussein. A. K. (2016). "Comparative Analysis of High-Rise Reinforced Concrete Structures According to International Seismic Design Codes." Journal of Civil Engineering and Architecture, 10, pp. 211-218.

4. Mohammed, A. H., Tayşi, N., Nassani, D. E., & Hussein, A. K. (2017). Finite element analysis and optimization of bonded post-tensioned concrete slabs. Cogent Engineering, 4(1), 1341288.

5. Kurtoglu, A. E., Hussein, A. K., Gulsan, M. E., Altan, M. F., & Cevik, A. (2018). Mechanical Investigation and Durability of HDPE-confined SCC Columns Exposed to Severe Environment. KSCE Journal of Civil Engineering, 22(12), 5046-5057.

Skills and Activities

Computer programs (Structural Programs)

Very good experience in STAAD.Pro, SAP2000, AutoCAD, ETAB, ANSYS.